FEUP FACULDADE DE ENGENHARIA
UNIVERSIDADE DO PORTO

A Unified Kinetics and Thermodynamics Model for Electrochemically Active Biofilms

Master's Dissertation in Bioengineering

Candidate:
Filipe António Nogueira da Cruz
Bachelor in Engineering Sciences

Institution granting the degree:
Department of Chemical Engineering
Faculty of Engineering, University of Porto

Institution where research was performed:
Department of Biotechnology
Faculty of Applied Sciences, Delft University of Technology

Supervisors:
Dr. C. Picioreanu, T.U. Delft
Dr. F. Harnisch, T.U. Braunschweig
Prof. Dr. L. Melo, U. Porto

Presented on June 21st, 2012,
at the Department of Biotechnology, T.U. Delft, Netherlands.

Abstract

Electrochemically active biofilms (EAB) are biofilms directly or indirectly accepting/donating electrons from/to a solid surface. For the first time, this work introduces a reversible kinetics and thermodynamics analytical model for these biofilms, applicable to processes involving extracellular electron transfer (EET): bioanodes, biocathodes and thus the generalized bioelectrode, as well as biocorrosion and spatially separated biogeochemical processes in marine sediment.

The two main subtypes of EET, mediated electron transfer (MET) and direct electron transfer (DET), are both mechanistically treated, using a combination of Butler-Volmer electrode kinetics and enzyme-inspired Ping-Pong microbial kinetics. Biofilm matrices are taken as conductive, either through diffusion of an intermediate redox molecule in MET or apparent metal-like conductivity in DET. The first-principles EET model is further complemented with predictions of biomass growth or endogenous respiration, thereby providing a complete base for scientific hypothesis development as well as engineering design calculations concerning EABs.

Additionally, for the first time, biomass redox states are predicted. These states are experimentally accessible in the form of redox-gradients, e.g. by Confocal Raman Microscopy. If measurements are shown to match predictions, the mathematical construct herein developed will not be restricted to global output predictions but may also explain internal system states, thus potentially giving rise to the first theory of electrochemically active biofilms.

Sumário

Biofilmes eletroquimicamente ativos são biofilmes que direta ou indiretamente aceitam/doam eletrões de/para uma superfície sólida. Pela primeira vez, esta dissertação introduz um modelo analítico reversível para a cinética e termodinâmica destes biofilmes, aplicável a processos que incluam transferência extracelular de eletrões: bioánodos, biocátodos e o bioeléctrodo generalizado; biocorrosão; e processos biogeoquímicos espacialmente isolados em sedimentos marinhos.

Tanto a transferência mediada de eletrões como a transferência direta de eletrões são abordadas sob uma perspetiva mecanística, através de uma combinação de cinéticas de elétrodo de Butler-Volmer e cinéticas microbianas inspiradas por mecanismos enzimáticos do tipo Ping-Pong. A matriz do biofilme é tomada como condutora, seja por difusão de um intermediário redox na transferência mediada, ou por condutividade aparente dos polímeros extracelulares que a constituem na transferência direta. Este modelo mecanístico para a transferência extracelular de eletrões é complementado com previsões de crescimento microbiano ou respiração endógena, proporcionando uma base de trabalho para o desenvolvimento de hipóteses científicas ou projeto de engenharia.

Adicionalmente, pela primeira vez, é previsto o estado redox da biomassa, variável mensurável por Microscopia Confocal Raman, permitindo assim a verificação experimental das previsões acerca desta varíavel interna do sistema. Torna-se assim possível verificar se a construção matemática desenvolvida neste trabalho corresponde fielmente à realidade física, potencialmente originando a primeira teoria cinética e termodinâmica para biofilmes eletroquimicamente ativos.

Acknowledgements

I would like to thank my supervisors, Dr. Cristian Picioreanu from T.U. Delft and Dr. Falk Harnisch from T.U. Braunschweig for adequate support and positive attitude. Also, I would like to thank Prof. Luís Melo for arranging my stay at T.U. Delft.

This work was partially funded by Agência Nacional PROLAV, under the framework of the Erasmus Programme, contract number 29233-IC-1-2007-1-PT-ERASMUS-EUCX-1.

Obrigado Mãe! Foram seis longos anos de Faculdade. Não sei o que teria sido de mim se não tivesse a família para me ancorar. Acho que sou uma pessoa melhor depois de tudo.

Table of Contents

Figures and Tables

Abbreviations, Nomenclature and Symbols

Abbreviations

ADP – Adenosine Diphosphate
AMP – Adenosine Monophosphate
AQDS – Anthraquinone-2,6-disulfonic acid
ATP – Adenosine Triphosphate
BES – Bioelectrochemical System
BV – Butler-Volmer (equation, model)
BVM – Butler-Volmer-Monod (equation, model)
cAMP – cyclic Adenosine Monophosphate
CAP – Catabolite Activator Protein
CV – Cyclic Voltammetry
DET – Direct Electron Transfer
DMRB – Dissimilatory Metal Reducing Bacteria
EAB – Electrochemically Active Biofilm
EET – Extracellular Electron Transfer
ET – Electron Transfer
ETC – Electron Transport Chain
FMN – Flavin Mononucleotide
HER – Hydrogen Evolution Reaction
MFC – Microbial Fuel Cell
MEC – Microbial Electrosynthesis Cell
MET – Mediated Electron Transfer
MV – Methyl Viologen
Mtr – Metal reducing (protein)
NADH – Nicotinamide Adenine Dinucleotide
NM – Nernst-Monod (equation, model)
Omc – Outer-membrane cytochrome
ORR – Oxygen Reduction Reaction
PMF – Proton Motive Force
RET – Reversed Electron Transport
RF – Riboflavin

Nomenclature

The notation herein described represents both the chemical species and its concentration or partial pressure.

A_{Ox} – Idealized oxidized electron acceptor
A_{Red} – Idealized reduced (post-acceptance) electron acceptor
D_{Ox} – Idealized oxidized (post-donation) electron donor
D_{Red} – Idealized reduced electron donor species

S_{Ox} – Idealized oxidized external substrate (other than mediator)
S_{Red} – Idealized reduced external substrate (other than mediator)
M_{Ox} – Idealized oxidized electron mediator
M_{Red} – Idealized reduced electron mediator

Electron acceptor: species that participates in cellular respiration as the final, external oxidant in electron transport chains, e.g. oxygen in aerobic respiration.

Electron donor: species that participates in cellular respiration as the initial, external or internal, reductant in electron transport chains, e.g. nitrite in nitrification (external) or NADH in organotrophy (internal).

Electron mediator: a donor or acceptor that may be regenerated to its original state by interaction with an extracellular solid surface, e.g. an electrode at an appropriate potential; opposite of external substrate. If the mediator is not regenerated by the surface for a particular set of conditions, then that mediator should be regarded as an external substrate in those conditions.

External substrate: a donor or acceptor that may not be regenerated to its original state by interaction with an extracellular solid surface; opposite of mediator. If the surface is so strongly electrically poised that it regenerates external substrate, e.g. a cathode abiotically evolving hydrogen used as donor by a microbial community, the substrate should be regarded as a mediator in those conditions.

Symbols

The symbols listed here apply to chapters 4, 5, 6, 7 and 8. Symbols in chapter 3.State-of-the-Art: EAB Kinetics Models may conflict with the meanings used in this report: refer to cited papers for their detailed significance.

α_a – Anodic charge transfer coefficient, dimensionless.
α_c – Cathodic charge transfer coefficient, dimensionless.
A_r – Heterogeneous reaction area, e.g. m^2.
$A_{biofilm}$ – Biofilm section area, e.g. m^2.
$a_{biofilm}$ – Biofilm internal surface area, $m^2_{interface}/m^3_{biofilm}$.
Γ_X – Surface concentration of X, e.g. mol/m^2.
γ_c – Degree of reduction of carbon source, e.g. e-mol/C-mol.
#C – Number of carbon atoms is a carbon source, e.g. e-mol/C-mol
$\Delta_f G°$ – Standard Gibbs energy of formation, subscript indicates reaction, e.g. J/mol.
$\Delta_r G°$ – Standard Gibbs energy of reaction, subscript indicates reaction, e.g. J/mol.
$\Delta_r G$ – Actual Gibbs energy of reaction, subscript indicates reaction, e.g. J/mol.
ΔG_{diss} – Dissipation energy, e.g. J/C-mol.
$\varepsilon_{biofilm}$ – Biofilm porosity, dimensionless.
E° – Standard reduction potential, subscript indicates redox pair, e.g. V.
E – Actual reduction potential, subscript indicates redox pair, e.g. V.

$\varphi_{electrode}$ – Electrode electrical potential, e.g. V.

φ_{matrix} – Matrix electrical potential, e.g. V.

$\varphi_{solution}$ – Solution electrical potential, e.g. V.

F – Faraday constant, e.g. 96485 C/e-mol.

i_{matrix} – Matrix homogeneous current density, e.g. A/m^2.

j – Heterogeneous current density, e.g. A/m^2.

j_{pc} – Cathodic peak heterogeneous current density, A/m^2.

j_{pa} – Anodic peak heterogeneous current density, A/m^2.

$j_{transfer}$ – Heterogeneous current density effectively transferred, e.g. A/m^2.

j_{growth} – Heterogeneous current density retained/released by growth, e.g. A/m^2.

K_a – Acidity constant, dimensionless.

K_{eq} – Equilibrium constant, dimensionless.

K_S – Half-saturation constant or coefficient for **S**, same units as **S** (may be a composite or exponentiated substrate).

k_1 – Homogeneous rate constant, units depend on stoichiometry.

k_{-1} – First-order homogeneous rate constant, e.g. 1/s.

k_2 – First-order homogeneous rate constant, e.g. 1/s.

k_{-2} – Homogeneous rate constant, units depend on stoichiometry.

k_3 – Homogeneous rate constant, units depend on stoichiometry.

k_{-3} – First-order homogeneous rate constant, e.g. 1/s.

k_4 – First-order homogeneous rate constant, e.g. 1/s.

k_{-4} – Homogeneous rate constant, units depend on stoichiometry.

k_f – Forward rate constant, units depend on stoichiometry.

k_r – Reverse rate constant, units depend on stoichiometry.

k° – Standard heterogeneous rate constant, e.g. m/s.

k_a – Anodic heterogeneous rate coefficient, e.g. m/s.

k_c – Cathodic heterogeneous rate coefficient, e.g. m/s.(m3/mol)$^{\boldsymbol{m}}$, where ***m*** is the number of protons participating in the cathodic reaction.

L_x – Biofilm thickness, e.g. m.

L_y – Biofilm height, e.g. m.

L_z – Biofilm depth, e.g. m.

M_X – Biomass molar mass, e.g. kg/C-mol.

m_G – Maintenance rate, e.g. J/(C-mol.s).

n – Number of electrons exchanged per unit reagent, e.g e-mol/mol.

σ_{matrix} – Matrix conductivity, e.g. S/m.

ρ_X – Biomass density, e.g. kg/m^3.

Q_r – Reaction quotient.

$q_{e,max}$ – Maximum catabolic turnover, e.g. e-mol/(C-mol.s).

q_G – Specific energy rate, e.g. J/(C-mol.s)

R – Ideal gas constant, e.g. 8.3145 J/(K.mol).

r – Reaction rate, subscript indicates reaction, superscript indicates conditions, e.g. mol/(m^3.s)

T – Temperature, e.g. K.

t – Time, e.g. s.

μ – Specific growth rate, e.g. 1/s.

$\nu_{X,an}$ – Anabolic stoichiometric coefficient, e.g. mol/C-mol.

V_f – Maximum forward reaction rate, e.g. mol/(m^3.s).

V_r – Homogeneous reaction volume, e.g. m^3 (chapter 5); Maximum reverse reaction rate, e.g. mol/(m^3.s).

$v_{biofilm}$ – Net biofilm growth rate (or velocity), e.g. m/s.

X – Oxidized biomass concentration or density, e.g. C-mol/m^3.

XH_n – Reduced biomass concentration or density, e.g. C-mol/m^3.

X_M – Biomass-mediator concentration or density, e.g. C-mol/m^3.

X_S – Biomass-substrate concentration or density, e.g. C-mol/m^3.

X_T – Total biomass concentration or density, e.g. C-mol/m^3.

z_e – Electron charge number, -1, dimensionless.

1. Motivation

Perhaps one of the most intriguing results in bioelectrochemical systems (BESs) literature is the one by Rozendal and co-workers (Rozendal et al., 2008). In their experiment, a mixed species biofilm was first grown on acetate, forming an anodic community on a graphite electrode. After sufficient growth was observed, the simultaneous carbon source and electron donor, i.e. acetate was replaced by an exclusive electron donor, spurge hydrogen, thus keeping the biofilm active but presumably arresting its growth. After some time, hydrogen was replaced with nitrogen, depriving cells of an electron donor, and the electrode potential was lowered significantly into the usual cathodic range. Microbial bioelectrocatalytic hydrogen evolution was observed.

What at first was an anode receiving electrons from hydrogen oxidation became a cathode donating electrons for proton reduction. Noteworthy, this inversion of biofilm catabolism was achieved simply by manipulating thermodynamics: changing the electrode potential and the hydrogen/proton ratio. Both the electrode material and microbial community remained the same. Also, a small negative current density was immediately observed upon the switch to cathodic-range potentials, meaning the same enzymatic machinery is capable of catalysing both the forward reaction, i.e. hydrogen oxidation and the reverse reaction, i.e. hydrogen evolution.

The objective of this dissertation is to provide a theoretical explanation to the reversibility of bioelectrochemical systems, using analytical modelling as the preferred approach. Therefore, the intended result is a set of reversible rate equations for electrochemically active biofilms (EABs), preferably based on first-principles kinetics and thermodynamics, so that results may be cross-checked with experimental data not only for macroscopic outputs, but also for internal system variables. By peering inside todays EAB black box from a fundamental perspective, I hope to provide the first quantitative kinetics and thermodynamics theory in the field. Thus, this dissertation should not only provide a profound scientific description of EABs, but also pave the way for future engineering of EAB technology.

2. Introduction

Electrochemically active biofilms (EABs) are biofilms composed of electroactive microorganisms, also called exo-electrogens or electrode-respiring bacteria and their self-produced extracellular polymeric substances (Lovley, 2008; Logan, 2009). The individual cells embedded in these biofilms may directly or indirectly donate/accept electrons to/from a solid surface. Spatially separated biogeochemical processes coupled by electric currents are an example, such as for instance the coupling of hydrogen sulphide oxidation in the anoxic region just below the sea floor and oxygen reduction just above – both processes are separated by a sediment layer up to several millimetres thick (Nielsen et al., 2010). Sulphur metabolizing bacteria are also present in biofilms responsible for accelerated low water corrosion (Beech and Campbell, 2008) – a form of aggressive biocorrosion that affects harbours around the world – although regular biocorrosion may be explained without the need for extracellular electron transfer (Picioreanu and Loosdrecht, 2002). Finally, electrochemically active biofilms are the cornerstone of microbial bioelectrochemical systems (Rabaey et al., 2010), usually growing on inert electrode materials such as carbon (Figure 1) or stainless steel, both in bioanodes (Torres et al., 2010) and biocathodes (Rosenbaum et al., 2011). This introduction will focus on bioelectrochemical systems as source of technical vocabulary, extracellular electron transfer as the core metabolic feature of EABs and the proposed theories for long-range direct electron transfer, arguably what is most unique about EABs.

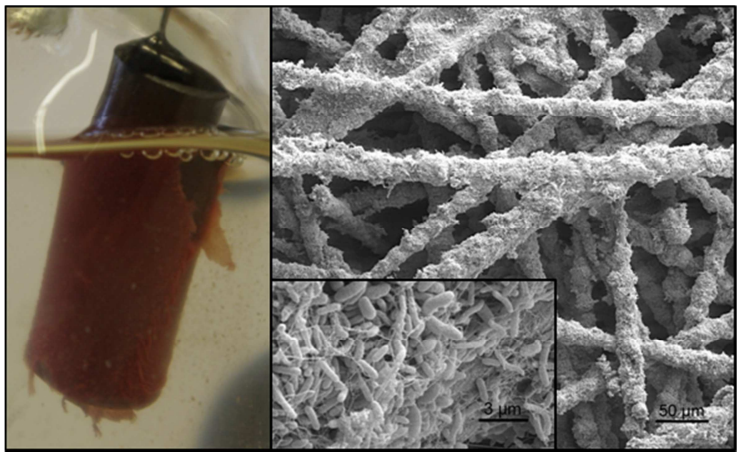

Figure 1 - Anodic biofilm of *Geobacter sp.* growing on a carbon electrode. In BESs, *Geobacter sp.* grows almost exclusively attached to the electrode, since it is natively capable of long-range DET but can't secrete soluble redox mediators. Used with permission of F. Harnisch (Harnisch and Schröder, 2012).

2.1. Bioelectrochemical Systems (BESs)

Bioelectrochemical systems (BESs) are a subtype of fuel cell technology, characterized by biocatalytic anodes, cathodes or both. The biocatalytic component is most often an attached microbial community, although suspended communities (Delaney et al., 1984) or enzyme-exclusive catalysts (Lapinsonnière et al., 2012) are also possible. Enzymatic fuel cells won't be further discussed here: a comprehensive review is available elsewhere (Cracknell et al., 2008). The general features of BESs are represented in Figure 2. One of the compartments is predominantly anoxic and anodic, where organic matter is oxidized to carbon dioxide, protons and electrons. Those electrons will then be transferred to a solid electrode and transverse an external circuit, where their reduction potential may be increased by a resistance or decreased by a source – for higher reduction potentials, the tendency of those electrons to reduce the terminal acceptor is lower. Finally, electrons reach the cathode and complete the electronic circuit. The circuit is closed by an ionic component, i.e. ion exchange between the two compartments. Most often, membranes selective for cations are used to separate the two chambers.

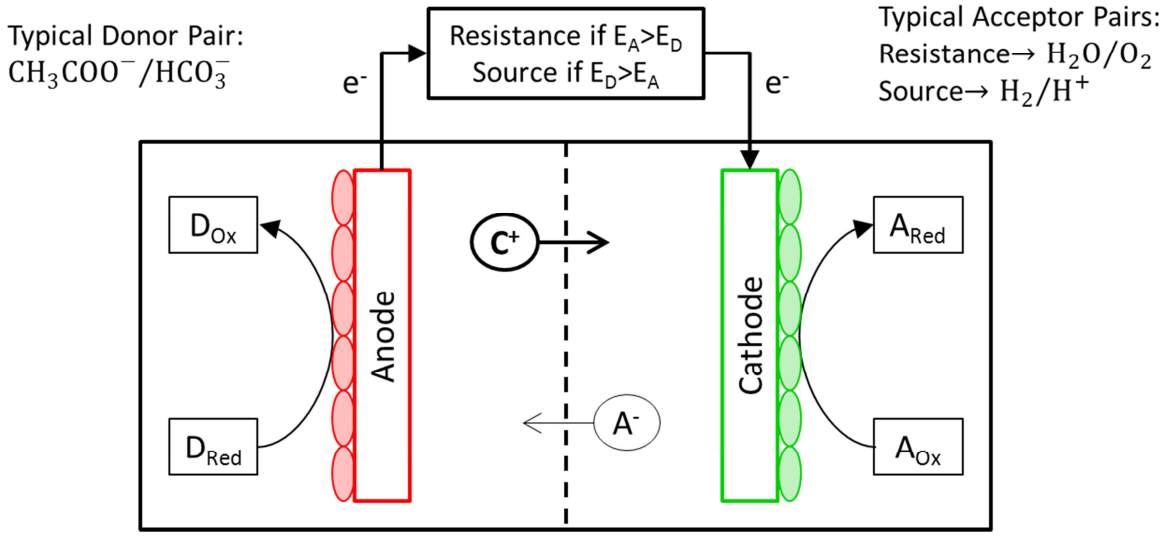

Figure 2 - Typical Bioelectrochemical System. Biofilms may be present on anode, cathode or both. If there is be no biological component in both electrodes, the system is a chemical fuel cell. Vertical dashed line: semi-permeable membrane, although configurations exist that don't require physical separation of compartments, e.g. if electrode potentials are poised using a potentiostat. **Legend:** C^+ – generic cation; A^- – generic anion; D_{Red}/D_{Ox} – redox pair that donates electrons for microbial catabolism; A_{Red}/A_{Ox} – redox pair that accepts electrons from microbial catabolism; Resistance – device that converts electrical potential into work or heat; Source – device that converts work or heat into electrical potential.

While anodic processes will typically generate protons, in the average BES it is mostly sodium that transverses the membrane (Harnisch and Schröder, 2009), since it is much more abundant than the hydronium ion: at neutral pH, 10^{-7} M of H_3O^+ are present, while typical anode feedstock contains 10^{-3} to 10^{-1} M of Na^+. Thus, acidification of anodic compartments and alkalinisation of cathodic compartments occurs, although this can usually be mitigated by a buffer.

When energy production is intended, cathodes perform the oxygen reduction reaction (ORR), and may be aerated with atmospheric air. However, if the objective is the hydrogen evolution reaction (HER), cathodes operate under anaerobic conditions, and most often electrons supplied by the anode must have their reduction potentials lowered by a source, thus implying energy consumption (Harnisch and Schröder, 2010), in a process now known as microbial electrosynthesis (Rabaey and Rozendal, 2010).

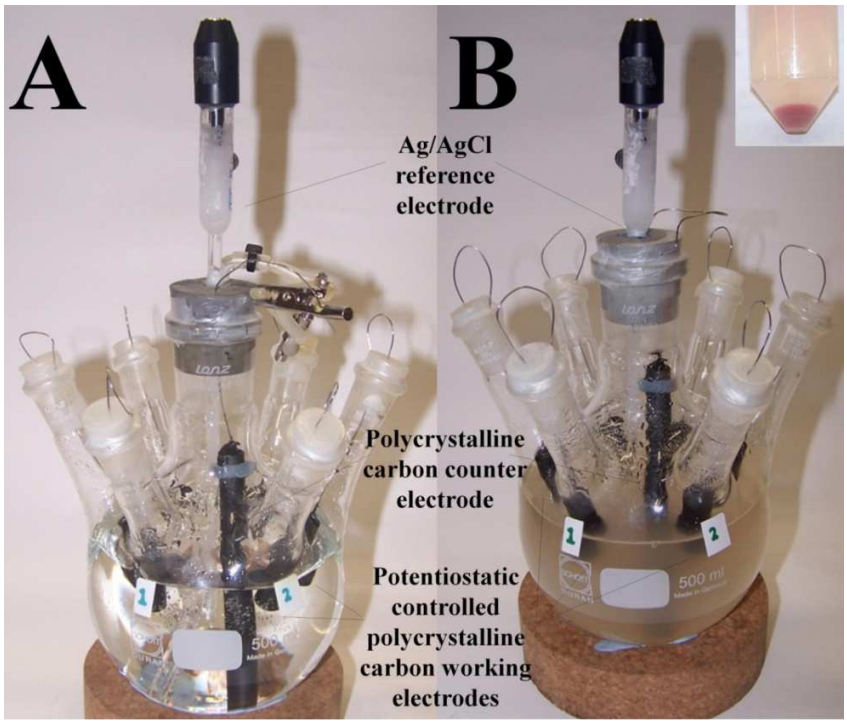

Figure 3 - Electrochemically active suspended culture. A) Sterile potentiostat-controlled BES. B) The same system now colonized by *Shewanella sp.*. Insert: centrifuged culture pellet. In BESs, *Shewanella sp.* may grow in suspended form and still interact with the electrode, since it is able to secrete soluble redox mediators of the flavin family. Used with permission of F. Harnisch. (Carmona-Martínez A., Harnisch F., et al., 2012).

In most fundamental BESs studies, acetate or lactate are the electron donors, since they are common organic acids in wastewater and also preferred substrates for the electrochemically active model organisms *Geobacter sulfurreducens* and *Shewanella oneidensis*, respectively (for their genome sequences and general microbiological information see respectively: Methé et al., 2003; Heidelberg et al., 2002). In nature, both

organisms belong to the group of dissimilatory metal reducing bacteria (DMRB), and their extracellular electron transfer capabilities allow them to reduce otherwise inaccessible terminal electron acceptors, such as iron(III) trapped in insoluble ferric oxides.

Biofilms are not strictly necessary for BES's operation. Given a soluble mediator molecule, it is possible that electrochemically active suspended cultures will form instead of biofilms (see Figure 3 for an example of the mediator producing genus *Shewanella*). However, most often biofilms are beneficial because they are a requirement for direct electron transfer.

Perhaps the dawn of modern microbial fuel cell (MFC) research – later expanded into bioelectrochemical systems research – is a pair of papers published in 1984 (Roller et al., 1984; Delaney et al., 1984), reporting the performance of MFCs operated with several microorganism-mediator-substrate combinations. Initially, bioelectrochemical systems research focused on electricity production via oxidation of organic compounds in anode compartments. However, since then the focus has started to shift towards biocathode research, both because hydrogen production has been report with such devices (Rozendal et al., 2008), but also because high abiotic cathodic overpotentials are one of the main reasons why both large scale organic matter oxidation and/or electrolytic hydrogen production are prohibitively expensive – platinum cathodes are required to drive down cathodic overpotentials sufficiently, yet capital costs are greatly inflated (Harnisch and Schröder, 2010).

2.2.Extracellular Electron Transfer (EET)

Extracellular electron transfer (EET) is the process by which cells donate/accept electron to/from a solid located outside the cell. Primarily regarded as a mechanism of dissimilatory metal reduction by bacteria in nature (Hernandez and Newman, 2001; Reguera et al., 2005; Marsili et al., 2008), and recently as part of the metabolism of marine sediment dwelling bacteria (Nielsen et al., 2010), EET is exploited in technological constructs such as bioelectrochemical systems. An overview of the two most common extracellular electron transfer mechanisms is provided in Figure 4: mediated electron transfer (MET) and contact direct electron transfer (DET).

2.2.1. Mediated Electron Transfer (MET)

MET is accomplished by cellular reduction/oxidation of a soluble electron shuttle, which will then diffuse away from the cell and reduce/oxidize an available solid. The shuttle may then diffuse back to the cell, specifically, to the cytoplasmic membrane, where it can be reused. Since the shuttle must diffuse back and forth, MET is only viable in low mass transport environments with relatively long residence times – such as batch BESs – otherwise mediator washout would occur. Continuous BESs based on MET are possible, but this would imply addition of exogenous mediator to the inflow, increasing operational

costs and generating pollution since mediators are not oxidized to carbon dioxide. It may be possible to operate endogenous MET based BESs in continuous, however retention times would have to be long, which may conflict with the need for substrate feed. MET has been known for some time, and was originally thought to be the only mechanism of EET (Hernandez and Newman, 2001). Alternatively, mediators may act as shuttles between species, in so called interspecies electron transfer (Harnisch and Rabaey, 2012).

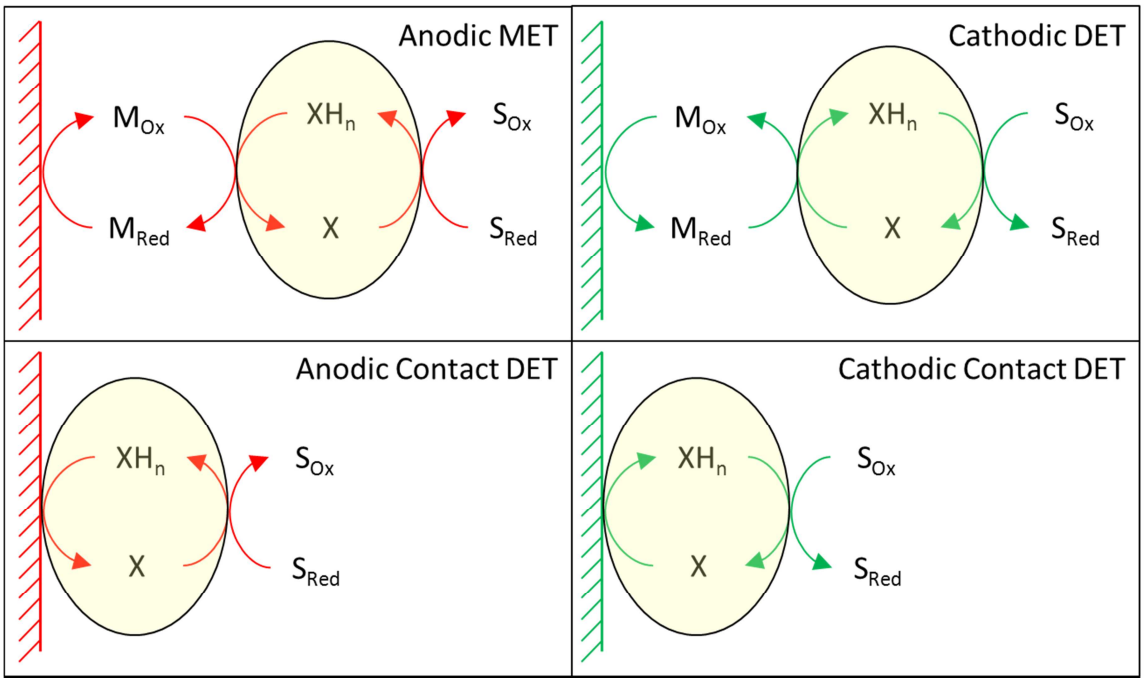

Figure 4 - Mediated electron transfer (MET) vs. *contact* direct electron transfer (DET), for both anodic and cathodic processes. **In MET**, a soluble mediator molecule M is oxidized/reduced at the solid surface. This mediator will then oxidize/reduce a biomass redox intermediate XH_n/X: this intermediate releases/captures n protons together with the n electrons transferred, to keep overall biomass neutrality. Finally, the biomass redox intermediate oxidizes/reduces an external substrate S. **In contact DET**, the sequence of events is similar, except the cellular redox intermediate directly interacts with the electrode.

MET may be further subdivided in two subtypes: endogenous and exogenous. Endogenous MET is observed in the model organism *Shewanella oneidensis*, capable of secreting mediators of the flavin family (Marsili et al., 2008). Specifically, flavin mononucleotide seems to be a growth associated product, whilst riboflavin seems to be secreted constitutively (Canstein et al., 2008). Exogenous MET occurs when a mediator is available in the environment or artificially supplied. For instance, both methyl viologen (Aulenta et al., 2007) and anthraquinone-2,6-disulfonate (Aulenta et al., 2010b) are redox shuttles usable by cathode grown cultures capable of reductive dechlorination. Most mediators belong to the quinone family of organic compounds, whose representatives are also a part of biological electron transport chains (ETC). It is thus not surprising that any

combination of mediator-microorganism seems to produce some sort of electrochemically active culture (Delaney et al., 1984), even if very inefficient: some components in respiratory chains may interact with mediators in a manner similar to their interactions with regular ETC quinones. Yet, from a technical perspective the use of exogenous mediators is now generally abandoned (Schröder, 2007).

2.2.2. Direct Electron Transfer (DET)

DET differs from MET in the vehicle for electron transport. Instead of soluble electron shuttles penetrating the outer-membrane of Gram-negative bacteria, in DET electrons are taken up via outer-membrane cytochromes, which may then further transfer those electrons to soluble intermediates located in the periplasmic space. These intermediates may diffuse to the cytoplasmic membrane, where they reduced an electron transport chain component. Of course, depending on conditions, electrons may also travel from the ETC to an outer-membrane component. An example is the MtrABC-OmcA system in *Shewanella oneidensis* (Carmona-Martínez et al., 2011; Richter et al., 2012). In this system, MtrA, a soluble periplasmic protein, is reduced at the terminus of the cytoplasmic respiratory chain. It may then diffuse to the outer-membrane where it reduces the transmembrane protein MtrB. MtrB transfers the electron to MtrC, anchored just outside the outer-membrane. Together with OmcA, MtrC reduces iron(III) oxides, the terminal acceptor. Carmona-Martínez and co-workers also speculated about the role of pil-type and msh-type pili, although they were unable to mechanistically distinguish this pathway from the better established MtrABC-OmcA system (Carmona-Martínez et al., 2011).

This type of DET, where outer-membrane cytochromes are touching the donor/acceptor solid surface is termed contact DET, and is biochemically possible so long as those cytochromes are present in tandem with periplasmic intermediates, regardless of how inefficient the process may be. For instance, reductive dechlorinating biocathodes, both of the pure – *Anaeromyxobacter dehalogenans* (Strycharz-Glaven et al., 2010) – and mixed culture type (Aulenta et al., 2010a), are capable of apparent contact DET. Results should be interpreted carefully however, since it is possible those cultures secrete previously unknown endogenous mediators (Aulenta et al., 2009), or in some cases cathodes themselves may produce mediators, e.g. in abiotic hydrogen evolution, which is subsequently oxidize by bacteria (Lohner et al., 2011). Additionally, contact DET alone can only sustain mono-layer biofilms, since cells must be touching the substratum. Thus, the ability of some species to perform contact DET without endogenous MET or other forms of DET to support it should, in my opinion, be regard as a biochemical coincidence, much like exogenous MET is also a fairly ubiquitous laboratory artefact: possible to some extent, but likely not viable in nature, and thus merely a side-effect of evolution.

2.3.Long-range DET

Some microorganisms are able to directly transfer electrons to/from a solid at a distance. Exactly how this long-range DET happens is yet unknown. Two main models have been proposed: metal-like conduction and superexchange (Figure 5).

2.3.1. Metal-like Conduction

Metal-like conduction was first proposed by Malvankar and co-workers (Malvankar et al., 2011), following previous measurements of conductivity in pili-like structures – dubbed nanowires – observed in electrochemically active biofilms of *Geobacter sulfurreducens* (Reguera et al., 2005). The hypothesis is based on the proportionally inverse relation between conductivity and temperature in the biologically relevant range of 275-300 K, similar to observations in metals. Outer-membrane cytochromes are still required at the cell/matrix and matrix/solid interfaces, with OmcZ specifically concentrated at anodic surfaces (Inoue et al., 2011).

Mechanistically, it has been proposed that π-stacking of delocalized molecular orbitals of aromatic aminoacid functionalities such as phenyl in tyrosine and benzyl in phenylalanine provide proteinaceous nanowires with conductive properties similar to the ones observed for metallic bonding: a single shared electronic cloud extending from solid to cell is the channel for extracellular electron transfer (Malvankar et al., 2011). So far, no definitive evidence of π-stacking of delocalized molecular orbitals in nanowires has been reported (Malvankar and Lovley, 2012).

For metal-like conduction, Ohm's law applies,

$$i = -\sigma.\nabla\varphi \qquad (2.3.1.–1)$$

where $\boldsymbol{i}$ is current density, e.g. $A.m^{-2}$, $\boldsymbol{\sigma}$ is conductivity, e.g. $S.m^{-1}$, and $\boldsymbol{\varphi}$ is electrical potential, e.g. V. As such, according to this model nanowires may be thought of as conductive extensions of the solid surface, or in other words, the solid plus biofilm matrix behave as a porous electrode.

2.3.2. Superexchange

Superexchange was first proposed by Strycharz-Glaven and co-workers (Strycharz-Glaven et al., 2011), based on reports of alignment of the outer-membrane cytochrome OmcS along *Geobacter sulfurreducens* nanowires (Leang et al., 2010). The model is an extension of the charge transport mechanism in electroactive polymers, where sequences of redox moieties spaced less than 2nm act as a series of stepping stones for electron transfer, so long as there is a potential gradient (Dalton et al., 1990). This in turn is an example of electron hopping, a phenomenon first reported by Kaufman and Engler, and later

demonstrated to be formally equivalent to the mass transfer of redox centres by diffusion and migration (Kaufman and Engler, 1979; Andrieux and Savéant, 1980; Laviron, 1980). This equivalence can be expressed using an electron diffusion coefficient (Savéant, 1986),

$$D_e \propto k_{ex}.C_T.\delta^2 \qquad (2.3.2.–1)$$

where $\boldsymbol{D_e}$ is the electron diffusion coefficient, e.g. $m^2.s^{-1}$, $\boldsymbol{k_{ex}}$ is the bimolecular rate constant for electron exchange between C_{Red} and C_{Ox}, e.g. $m^3.mol^{-1}.s^{-1}$, $\boldsymbol{C_T}$ is the total concentration of redox centres, e.g. $mol.m^{-3}$, and $\boldsymbol{\delta}$ is the hopping distance, e.g. m. The proportionality constant implicit is 1/6 for fixed redox centres (Blauch and Savéant, 1992). Interestingly, in the original report of OmcS alignment along nanowires (Leang et al., 2010), and based on analogy with electroactive polymers, the authors concluded that cytochrome spacing – 28.6±10.5 nm – was too large to allow electron hopping, since Dalton and co-workers predicted a distance of circa 2 nm as the tipping point above which electron hopping between adjacent moieties is no longer viable (Dalton et al., 1990). Thus OmcS would serve as an exit/entry-point to the acceptor/donor solid, much like OmcZ is thought to behave in the metal-like conduction model. It should be said however that the distance measured is, technically, the distance between gold particles in gold-labelled antibodies, and that *Geobacter sulfurreducens* encodes 111 putative *c*-type cytochromes, as deducted from genome sequencing (Methé et al., 2003).

A variation to the superexchange model was proposed by Okamoto and co-workers (Okamoto et al., 2012). Based on whole-cell voltammetry measurements on multilayer *Shewanella oneidensis* biofilms, not known to produce conductive biofilm matrices, the authors propose a model of long-range DET in which matrix embedded cells have limited motility, and are thus able to adjust the relative positions of cytochromes located at the outer-membrane, closing redox centre gaps as needed for electron hopping. Superexchange would thus not only be a process of electron percolation through fixed redox sites, but also a process of displacement of redox sites, as generally described by Blauch and Savéant (Blauch and Savéant, 1992). Still, no definitive evidence of the network of cytochromes necessary for superexchange is available (Bond et al., 2012), although, in my opinion, should the nuances proposed by Okamoto and co-workers prove correct, it is the more likely candidate to explain long-range DET.

Although the proposed theories for long-range DET are mechanistically different, from a modelling perspective both are compatible with an equivalent conductivity $\boldsymbol{\sigma}$, even if this apparent parameter only matches physical reality in metal-like conduction.

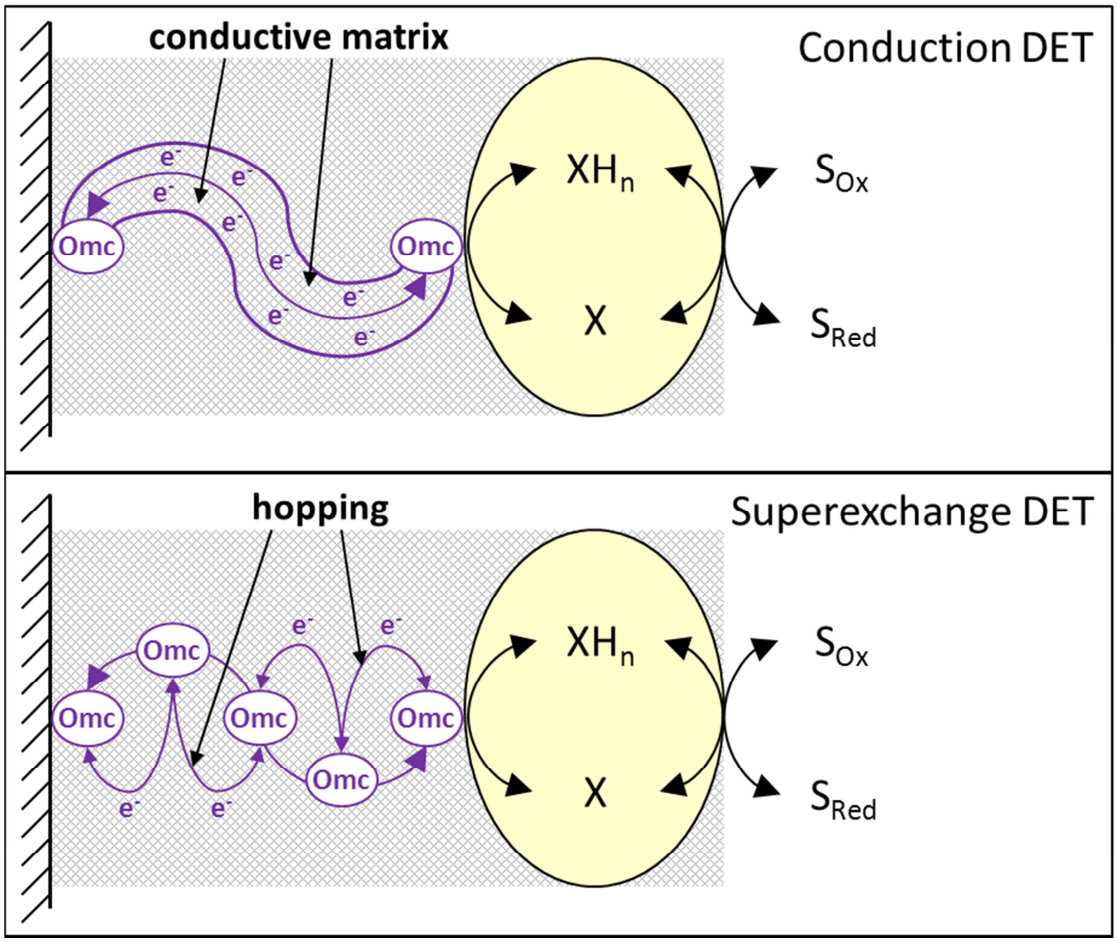

Figure 5 - Proposed mechanisms of long-range DET. **In metal-like conduction**, cellular extensions dubbed nanowires conduct electrons in a manner similar to metals (Malvankar et al., 2011). The mechanism requires yet unproven (Malvankar and Lovley, 2012) π-stacking of delocalized molecular orbitals of aromatic aminoacid side chains, thus creating a single electronic cloud extending from the outer-membrane to the solid surface, in a manner analogous to the metallic bonding model (Atkins et al., 2009). Outer-membrane type cytochromes are required at the cell/matrix and matrix/solid interfaces. **In superexchange**, electrons hop across nanowire-contained cytochrome chains extending through the biofilm matrix (Strycharz-Glaven et al., 2011). The mechanism requires yet unproven (Bond et al., 2012) uniform cytochrome spacing of no more than 2nm, thus forming a series of individual redox entities, with each cytochrome sequentially oxidizing an upstream donor and reducing a downstream acceptor, in a manner analogous to electron hopping along the redox moieties of electroactive polymers (Dalton et al., 1990). As in metal-like conduction, outer-membrane type cytochromes are required at the cell/matrix and matrix/solid interfaces. **Legend:** e^- - electron; Omc – outer-membrane cytochrome; S_{Red}/S_{ox} – redox pair that either provides or donates electrons for microbial catabolism; XH_n/X – redox pair that represents the redox state of biomass, XH_n is the reduced form and X is the oxidized form.

3. State-of-the-Art: EAB Kinetics Models

This review will focus on kinetic models of electrochemically active biofilms, since, to the best of my knowledge, no attempts at incorporating microbial thermodynamics have so far been made, apart simple net thermodynamic calculations (Schröder, 2007; Harnisch and Schröder, 2010). Also, all models discussed were developed with anodic biofilms in mind, and thus none of them incorporates the concept of EAB catabolic reversibility, experimentally demonstrated by Rozendal and co-workers (Rozendal et al., 2008). Historically, models are categorized as mediated or direct electron transfer models, and both transport and kinetics equations are required.

3.1.MET Models

The kinetics of anodic mediated electron transfer is modelled by Picioreanu and co-workers in a series of papers (Picioreanu et al., 2007; Picioreanu et al., 2008; Picioreanu et al., 2010a; Picioreanu et al., 2010b). These studies include: suspended and attached microbial populations; two-dimensional and three-dimensional simulations; and the effects of pH, electrode geometry and to some extent hydrodynamics on microbial fuel cell performance. Multispecies populations and their interactions are also simulated, specifically the ones observed in wastewater treatment and anaerobic digestion, e.g. glucose fermentation to organic acids – acidogenesis – followed by oxidation to acetate, hydrogen and bicarbonate – acetogenesis – and lastly methanogenesis, either by hydrogen oxidation and bicarbonate reduction, or by dismutation of acetate into bicarbonate and methane. Each genesis process is performed by a different microbial entity.

3.1.1. Transport in MET

The models themselves are implemented in a computational mesh and accompanied by the necessary mass transport mathematical structure. Thus, and unlike other extracellular electron transfer models, the work by Picioreanu and co-workers yields concentration profiles for all relevant chemical species within and around biofilms. To illustrate the general case for a charged species **A**, subjected to diffusion, (electro-) migration and convection, the Nernst-Plank equation applies (Bard and Faulkner, 2001),

$$J_A = -D_A.\nabla C_A - z_A.\frac{D_A}{R.T}F.C_A.\nabla\varphi + u.C_A \qquad (3.1.1.–1)$$

$$\text{Diffusion}\left[\text{mol.m}^{-2}.\text{s}^{-1}\right] = -D_A\left[\text{m}^2.\text{s}^{-1}\right].\nabla C_A\left[\text{mol.m}^{-4}\right]$$

$$\text{Migration}\left[\text{mol}.\text{m}^{-2}.\text{s}^{-1}\right] = -z_A[-].\frac{D_A}{R.T}\left[\text{m}^2.\text{mol}.\text{s}^{-1}.J^{-1}\right].F\left[\text{C}.\text{mol}^{-1}\right].C_A\left[\text{mol}.\text{m}^{-3}\right].\nabla\varphi\left[\text{V}.\text{m}^{-1}\right]$$

$$\text{Convetion}\left[\text{mol}.\text{m}^{-2}.\text{s}^{-1}\right] = +u\left[\text{m}.\text{s}^{-1}\right].C_A\left[\text{mol}.\text{m}^{-3}\right]$$

Evidently, each of the transport components requires its own driving force: a concentration gradient for diffusion, an electrical potential gradient for migration and a velocity field for convection. Usually, in electrochemical experiments, an electrolyte is used, such that liquid phase electric potential gradients are negligible (Bard and Faulkner, 2001).

3.1.2. Kinetics in MET

With a realistic mass transfer environment in place, rate equations for localized substrate concentrations may be developed. In the work of Picioreanu and co-workers, a division is made between electrode kinetics and microbial kinetics. Mediator cycling at the electrode surface is implemented using the Butler-Volmer equation (Bard and Faulkner, 2001),

$$\text{M}_{\text{Red}} \underset{\text{k}_c}{\overset{\text{k}_a}{\rightleftharpoons}} \text{M}_{\text{Ox}} + \text{n}.\text{e}^-$$

$$j = n.F.\left(k_a.M_{Red} - k_c.M_{Ox}\right) \tag{3.1.2.–1}$$

$$k_a = k^{\circ}.\exp\left(+\alpha_a \frac{n.F}{R.T}.\left\{\left[\varphi_{electrode} - \varphi_{solution}\right] - E^{\circ}_{M_{Red}/M_{Ox}}\right\}\right) \tag{3.1.2.–2}$$

$$k_c = k^{\circ}.\exp\left(-\alpha_c \frac{n.F}{R.T}.\left\{\left[\varphi_{electrode} - \varphi_{solution}\right] - E^{\circ}_{M_{Red}/M_{Ox}}\right\}\right) \tag{3.1.2.–3}$$

It has to be noted this reaction is heterogeneous, meaning the apparently imbalanced electrons are donated/accepted by the electrode. Furthermore, it is also worth mentioning the two distinct driving forces for this reaction: chemical potential – the difference in the near-surface concentrations of M_{Red} and M_{Ox}; and electrical potential – the difference between the potential provided by the electrode, $\left[\varphi_{electrode} - \varphi_{solution}\right]$, or in other words, the change in electron potential when traversing the phase boundary, and the electrical potential required for mediator reduction when the chemical potential is null, also known as standard reduction potential. As such, equilibrium of electrode processes is only observed when both driving forces are null or cancel each other out, i.e. the net electrochemical

potential is null. Conversion of the heterogeneous current density ***j*** into homogeneous rates of consumption/production is straightforward if the surface area of the electrode is known.

Hyperbolic kinetics can be used to express microbial growth, specifically an extension of the single-limiting substrate Monod model (Monod, 1949) to two substrates: for anode, oxidized mediator as electron acceptor and a simultaneous organic electron donor and carbon source,

$$\mu = \mu_{max} \cdot \frac{S}{K_S + S} \cdot \frac{M_{Ox}}{K_{M_{Ox}} + M_{Ox}} \qquad (3.1.2.–4)$$

The conversion of growth rate into consumption/production of chemical species requires knowledge of the respective biomass yields. This is achieved using a thermodynamics-based method introduced by Heijnen and co-workers (Heijnen et al., 1992). Let us take methyl viologen as mediator and acetate as carbon source and electron donor. First, the net catabolic reaction is written as follows,

$$\text{Half-oxidation}: CH_3COO^-(aq) + 4\,H_2O(l) \longrightarrow 2\,HCO_3^-(aq) + 9\,H^+(aq) + 8\,e^-$$

$$\text{Half-reduction}: MV^{\bullet -}(aq) + e^- \longrightarrow MV^{2-}(aq)$$

$$\text{Net-catabolism}: CH_3COO^-(aq) + 4\,H_2O(l) + 8\,MV^{\bullet -}(aq) \longrightarrow 2\,HCO_3^-(aq) + 9\,H^+(aq) + 8\,MV^{2-}(aq)$$

From this chemical equation, the Gibbs energy of reaction $\Delta_r G_{cat}$ is calculated. For anabolism, assuming ammonium is the nitrogen source, from elemental balances to carbon, hydrogen, oxygen and nitrogen, and a charge balance (see 7.1.Stoichiometry for a detailed procedure),

$$\text{Anabolism}: 0.525\,CH_3COO^-(aq) + 0.2\,NH_4^+(aq) + 0.275\,H^+(aq) \longrightarrow CH_{1.8}O_{0.5}N_{0.2}(s) + 0.05\,HCO_3^-(aq) + 0.4\,H_2O(l)$$

This result shows how the oxidation of acetate to bicarbonate is the source of electrons for acetate reduction to biomass. From the anabolic chemical equation, the Gibbs energy of reaction $\Delta_r G_{an}$ is calculated, using reported values of $\Delta_f G^{\circ}_{biomass}$ (Heijnen et al., 1992). Furthermore, a third component is necessary to reflect the losses in the coupling of catabolism and anabolism, designated dissipation energy. For heterotrophic growth (Heijnen et al., 1992),

$$\Delta G_{diss} = -\left[200 + 18.\left(6 - \#C\right)^{1.8} + \exp\left\{\left(\left(3.8 - \gamma_C\right)^2\right)^{0.16}.\left(3.6 + 0.4\#C\right)\right\}\right] \quad (3.1.2.–5)$$

where ΔG_{diss} is in e.g. kJ.c-mol^{-1}, and ***#C*** is the number of carbon atoms in the carbon source and γ_c is the average degree of reduction of those atoms. ΔG_{diss} is always negative since it represents energy dissipated as heat. The metabolic factor f_{cat} can then be calculated,

$$f_{cat}.\Delta_r G_{cat} = -\left(\Delta_r G_{an} - \Delta G_{diss}\right) \quad (3.1.2.–6)$$

This parameter represents the number of times that the basic catabolic reaction must be repeated to sustain the biosynthesis of 1 C-mol of biomass. Once this factor is known, calculation of all biomass yields and thus conversion of growth rate into consumption/production of chemical species is straightforward.

3.2.DET Models

In MET, electrons are transported from electrode to cell by soluble redox shuttles, for which standard mass transfer equations apply. In DET however, since there is no agreement on the mechanism of long-range transfer, the problem of electron transport may be formulated in different ways. In 2.3.Long-range DET, two different formulations were presented: first, Ohm's law, thought to be the governing equation for electron transport in metal-like conduction; second, the equivalent electron diffusion coefficient proposed for superexchange, derived via the Laviron approach to space distributed redox modified electrodes, i.e. electrodes coated by a redox polymer or several layers of an adsorbed electroactive substance (Laviron, 1980; Laviron et al., 1980), or in this case, an EAB. The more superexchange oriented formulation of transport is compatible with the rate equations used in MET, while conduction-based electron transfer along the biofilm requires a different type of rate law.

3.2.1. DET according to Superexchange

When applied to biofilms, the Laviron method for enzyme electrochemistry may be re-formulated as follows: consider a biofilm on a surface at position x=0, growing along the **x** axis. In each infinitesimal layer there are oxidized and reduced redox moieties – e.g. cytochromes – at concentrations C_{Ox} and C_{Red}, expressed in e.g. mol.m^{-3}. The flux of electrons at height x along the **x** axis may be expressed as,

$$J_e\big|_x = -k_e.C_{Red}\big|_{x+dx}.C_{Ox}\big|_x + k_e.C_{Ox}\big|_{x+dx}.C_{Red}\big|_x \qquad (3.2.1.–1)$$

where $\boldsymbol{k_e}$ is the heterogeneous bimolecular rate constant of electron exchange between C_{Ox} and C_{Red} in adjacent layers, in e.g. $m^4.mol^{-1}.s^{-1}$. This rate constant is heterogeneous since, in pure electron hopping, electron exchange reactions occur between unmixable layers of redox moieties. Given this formula refers to flux along **x**, a negative sign is assigned to the transfer of electrons towards the surface. If the concentration of redox moieties is constant throughout the film,

$$C_T\big|_{x+dx} = C_{Red}\big|_{x+dx} + C_{Ox}\big|_{x+dx} = C_T\big|_x = C_{Red}\big|_x + C_{Ox}\big|_x = C_T \qquad (3.2.1.–2)$$

$$\Rightarrow J_e\big|_x = -k_e.C_T.\left(C_{Red}\big|_{x+dx} - C_{Red}\big|_x\right) \qquad (3.2.1.–3)$$

$$\Rightarrow J_e\big|_x = -k_e.C_T.dx.\frac{dC_{Red}}{dx} \qquad (3.2.1.–4)$$

This result is analogous to Fick's first law of diffusion, with diffusion coefficient $D_e = k_e.C_T.dx$. The derivation procedure here presented is different from the one used by Savéant (Savéant, 1986) as discussed in **2.3.Long-range DET**, but the result is the same: electron transport by hopping is mathematically equivalent to diffusion. Equations such as Butler-Volmer for electrode kinetics and Monod for microbial kinetics can be used together with this transport formalism: once electron transport is shown to be equivalent to redox moiety diffusion, DET can be modelled in much the same way as MET (Richter et al., 2009; Strycharz et al., 2011; Strycharz-Glaven et al., 2012). However, this approach fails to produce insights into the mechanics of direct electron transfer.

3.2.2. DET according to Metal-like Conduction

Two main approaches have been proposed so far: the Nernst-Monod model and the Butler-Volmer-Monod model. The equations presented in the following two chapters are faithful reproductions of cited publications, including possible errors and inconsistencies.

3.2.2.1. Nernst-Monod Model

Should electron transport be modelled according to the metal-like conduction hypothesis, that is using Ohm's law, electrons reach/leave the cell at a certain electrical potential, which is the *de facto* substrate for catabolism. Marcus and co-workers literally implemented this concept in the development of the Nernst-Monod model for bioanodes (Marcus et al., 2007; Torres et al., 2008; Lee et al., 2009).

The crux of the Nernst-Monod model is the relation between concentrations of a redox pair and its reduction potential, expressed by the Nernst equation,

$$E_{Red/Ox} = E^{\circ}_{Red/Ox} - \frac{R.T}{n.F}.\ln\left(\frac{C_{Red}}{C_{Ox}}\right) \qquad (3.2.2.1.–1)$$

Let us consider an electron acceptor **A** and define the respective microbial half-saturation constant for the oxidized form $K_{A_{Ox}}$. Further, let's define a half-saturation reduction potential $E_{K_{A_{Ox}}}$. Marcus and co-workers write the Nernst equation using a reference concentration instead of reduced acceptor,

$$\begin{cases} E_{A_{Ox}} = E^{\circ}_{A_{Red}/A_{Ox}} - \frac{R.T}{n.F}.\ln\left(\frac{A^{\circ}_{Ox}}{A_{Ox}}\right) \\ E_{K_{A_{Ox}}} = E^{\circ}_{A_{Red}/A_{Ox}} - \frac{R.T}{n.F}.\ln\left(\frac{A^{\circ}_{Ox}}{K_{A_{Ox}}}\right) \end{cases} \Leftrightarrow \begin{cases} A_{Ox} = A^{\circ}_{Ox}.\exp\left(\frac{n.F}{R.T}.\left[E_{A_{Ox}} - E^{\circ}_{A_{Red}/A_{Ox}}\right]\right) \\ K_{A_{Ox}} = A^{\circ}_{Ox}.\exp\left(\frac{n.F}{R.T}.\left[E_{K_{A_{Ox}}} - E^{\circ}_{A_{Red}/A_{Ox}}\right]\right) \end{cases} \qquad (3.2.2.1.–2)$$

Now let's consider a Monod law for growth limited by a reduced donor and an oxidized acceptor,

$$\mu = \mu_{max}.\frac{D_{Red}}{K_{D_{Red}} + D_{Red}}.\frac{A_{Ox}}{K_{A_{Ox}} + A_{Ox}} \qquad (3.2.2.1.–3)$$

and define relations between the derived reduction potentials and the respective biofilm conductive matrix potentials – the authors specifically assume the half-saturation potential is null,

$$\varphi_{matrix} = E_{A_{Ox}} \qquad (3.2.2.1.–4)$$

$$\varphi_{K_{matrix}} = E_{K_{A_{Ox}}} = 0 \qquad (3.2.2.1.–5)$$

Substituting and rearranging yields the Nernst-Monod equation,

$$\mu = \mu_{max} . \frac{D_{Red}}{K_{D_{Red}} + D_{Red}} . \frac{1}{1 + \exp\left(-\frac{n.F}{R.T} . \varphi_{matrix} \right)} \qquad (3.2.2.1.–6)$$

Essentially, conversion of substrate concentrations into reduction potentials using the Nernst equation is equivalent to converting hyperbolic into sigmoid kinetics (Figure 6). Using the derived microbial kinetics and further considering electrons produced by endogenous respiration, the rate at which electrons are transferred to the conductive matrix may be expressed as follows,

$$-\frac{d}{dx} i_{matrix} = n_{Donor} . F . \frac{oxidized\_donor}{total\_consumed\_donor} . \frac{\mu . X}{Y_{X/Donor}} + n_X . F . q_{decay} . X \qquad (3.2.2.1.–7)$$

where n_{Donor} is the number of electrons transferred per oxidized donor molecule, and n_X is the number of electrons transferred per unit biomass oxidized in endogenous respiration, e.g. mol of e^- / C-mol. The electron donor is assumed to be organic, and since some of it will be reduced for biosynthesis, only the fraction of oxidized donor is accounted for in electrons transferred to matrix – that is, coulombic efficiency must be accounted for.

This result may be further combined with Ohm's law, yielding a differential equation for simultaneous conduction and heterogeneous transfer of electrons,

$$\sigma_{matrix} . \frac{d^2}{dx^2} \varphi_{matrix} = n_{Donor} . F . \frac{oxidized\_donor}{total\_consumed\_donor} . \frac{\mu . X}{Y_{X/Donor}} + n_X . F . q_{decay} . X \qquad (3.2.2.1.–8)$$

a Poisson's equation whose solution yields the electrical potential profile in the biofilm matrix, and through Ohm's law the current density profile.

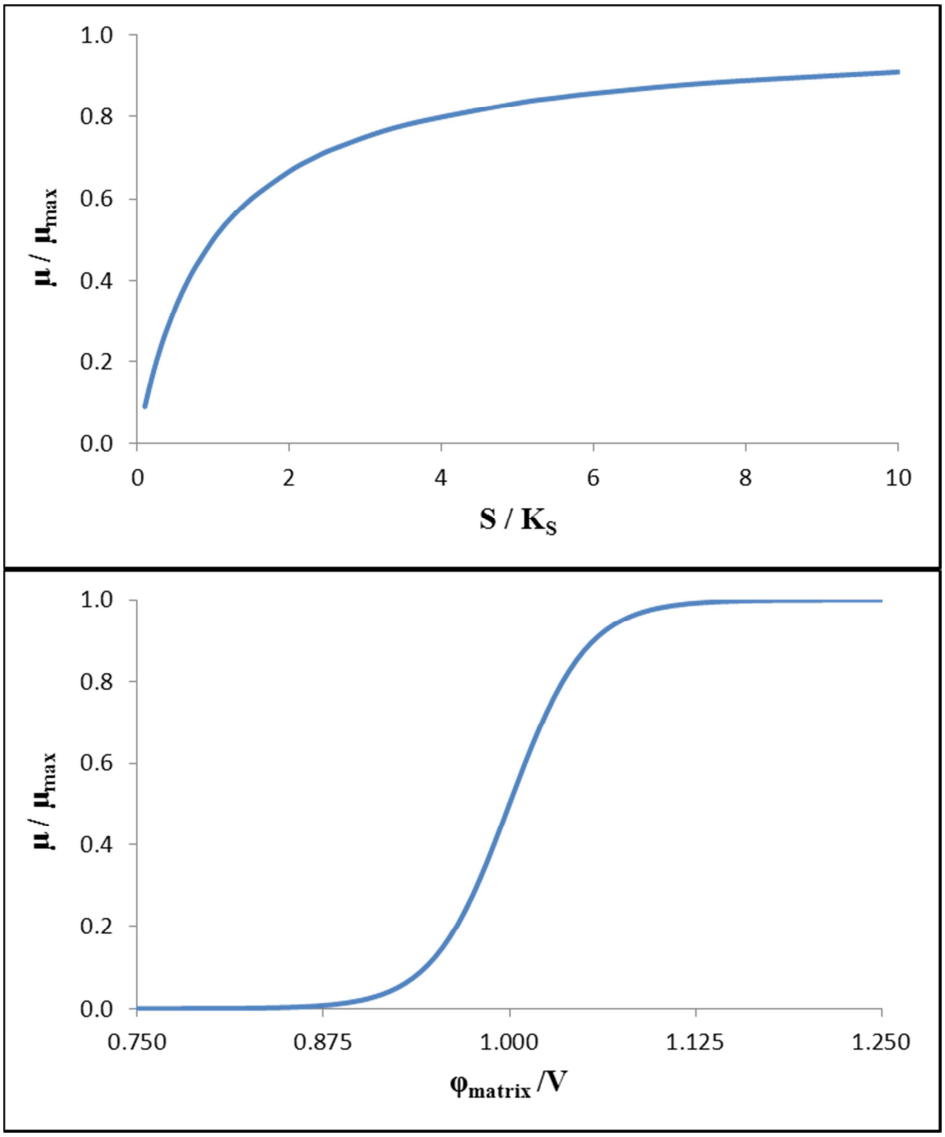

Figure 6 - Standard Monod kinetics (top) *vs.* its Nernst-Monod counterpart (bottom) for a single substrate scenario. Conversion of substrate concentrations into reduction potentials as performed by Marcus and co-workers effectively means converting hyperbolic into sigmoid kinetics (Marcus et al., 2007).

3.2.2.2. Butler-Volmer-Monod Model

Although the Butler-Volmer-Monod model developed by Hamelers and co-workers (Hamelers et al., 2011; Stein et al., 2011) is not explicitly a conduction-based model, it is formulated for cells touching an electrode at $\varphi_{electrode}$, whereas in conduction based DET cells are in contact with a matrix at φ_{matrix}. The same kinetics formalism applies to both cases. Additionally, at the electrode surface, $\varphi_{matrix}\big|_{x=0} = \varphi_{electrode}$, meaning the Butler-

Volmer-Monod model can be applied to any point in the biofilm, since the electrode surface is a specific location in that matrix.

The Butler-Volmer-Monod model exploits the concept of biomass redox state applied to anodic processes: upon contact with an anode, an unspecified biomass component, previously reduced by a chemical electron donor, transfers its valence electrons to the anode, becoming oxidized in the process (Hamelers et al., 2011). The oxidized component is then free to interact with another donor molecule, resetting the cycle (Figure 7).

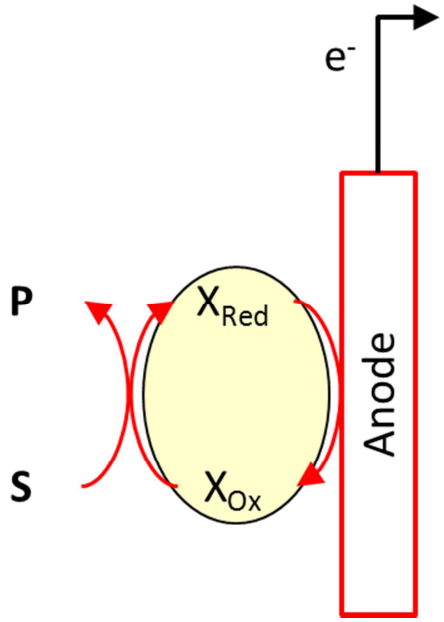

Figure 7 - Conceptual basis for the Butler-Volmer-Monod model. A reduced electron donor **S** interacts with an oxidized biomass redox intermediate $\mathbf{X_{Ox}}$, becoming oxidized to product **P**. The now reduced biomass intermediate $\mathbf{X_{Red}}$ will then transfer the electrons it received onto the anode.

The following chemical equations apply,

$$S + X_{Ox} \underset{k_2}{\overset{k_1}{\rightleftarrows}} X_C \underset{k_4}{\overset{k_3}{\rightleftarrows}} P + X_{Red}$$

$$X_{Red} \underset{k_6}{\overset{k_5}{\rightleftarrows}} X_{Ox} + e^-$$

where the heterogeneous rate coefficients k_5 and k_6 bare their usual meanings, according to the Butler-Volmer equation. As formulated by the authors,

$$j = n.F.\left(k_5.X_{Red} - k_6.X_{Ox}\right) \qquad (3.2.2.2.–1)$$

$$k_5 = k^{\circ}.\exp\left(+\alpha_a \frac{F}{R.T}.\left\{\varphi_{electrode} - E^{\circ}_{X_{Red}/X_{Ox}}\right\}\right) \quad (3.2.2.2.–2)$$

$$k_c = k^{\circ}.\exp\left(-\alpha_c \frac{F}{R.T}.\left\{\varphi_{electrode} - E^{\circ}_{X_{Red}/X_{Ox}}\right\}\right) \quad (3.2.2.2.–3)$$

Hamelers and co-workers also assumed quasi-steady-state, meaning the concentrations of intermediate biocatalyst forms do not change over time. The following differential balances for X_{Ox} and X_{Red} are written, alongside a mass balance to the biocatalyst

$$\frac{d}{dt}X_{Ox} : 0 = -k_1.S.X_{Ox} + k_2.X_C + \left(k_5.X_{Red} - k_6.X_{Ox}\right) \quad (3.2.2.2.–4)$$

$$\frac{d}{dt}X_{Red} : 0 = +k_3.X_C - k_4.P.X_{Red} - \left(k_5.X_{Red} - k_6.X_{Ox}\right) \quad (3.2.2.2.–5)$$

$$X_T = X_{Ox} + X_{Red} + X_C \quad (3.2.2.2.–6)$$

The method used by the authors requires substitution of X_{Ox} and X_{Red} in the Butler-Volmer formula, and if possible elimination of the rate constants k_1 through k_4. Using a definition of half-saturation constant analogous to that of Michaelis-Menten enzyme kinetics (Johnson and Goody, 2011), substrate affinity and product inhibition are defined,

$$K_S = \frac{k_2 + k_3}{k_1} \quad (3.2.2.2.–7)$$

$$K_P = \frac{k_2 + k_3}{k_4} \quad (3.2.2.2.–8)$$

Furthermore, by assuming microbial kinetics is limiting in the overall anode performance, Hamelers and co-workers define a maximum current density when all biomass is about to generate reduced intermediate,

$$j_{max} = n.F.k_3.X_T \quad (3.2.2.2.–9)$$

which in turn will transfer electrons to the anode, thus producing maximal anodic current. Also, the exchange current density is also defined, assuming the system will be at equilibrium when the electrode potential equals the reduction potential of the electron donor pair,

$$at\ \ equilibrium: \varphi_{electrode} = E_{S/P} \tag{3.2.2.2.–10}$$

$$\Rightarrow j_0 = n.F.k^{\circ}.X_T.\exp\left(+\alpha_a \frac{n.F}{R.T}.\left\{E_{S/P} - E^{\circ}_{X_{Red}/X_{Ox}}\right\}\right) \tag{3.2.2.2.–11}$$

Lastly, overpotential is defined as deviation from the equilibrium condition,

$$\eta = \varphi_{electrode} - E_{S/P} \tag{3.2.2.2.–12}$$

Combining all definitions with the differential balances to biomass redox intermediates yields the Butler-Volmer-Monod equation,

$$j = j_{max}.\frac{1-\exp\left(-\frac{F}{R.T}.\eta\right)}{K_1.\exp\left(-\alpha_a.\frac{F}{R.T}.\eta\right)+K_2.\exp\left(-\frac{F}{R.T}.\eta\right)+\left(\frac{K_S}{S}+1\right)} \tag{3.2.2.2.–13}$$

with parameters K_1 and K_2 defined as,

$$K_1 = \frac{j_{max}}{j_0}.\left(1+P.\frac{k_3}{k_4}+\exp\left(+\frac{F}{R.T}.\left\{E_{S/P} - E^{\circ}_{X_{Red}/X_{Ox}}\right\}\right)\right) \tag{3.2.2.2.–14}$$

$$K_2 = \frac{k_3}{k_2}.\left(1+\frac{K_P}{P}\right) \tag{3.2.2.2.–15}$$

Figure 8 provides a kinetic outlook on the properties of this result. Unlike the Nernst-Monod model, where substrate dependence is hyperbolic and potential dependence is sigmoidal, in the Butler-Volmer Monod model, the opposite is observed. For electrical potential, this could be because the model only applies to overpotentials above zero: extension into the negative range would reveal a more hyperbolic curvature. As for substrate, this can assigned to the fact that parameter K_1 includes the reduction potential of the substrate/product pair, and thus substrate concentrations indirectly change one of the parameters even if product concentrations are kept constant.

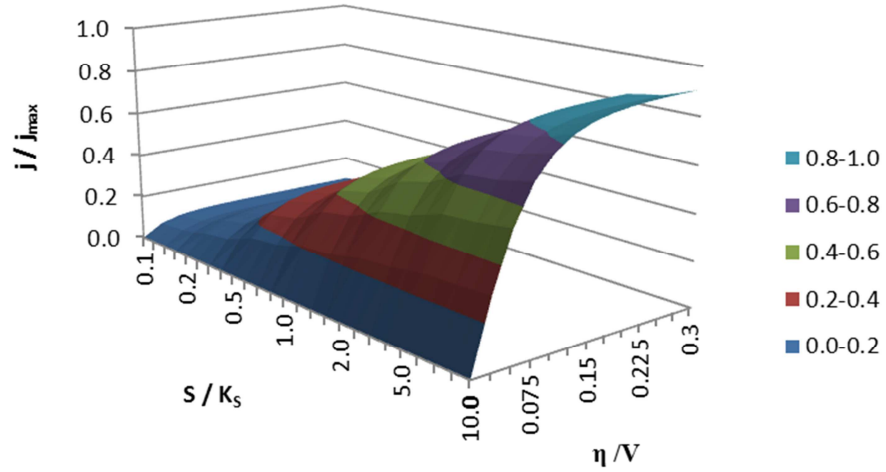

Figure 8 - Butler-Volmer-Monod model for $K_1=K_2=1$ and $\alpha_a=0.5$. The model is sigmoidal in substrate concentration and hyperbolic in overpotential, contrary to the Nernst-Monod model (see Figure 6).

The Butler-Volmer-Monod model is exclusively catabolic and the authors do not speculate about ways to incorporate growth into their model (Hamelers et al., 2011), although they have attempted to extend the model to inhibition scenarios (Stein et al., 2011).

3.3.Shortcomings of Existing Models

At the start of this state-of-the-art review, the lack of thermodynamics based approaches and reversible rate equations was mentioned, and later verified in the review itself. On the subject, it should be said the Butler-Volmer model of electrode kinetics is both reversible and thermodynamics based, at least in its basic one-step, one-electron derivation (Bard and Faulkner, 2001). However, the Monod based approaches to microbial kinetics, both in the work of Picioreanu and co-workers and the Nernst-Monod model are intrinsically incompatible with reversible microbial metabolic pathways and thus rates. One could in fact say that thermodynamics and reversibility are complementary in the sense that the concept of equilibrium is central to both.

But why are reversible microbial rates necessary if they are only relevant in near equilibrium conditions? Certainly in nature life attempts to evolve towards the exploitation of far-from-equilibrium reactions, so that energy sources will last longer at high yields. Also, in the fermentation industry, where the desired product is often biomass or another growth associated product, conditions are strongly shifted away from equilibrium to increase productivity. However, in bioelectrochemical systems, it is advantageous to operate close to equilibrium. In microbial fuel cells, if the anodic and cathodic biofilms are

at near equilibrium conditions, then the fraction of energy they retain is minimal, thus maximizing the energy available at the external circuit. Also, in microbial electrosynthesis cells, if the biofilms are near equilibrium, then the energy retained by bacteria is minimal, meaning the power supplied by the external source is almost fully committed to the synthesis itself. In BESs it is thus advantageous to spend as little energy as possible on bioelectrocatalyst sustenance.

Of course the same could be said of non-growth associated fermentation products. However, such products are often highly valuable, e.g. pharmaceuticals, meaning a tight management of substrate allocation is not important and not necessary for industrial applications. Also, considering the disproportionally high costs of purification for such products, substrate management becomes almost completely irrelevant from an economics perspective. *What about BESs?* Bioelectrochemical systems are often envisioned with one of two purposes in mind: 1. Microbial fuel cells to produce electricity from wastewater; 2. Microbial electrosynthesis cells to produce value-added compounds such as hydrogen from e.g. renewable electricity. Unlike fine chemicals, these are the sort of mass energy production applications that must operate with high efficiency, therefore the thermodynamics of bioelectrocatalytic biofilms should be kept close to equilibrium. Furthermore, this isn't the type of equilibrium where growth is arrest due to lack of substrate, but rather due to the low energy yield of an abundant substrate, such that high catabolic turnovers and near zero growth coexist.

Bioelectrochemical systems are not only unique in the – dare I say – need to operate the biological component at near equilibrium conditions, but also on the ease with which this might be achieved: simply poise electrode potentials as needed. Tight control of residence times, substrate or product concentrations would not be necessary, although of course, backup control loops for those variables should be in place.

The chemical equations proposed in the Butler-Volmer-Monod model are a good way to approach the problem of reversibility in DET. Nonetheless, when defining maximal and exchange current densities, Hamelers and co-workers (Hamelers et al., 2011) opted for an anodic viewpoint that compromises the reversibility of the final result, i.e. a minimal (negative) cathodic current density might have also been defined,

$$\begin{cases} anodic: j_{max} = n.F.k_3.X_T \\ cathodic: j_{nim} = -n.F.k_2.X_T \end{cases} \qquad (3.3.–1)$$

and the exchange current density, according to their definition (Hamelers et al., 2011), could have also been written from a cathodic perspective,

$$\begin{cases} anodic: j_0 = n.F.k^{\circ}.X_T.\exp\left(+\alpha_a \dfrac{n.F}{R.T}.\left\{E_{S/P} - E^{\circ}_{X_{Red}/X_{Ox}}\right\}\right) \\ cathodic: j_0 = n.F.k^{\circ}.X_T.\exp\left(-\alpha_c \dfrac{n.F}{R.T}.\left\{E_{S/P} - E^{\circ}_{X_{Red}/X_{Ox}}\right\}\right) \end{cases} \quad (3.3.–2)$$

Thus, concerning direct electron transfer, this dissertation will build on the approach brought forth by Hamelers and co-workers, and attempt to, in the most rigorous way possible, establish a truly reversible system of rate equations. As for mediated electron transfer, a completely new approach to the problem, inspired by Ping-Pong enzyme kinetics for two substrates and two products (Cleland, 1963), will be formulated.

4. Conceptualization of Respiratory Reversibility

The problem of EAB reversibility is essentially a matter of respiratory reversibility, since the cellular entry/exit points for electrons in cathodic/anodic EET are outer-membrane cytochromes, which communicate with cytoplasmic membrane electron transport chains (ETCs) via periplasmic intermediates, e.g. the MtrABC-OmcA system in *Shewanella oneidensis* (Carmona-Martínez et al., 2011; Richter et al., 2012). Thus, to understand EET reversibility, there is a need to envision how ETCs behave near equilibrium conditions.

4.1. The Meaning of *Donor* and *Acceptor*

Take for instance the omnipresent respiratory electron acceptor oxygen. In today's atmosphere, oxygen partial pressures are such that in nearly all redox reactions that it participates, oxygen is the oxidant, or as a microbiologist would put it, the terminal electron acceptor. If we write its half-reduction reaction,

$$O_2(g) + 4.H^+(aq) + 4.e^- \underset{\text{Oxidation}}{\overset{\text{Reduction}}{\rightleftharpoons}} 2.H_2O(l)$$

And calculate its reduction potential in the conditions most often found in nature,

$\text{pH} = 7$

$T = 298.15\,\text{K}$

$pO_2 = 0.21\,\text{bar}$ (atmospheric)

$E^{o}_{H_2O/O_2} = +1.23\,\text{V}$ (Rabaey et al., 2010)

$$\Rightarrow E_{H_2O/O_2} = E^{o}_{H_2O/O_2} - \frac{R.T}{4.F}.\ln\left(\frac{1}{pO_2.\left[H^+\right]^4}\right) = +0.81\,\text{V}$$

The resulting reduction potential is high enough to oxidize most organic compounds used by microorganisms in nature, in all the usable concentration ranges. This is perhaps why designations such as *donor* and *acceptor* are strongly associated with certain chemical species in microbiology. However, thermodynamics tells us that reduction potentials are relative measures of the tendency to undergo reduction: we need only look at the Nernst equation to conclude that,

$pO_2 \to 0$

$\Rightarrow E_{H_2O/O_2} = -\infty$

meaning that, from a thermodynamics perspective, if there is no oxygen available, in theory water could be a perfectly viable electron donor. Even if there is oxygen at atmospheric pressures, it is possible to use an external energy source to drive the otherwise unspontaneous water oxidation, such as sunlight in photosynthesis (Nelson and Cox, 2009).

Biological systems can thus perform the exact same half-reaction, in the exact same environmental conditions, in both forward and reverse directions, with one of the redox pairs that is normally farther away from equilibrium. Therefore, the designations *donor* and *acceptor* should perhaps be interpreted as relative to a certain *acceptor* and *donor*, respectively. However, since sunlight is required in photosynthesis, one could argue that unless there is a redox pair that can spontaneously be *donor* or *acceptor*, then this is merely a chemical concept with no biological relevance. Let us consider the redox pair succinate/fumarate,

$$\mathrm{Fumarate^{2-}(aq) + 2.H^{+}(aq) + 2.e^{-} \underset{\text{Oxidation}}{\overset{\text{Reduction}}{\rightleftharpoons}} Succinate^{2-}(aq)}$$

whose standard biochemical reduction potential is $E^{o'} = +0.03\,V$ (Madigan et al., 1999). For the model organism *Escherichia coli*, if oxygen is available, succinate is a potential donor (Condon et al., 1985), as expected for most organic compounds *vs.* O_2. However, if favourable acceptors such as oxygen or nitrate are absent, fumarate is a potential acceptor (Iverson et al., 1999). In fact the respiratory entry-point from succinate, succinate dehydrogenase, and the respiratory exit-point into fumarate, fumarate reductase, are not only functionally but also structurally very similar (Cecchini et al., 2002). Of course, succinate dehydrogenase has better affinity for the reduced species of the pair and fumarate reductase for the oxidized chemical, but still, macroscopically, affinities are kinetic properties, and thus not relevant from the perspective of thermodynamical reversibility: whether inversion of catabolism is fast or slow is of no concern to the present argument.

4.2. Respiratory Reversibility

Generalization of the succinate/fumarate case produces the conceptual model depicted in Figure 9. Thermodynamically, which redox pair is the donor and which is the acceptor will depend on their relative reduction potentials. Kinetically, the affinity of the first ETC transporter – entry-point – for the reduced species of each pair and the affinity of the last ETC transporter – exit-point – for the respective oxidized species determines how fast the forward and reverse reactions proceed. Naturally, combinations of affinity values that would violate thermodynamic spontaneity are impossible, which immediately hints at a relation between kinetics and thermodynamics: maximum rates must be thermodynamically definable.

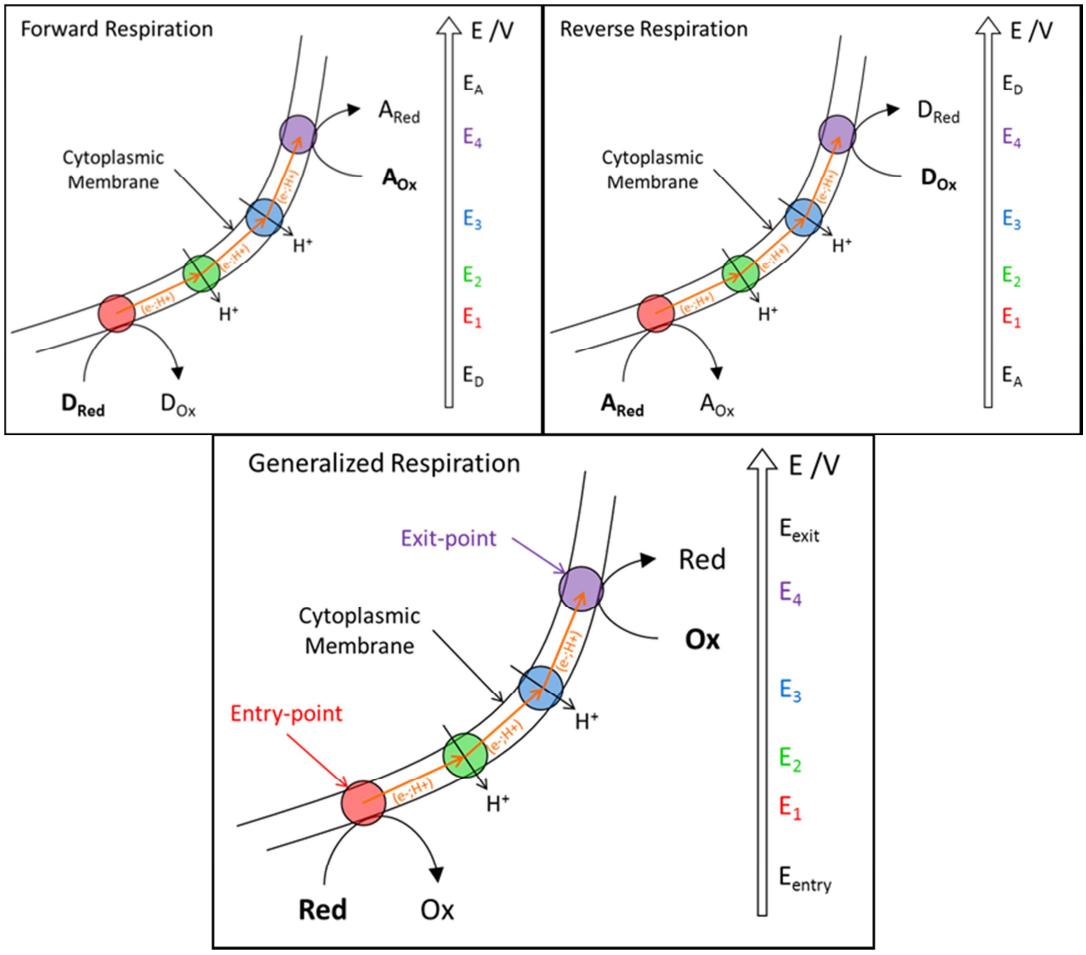

Figure 9 - Conceptualization of respiratory reversibility. In **Forward Respiration**, a reduced compound D_{Red} acts as donor and an oxidized compound A_{Ox} acts as acceptor. However, if the reduction potentials of the D and A redox pairs change in such a way that A_{Red} in now able to donate electrons and D_{Ox} is able to accept electrons, **Reverse Respiration** occurs. Thus, the designations *donor* and *acceptor* are an indicator of thermodynamic spontaneity and are not an intrinsic property of chemical species. Instead of *donor* one could use *reductant* and instead of *acceptor* one could use *oxidant*. Therefore, given two redox pairs, which is the donor and which is the acceptor depends on their reduction potentials only. How fast electron transport chains can execute either forward or reverse respiration depends on: 1. entry-point affinities for the reduced species in each redox pair; 2. exit-point affinities for the oxidized species in each redox pair; 3. how far is the reaction from equilibrium.

Although thermodynamic reversibility is always theoretically possible, there are instances where the gap in reduction potential between donor and acceptor is so large that, in practice, catabolic inversion will never occur. This is the case for aerobic oxidation of organics. However, in energy poor catabolic systems, such as many instances of anaerobic respiration, the gap in reduction potential is less significant. Bioelectrochemical systems,

which energy-wise are similar to anaerobic environments – and being operated anaerobically themselves, expect for ORR bioelectrocatalysis – are the sort of medium where the difference in reduction potential between donor/acceptor and anode/cathode is manipulated to be as small as possible, therefore creating the ideal context for practical catabolic reversibility.

4.3.A Generalized Notation

Development of applicable general rate equations can be quite troublesome – and potentially not useful for practical applications – without a method to quickly convert abstract representations such as D_{Red} for reduced donor or A_{Ox} for oxidized acceptor, into concentrations or partial pressures of real chemical species in real reactions. Let us consider a general substrate **S** and its half-reduction reaction,

$$S_{Ox} + n.e^- \underset{k_r}{\overset{k_f}{\rightleftharpoons}} S_{Red}$$

which would read as "idealized compound $\mathbf{S_{Ox}}$ is reduced by a certain number of electron **n** into its reduced counterpart $\mathbf{S_{Red}}$". Using the homogeneous rate constants k_f and k_r, the rate equation reads as,

$$r = k_f.S_{Ox} - k_r.S_{Red} \qquad (4.3.–1)$$

The chemical equilibrium for this (half-)reaction can also be written in a similar way,

$$K_{eq} = \frac{k_f}{k_r} = \frac{S_{Red}}{S_{Ox}} \qquad (4.3.–2)$$

To avoid clutter, when working with idealized species, the concentration brackets [A] are not utilized. Since the example is a redox (half-)reaction, we may also write the respective Nernst equation,

$$E_{S_{Red}/S_{Ox}} = E^{\circ}_{S_{Red}/S_{Ox}} - \frac{R.T}{n.F}.\ln\left(\frac{S_{Red}}{S_{Ox}}\right) \qquad (4.3.–3)$$

We could continue with other thermodynamic or kinetic formula. This notation is very powerful since it greatly simplifies a large number of procedures common in Physical Chemistry. As for conversion of idealized into real species, S_{Red} should be the multiplicand of concentrations or partial pressures of those, respectively, solutes and gases that appear

on the right-hand side of the half-reduction reaction, elevated to their stoichiometric coefficients. S_{Ox} has equivalent meaning for the left-hand side of the same reaction, while liquids and solids of constant activity are represented by **1** in the multiplicands.

Furthermore, redox pairs may be designated by **S** for (external) substrate, **A** for acceptor, **D** for donor or **M** for mediator, depending on the intended usage.

4.3.1. Example 1: Oxygen Reduction Reaction

For instance, consider the microbially catalysed ORR reaction,

$$\mathrm{O_2(g) + 4.H^+(aq) + 4.e^- \underset{k_r}{\overset{k_f}{\rightleftharpoons}} 2.H_2O(l)}$$

and write down the conversion rules for an idealized acceptor **A**, the usual role of oxygen in biological systems,

$$\begin{cases} A_{Red} = 1 \\ A_{Ox} = pO_2.\left[H^+\right]^4 \end{cases} \tag{4.3.1.–1}$$

Verifying the rate equation, equilibrium constant and Nernst equation,

$$r = k_f.A_{Ox} - k_r.A_{Red} \Leftrightarrow r = k_f.pO_2.\left[H^+\right]^4 - k_r \tag{4.3.1.–2}$$

$$K_{eq} = \frac{A_{Red}}{A_{Ox}} \Leftrightarrow K_{eq} = \frac{1}{pO_2.\left[H^+\right]^4} \tag{4.3.1.–3}$$

$$\begin{aligned} & E_{A_{Red}/A_{Ox}} = E^\circ_{A_{Red}/A_{Ox}} - \frac{R.T}{n.F}.\ln\left(\frac{A_{Red}}{A_{Ox}}\right) \\ & \Leftrightarrow E_{H_2O/O_2} = E^\circ_{H_2O/O_2} - \frac{R.T}{4.F}.\ln\left(\frac{1}{pO_2.\left[H^+\right]^4}\right) \end{aligned} \tag{4.3.1.–4}$$

4.3.2. Example 2: The Succinate/Fumarate Pair

Another example would be the fumarate/succinate pair,

$$\mathrm{Fumarate^{2-}(aq) + 2.H^+(aq) + 2.e^- \underset{k_r}{\overset{k_f}{\rightleftharpoons}} Succinate^{2-}(aq)}$$

which may either be a donor or an acceptor in *E. coli* (Condon et al., 1985; Iverson et al., 1999), and is thus labelled as an idealized substrate **S**,

$$\begin{cases} S_{Red} = \left[Succinate^{2-} \right] \\ S_{Ox} = \left[Fumarate^{2-} \right].\left[H^{+} \right]^{2} \end{cases} \quad (4.3.2.–1)$$

Again, verification of the rate equation, equilibrium constant and Nernst equation yields,

$$\begin{aligned} & r = k_f.S_{Ox} - k_r.S_{Red} \\ & \Leftrightarrow r = k_f.\left[Fumarate^{2-} \right].\left[H^{+} \right]^{2} - k_r.\left[Succinate^{2-} \right] \end{aligned} \quad (4.3.2.–2)$$

$$K_{eq} = \frac{S_{Red}}{S_{Ox}} \Leftrightarrow K_{eq} = \frac{\left[Succinate^{2-} \right]}{\left[Fumarate^{2-} \right].\left[H^{+} \right]^{2}} \quad (4.3.2.–3)$$

$$\begin{aligned} & E_{S_{Red}/S_{Ox}} = E^{\circ}_{S_{Red}/S_{Ox}} - \frac{R.T}{n.F}.\ln\left(\frac{S_{Red}}{S_{Ox}} \right) \\ & \Leftrightarrow E_{Suc./Fum.} = E^{\circ}_{Suc./Fum.} - \frac{R.T}{2.F}.\ln\left(\frac{\left[Succinate^{2-} \right]}{\left[Fumarate^{2-} \right].\left[H^{+} \right]^{2}} \right) \end{aligned} \quad (4.3.2.–4)$$

4.3.3. Example 3: Flavin Mediators

A third example is the flavin-family compound riboflavin,

$$\mathrm{RF(aq) + 2.H^{+}(aq) + 2.e^{-} \underset{k_r}{\overset{k_f}{\rightleftharpoons}} RFH_2(aq)}$$

which is an endogenous mediator produced by *Shewanella oneidensis* (Marsili et al., 2008), and can thus be labelled as an idealized mediator **M**,

$$\begin{cases} M_{Red} = \left[RFH_2 \right] \\ M_{Ox} = \left[RF \right].\left[H^{+} \right]^{2} \end{cases} \quad (4.3.3.–1)$$

Writing down the rate equation, equilibrium constant and Nernst equation,

$$r = k_f.M_{Ox} - k_r.M_{Red} \Leftrightarrow r = k_f.[RF].\left[H^+\right]^2 - k_r.[RFH_2] \qquad (4.3.3.–2)$$

$$K_{eq} = \frac{M_{Red}}{M_{Ox}} \Leftrightarrow K_{eq} = \frac{[RFH_2]}{[RF].\left[H^+\right]^2} \qquad (4.3.3.–3)$$

$$E_{M_{Red}/M_{Ox}} = E^{\circ}_{M_{Red}/M_{Ox}} - \frac{R.T}{n.F}.\ln\left(\frac{M_{Red}}{M_{Ox}}\right)$$
$$\Leftrightarrow E_{RFH_2/RF} = E^{\circ}_{RFH_2/RF} - \frac{R.T}{2.F}.\ln\left(\frac{[RFH_2]}{[RF].\left[H^+\right]^2}\right) \qquad (4.3.3.–4)$$

5. Catabolic Rate of Mediated Electron Transfer

Kinetically, and from a catabolic perspective, MET is divided in two discrete operations: electrode kinetics and microbial kinetics. The two components are interconnected by an electron shuttle, termed redox mediator or just mediator. Thus, and taking the forward direction as cathodic, the sequence of events in MET may be summarized as follows,

$$M_{Ox} + n.e^- \underset{k_a}{\overset{k_c}{\rightleftharpoons}} M_{Red}$$

Diffusion of M_{Red} towards cells.

$$M_{Red} + X + n.H^+ \underset{k_{-1}}{\overset{k_1}{\rightleftharpoons}} X_M \underset{k_{-2}}{\overset{k_2}{\rightleftharpoons}} M_{Ox} + XH_n$$

$$S_{Ox} + XH_n \underset{k_{-3}}{\overset{k_3}{\rightleftharpoons}} X_S \underset{k_{-4}}{\overset{k_4}{\rightleftharpoons}} S_{Red} + X + n.H^+$$

The specificities of each chemical equation will be discussed in subsequent sections. Of course, the mediator may also diffuse back to the electrode once it has been oxidized, and the external substrate also needs to reach the cells. This derivation won't take into account transport phenomena: all concentrations herein implied are localized. For information on how to deal with the mass transfer sub-problem, refer to **3.1.1.Transport in MET**, or directly to the papers by Picioreanu and co-workers (Picioreanu et al., 2007; Picioreanu et al., 2008; Picioreanu et al., 2010a; Picioreanu et al., 2010b).

5.1.Electrode Kinetics in MET

Following the approach of Picioreanu and co-workers for mediator regeneration (Picioreanu et al., 2007; Picioreanu et al., 2008; Picioreanu et al., 2010a; Picioreanu et al., 2010b), the heterogeneous reaction at the electrode surface is modelled using Butler-Volmer kinetics,

$$j = n.F.\left(k_a.M_{Red} - k_c.M_{Ox}\right) \qquad (5.1.–1)$$

where $\boldsymbol{j}$ is heterogeneous current density, e.g. $A.m^{-2}$, and $\boldsymbol{k_a}$ and $\boldsymbol{k_c}$ are, respectively, the anodic and cathodic heterogeneous rate coefficients, which according to the Butler-Volmer model (Bard and Faulkner, 2001) are a function of electrode potential, such that,

$$k_a = k^\circ.\exp\left(+\alpha_a.\frac{n.F}{R.T}.\left\{\left[\varphi_{electrode} - \varphi_{solution}\right] - E^o_{M_{Red}/M_{Ox}}\right\}\right) \qquad (5.1.–2)$$

$$k_c = \frac{k^\circ}{\left(\left[H^+\right]^\circ\right)^m}.\exp\left(-\alpha_c.\frac{n.F}{R.T}.\left\{\left[\varphi_{electrode}-\varphi_{solution}\right]-E^o_{M_{Red}/M_{Ox}}\right\}\right) \qquad (5.1.–3)$$

where ***m*** is the stoichiometry coefficient for protons in the actual half-reduction reaction – which is zero should there be no protons involved – and $\left[\mathrm{H}^+\right]^o$ is a reference hydronium concentration.

5.1.1. Reference Hydronium Concentration

Understanding the purpose of a reference hydronium concentration in the formula for the cathodic heterogeneous rate coefficient requires knowledge of the typical mediator half-reduction reaction. Mediators are compounds that, upon reduction/oxidation, only accept/donate electrons and protons – most exogenous mediators are in fact members of the quinone family of organic compounds (McNaught and Wilkinson, 1997). A few examples of mediators include methyl viologen,

$$\mathrm{MV}^{2+}(\mathrm{aq}) + \mathrm{e}^- \underset{k_a}{\overset{k_c}{\rightleftharpoons}} \mathrm{MV}^{\bullet+}(\mathrm{aq})$$

anthraquinone-2,6-disulfonate,

$$\mathrm{AQDS}^{2-}(\mathrm{aq}) + 2.\mathrm{H}^+(\mathrm{aq}) + 2.\mathrm{e}^- \underset{k_a}{\overset{k_c}{\rightleftharpoons}} \mathrm{AQDSH}_2^{2-}(\mathrm{aq})$$

the endogenous mediator riboflavin,

$$\mathrm{RF}(\mathrm{aq}) + 2.\mathrm{H}^+(\mathrm{aq}) + 2.\mathrm{e}^- \underset{k_a}{\overset{k_c}{\rightleftharpoons}} \mathrm{RFH}_2(\mathrm{aq})$$

or even, should an hydrogenotrophic culture coexist with a cathode capable of abiotic HER, hydrogen,

$$2.\mathrm{H}^+(\mathrm{aq}) + 2.\mathrm{e}^- \underset{k_a}{\overset{k_c}{\rightleftharpoons}} \mathrm{H}_2(\mathrm{g})$$

Despite the fact that protons are often involved in such reactions – methyl-viologen is a good exception – studies of electrode kinetics are often performed at constant pH, and thus hydronium concentrations are ignored when fitting the Butler-Volmer (BV) model to results – here the HER is a good exception, since ignoring the only substrate wouldn't be

logical. Let us focus on riboflavin for a moment, and write the BV equation specifically for this mediator,

$$j = n.F.\left(k_a.\left[RFH_2\right] - k_c.\left[RF\right].\left[H^+\right]^2\right) \qquad (5.1.1.–1)$$

We see that, for variable hydronium concentrations, $\boldsymbol{k_c}$ would be a third order heterogeneous rate coefficient, with units e.g. $[m.s^{-1}].[m^3.mol^{-1}]^2$. Furthermore, since we can expect literature values of the standard heterogeneous rate constant $\boldsymbol{k°}$ to be reported at a certain reference pH, we must correct it when calculation $\boldsymbol{k_c}$ in order to maintain dimensional consistency. For clarity, let us substitute the rate coefficient formulas into the main BV equation, still with the example of riboflavin,

$$j = n.F.k^{\circ}.\left(+\left[RFH_2\right].\exp\left(+\alpha_a.\frac{n.F}{R.T}.\left\{\left[\varphi_{electr.} - \varphi_{sol.}\right] - E^{o}_{M_{Red}/M_{Ox}}\right\}\right) - \left[RF\right].\left(\frac{\left[H^+\right]}{\left[H^+\right]^{\circ}}\right)^2.\exp\left(-\alpha_c.\frac{n.F}{R.T}.\left\{\left[\varphi_{electr.} - \varphi_{sol.}\right] - E^{o}_{M_{Red}/M_{Ox}}\right\}\right)\right) \qquad (5.1.1.–2)$$

Thus, since $\boldsymbol{k°}$ is measured at a reference pH, we normalize hydronium concentrations. Of course, $\boldsymbol{k_a}$ is not affected, since protons are not a reagent in this anodic process.

5.1.2. Multi-proton | Multi-electron Mediators

On the topic of riboflavin as mediator, the fully oxidized **RF** and fully reduced **RFH_2** forms are not the only mediator states. Consider a two-proton, two-electron mediator, e.g. riboflavin or AQDS. The net half-reduction reaction may be represented as follows,

$$\mathrm{M(aq) + 2.H^+(aq) + 2.e^- \underset{k_a}{\overset{k_c}{\rightleftharpoons}} MH_2(aq)}$$

Theoretically (Jacq, 1971; Bard and Faulkner, 2001), this net reaction is a sequence of discrete one-proton and one-electron transfer steps. Furthermore, and due to *p*-orbital delocalization, quinone radicals may be stable (March, 1985). It is thus necessary to know if the existence of stable reaction intermediates invalidates the BV equations, originally derived for one-electron, one-step reactions (Bard and Faulkner, 2001). Specifically, it is important to know if the electrochemical driving force,

$$\left\{\left[\varphi_{electrode}-\varphi_{solution}\right]-E^{o}_{M_{Red}/M_{Ox}}\right\} \tag{5.1.2.–1}$$

is affected. Furthermore, since electrode potentials are not a function of mediator states, knowing if the electrochemical driving force is affected is a matter of understanding how the standard reduction potential of the net reaction relates to the standard reduction potentials and acid-base equilibrium constants of the individual one-proton, one-electron transfer steps.

The properties of two-proton, two-electron redox systems have been previously summarized as depicted in Figure 10 (Jacq, 1971; Batchelor-McAuley et al., 2010). Consider for instance pathway **1**, and write down the acid-base and redox equilibria,

$$pK_{a_1}=pH+\log_{10}\left(\frac{\left[MH^{+}\right]}{\left[M\right]}\right) \tag{5.1.2.–2}$$

$$pK_{a_4}=pH+\log_{10}\left(\frac{\left[MH_2^{2+}\right]}{\left[MH^{+}\right]}\right) \tag{5.1.2.–3}$$

$$E^{\circ}_{5}=\frac{R.T}{F}.\frac{1}{\log_{10}(e)}.\log_{10}\left(\frac{\left[MH_2^{\bullet+}\right]}{\left[MH_2^{2+}\right]}\right) \tag{5.1.2.–4}$$

$$E^{\circ}_{6}=\frac{R.T}{F}.\frac{1}{\log_{10}(e)}.\log_{10}\left(\frac{\left[MH_2\right]}{\left[MH_2^{\bullet+}\right]}\right) \tag{5.1.2.–5}$$

Summing and rearranging,

$$\begin{aligned}&\frac{R.T}{2.F}.\frac{1}{\log_{10}(e)}.\log_{10}\left(\frac{\left[MH_2\right]}{\left[M\right]}\right)\Bigg|_{1}\\&=\frac{E^{\circ}_{5}+E^{\circ}_{6}}{2}+\frac{R.T}{F}.\frac{1}{\log_{10}(e)}.\left(\frac{pK_{a_1}+pK_{a_4}}{2}-pH\right)\end{aligned} \tag{5.1.2.–6}$$

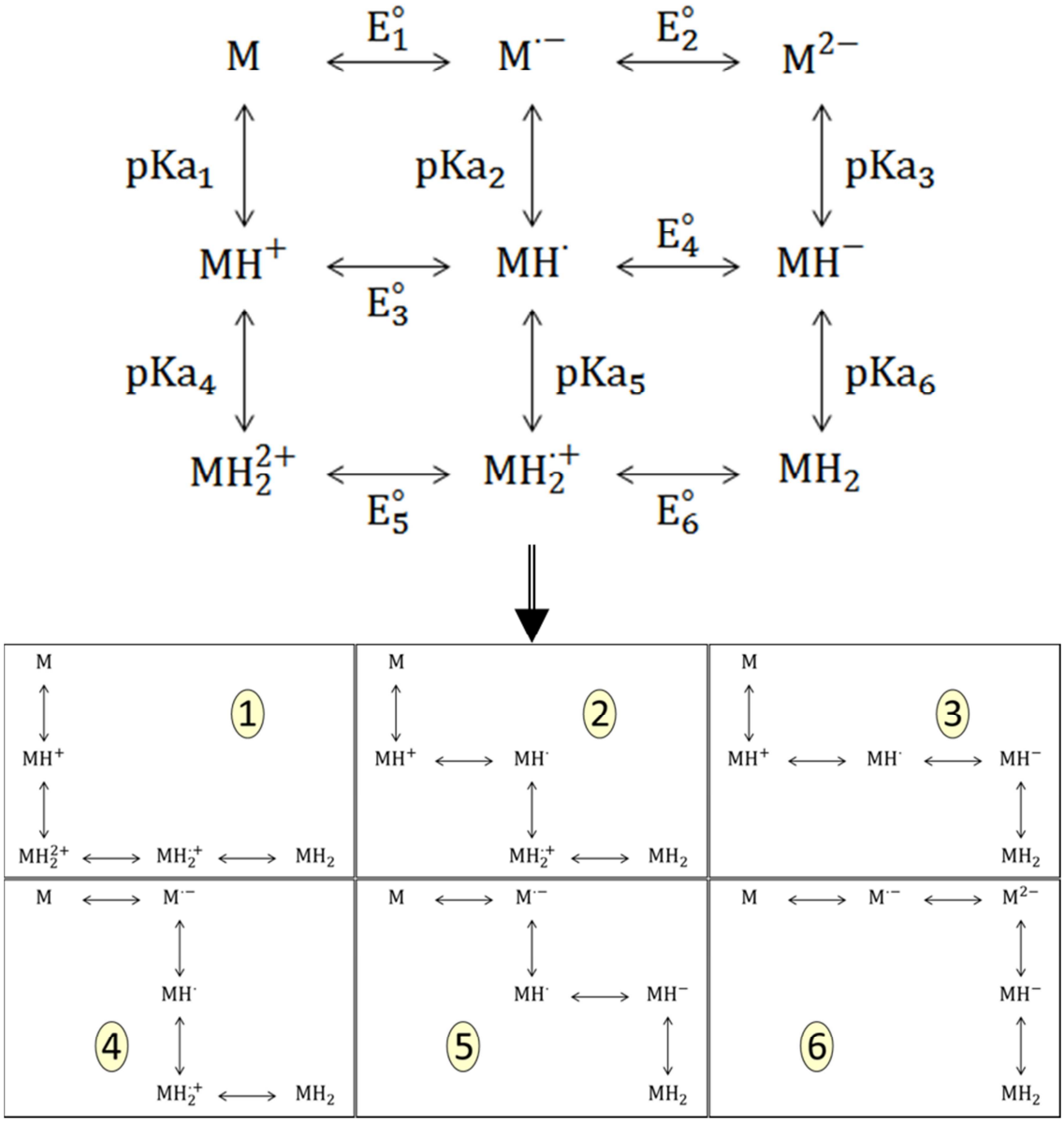

Figure 10 - Scheme of squares for two-proton, two-electron mediator **M**. Vertical steps represent acid-base equilibria while horizontal steps represent redox equilibria. The complete scheme is assumed to be in equilibrium, since its purpose is derivation of the net standard reduction potential. Top: Complete mapping of the redox system. Bottom: Possible pathways connecting the fully oxidized form **M** with the fully reduced form $\mathbf{MH_2}$.

The same procedure also applies to all other pathways, yielding equivalent results: for each pathway, the respective one-step standard reduction potentials and acidity constants will be represented. A simple average of the six pathways yields,

$$\frac{R.T}{2.F}.\frac{1}{\log_{10}(e)}.\log_{10}\left(\frac{[MH_2]}{[M]}\right)\Bigg|_m = E_m^\circ + \frac{R.T}{F}.\frac{1}{\log_{10}(e)}.\left(pK_{a_m} - pH\right) \qquad (5.1.2.–7)$$

with mean one-step properties E_m° and pK_{a_m} as follows,

$$E_m^\circ = \frac{3.E_1^\circ + 1.E_2^\circ + 2.E_3^\circ + 2.E_4^\circ + 1.E_5^\circ + 3.E_6^\circ}{12} \qquad (5.1.2.–8)$$

$$pK_{a_m} = \frac{3.pK_{a_1} + 2.pK_{a_2} + 1.pK_{a_3} + 1.pK_{a_4} + 2.pK_{a_5} + 3.pK_{a_6}}{12} \qquad (5.1.2.–9)$$

A simple average of pathways is thus equivalent to a weighted average of one-step reactions, since some of those steps are shared by multiple paths. Also, no weighting is necessary when calculating pathway averages, since the one-step standard reduction potentials and acidity constants are intrinsically weighing factors. On the other hand, if we write down the net redox equilibrium,

$$\begin{aligned} E_{MH_2/M}^\circ &= \frac{R.T}{2.F}.\ln\left(\frac{[MH_2]}{[M].[H^+]^2}\right) \\ &= \frac{R.T}{2.F}.\frac{1}{\log_{10}(e)}.\log_{10}\left(\frac{[MH_2]}{[M]}\right) + \frac{R.T}{F}.\frac{1}{\log_{10}(e)}.pH \end{aligned} \qquad (5.1.2.–10)$$

and substitute the mean result obtained from the scheme of squares,

$$E_{MH_2/M}^\circ = E_m^\circ + \frac{R.T}{F}.\frac{1}{\log_{10}(e)}.pK_{a_m} = constant \qquad (5.1.2.–11)$$

Thus, from a set of elementary one-step reactions, we demonstrate that variations in concentration of the seven intermediate forms for two-proton, two-electron mediators do not affect the electrochemical driving force in the BV model. Therefore, for computational purposes, the mediator can be solely represented by the fully oxidized **M** and fully reduced **MH_2** forms.

5.2.Microbial Kinetics in MET

As described in section 4.Conceptualization of Respiratory Reversibility, the entry-point and exit-point for electron transport chains are separate entities. Thus, and since electrons must be transferred from entry to exit before acceptor reduction can occur, respiratory chains oscillate between two stable states: oxidized, after acceptor reduction but before donor oxidation; reduced, after donor oxidation but before acceptor reduction. This mechanism closely resembles Ping-Pong enzyme kinetics, where the enzyme oscillates between stable states (Cleland, 1963). Furthermore, respiratory ubi- and menaquinones always take up electrons together with protons (Nelson and Cox, 2009), to preserve their hydrophobicity and thus remain embedded in the cytoplasmic membrane. Also, it has been recently demonstrated that the *c*-type cytochrome PpcA of *Geobacter sulfurreducens* also performs coordinated electron and proton transfer (Morgado et al., 2012). Thus, any representation of a biomass redox half-reaction would have to include an equal number of protons and electrons,

$$X + n.e^- + n.H^+ \underset{\text{Oxidation}}{\overset{\text{Reduction}}{\rightleftharpoons}} XH_n \Leftrightarrow XH_n \underset{\text{Reduction}}{\overset{\text{Oxidation}}{\rightleftharpoons}} X + n.e^- + n.H^+$$

Brackets will not be used when dealing with the concentration of biomass species, since they aren't actual chemical compounds. This biomass redox component would be best interpreted as an average representation of the pool of cellular redox intermediates. This pool includes, for instance, NADH/NAD^+, which is the prime internal donor/acceptor for metabolism, but also refers to membrane anchored redox intermediates, such as cytochromes and quinones, with their prominent roles in cellular respiration (Nelson and Cox, 2009). Although at first glance these are rather different entities, in truth all cellular redox systems are interconnected and in relative equilibrium, such that the cell can at any time call upon the pool of valence electrons distributed through all redox intermediates. Qualitatively, biomass redox state is thus how many valence electrons are available in this pool relative to its full capacity.

Let us also consider the half-oxidation of a mediator **M** and the half-reduction of an external substrate **S**,

$$M_{Red} \underset{\text{Reduction}}{\overset{\text{Oxidation}}{\rightleftharpoons}} M_{Ox} + n.e^-$$

$$S_{Ox} + n.e^- \underset{\text{Oxidation}}{\overset{\text{Reduction}}{\rightleftharpoons}} S_{Red}$$

Combining biomass half-reduction with mediator half-oxidation,

$$M_{Red} + X + n.H^+ \underset{k_{-1}}{\overset{k_1}{\rightleftharpoons}} X_M \underset{k_{-2}}{\overset{k_2}{\rightleftharpoons}} M_{Ox} + XH_n$$

where X_M is a transient complex of the two components. Similarly, combining biomass half-oxidation with external substrate half-reduction,

$$S_{Ox} + XH_n \underset{k_{-3}}{\overset{k_3}{\rightleftharpoons}} X_S \underset{k_{-4}}{\overset{k_4}{\rightleftharpoons}} S_{Red} + X + n.H^+$$

where X_S is also a transient complex.

5.2.1. Quasi-steady-state

Approaching this set of chemical equations from an enzyme kinetics perspective inevitably requires the classical quasi-steady-state assumption introduced by Briggs and Haldane (Briggs and Haldane, 1925), which would be formulated as follows,

Assumption: Quasi-steady-state.

$$\frac{d}{dt}X = \frac{d}{dt}X_M = \frac{d}{dt}XH_n = \frac{d}{dt}X_S = 0 \qquad (5.2.1.–1)$$

$$\Rightarrow \frac{d}{dt}X_T = 0 \wedge -\frac{d}{dt}M_{Red} = \frac{d}{dt}M_{Ox} = -\frac{d}{dt}S_{Ox} = \frac{d}{dt}S_{Red} \qquad (5.2.1.–2)$$

meaning the concentrations of intermediate biocatalyst forms don't change over time, which implies the preservation of overall biocatalyst concentration and equal turnovers for all substrates and products. From a practical perspective, this assumption could best be stated as follows: variations in the concentrations of intermediate biocatalyst forms are much slower than variations in substrate or product concentrations.

How can the application of this assumption to whole microorganisms – not just enzymes – be justified? Certainly for growing suspended cultures this is not remotely true. If growth means an increase in biomass concentration, it's impossible for all biomass intermediates to remain at a constant level. However, biofilms grow in volume, while preserving approximately the same density. Of course there are occasional sudden rearrangements of biofilm structure, e.g. sloughing, with concomitant changes in localized biomass density. However, those phenomena are both temporary and only imply a fluctuation of biofilm density around an optimal value. Thus, one could rewrite the mathematical formulation of the quasi-steady-state assumption to better express the role of these fluctuations,

$$\frac{d}{dt}X \approx \frac{d}{dt}X_M \approx \frac{d}{dt}XH_n \approx \frac{d}{dt}X_S \approx 0 \qquad (5.2.1.–3)$$

$$\Rightarrow \frac{d}{dt} X_T \approx 0 \wedge -\frac{d}{dt} M_{Red} \approx \frac{d}{dt} M_{Ox} \approx -\frac{d}{dt} S_{Ox} \approx \frac{d}{dt} S_{Red} \qquad (5.2.1.–4)$$

which we may perhaps term as **weak quasi-steady-state**. As for long-term processes of biofilm restructuring – also known as consolidation (Alpkvist et al., 2006) – in which the *de facto* optimal biomass density might change over a long period of time, the practical formulation of the quasi-steady-state assumption applies: the localized concentrations of substrates and products vary much faster than local biomass density.

With the quasi-steady-state assumption, the following balances apply,

$$\frac{d}{dt} X : 0 = -k_1 . M_{Red} . X . \left[H^+ \right]^n + k_{-1} . X_M + k_4 . X_S - k_{-4} . S_{Red} . X . \left[H^+ \right]^n \qquad (5.2.1.–5)$$

$$\frac{d}{dt} X_M : 0 = +k_1 . M_{Red} . X . \left[H^+ \right]^n - k_{-1} . X_M - k_2 . X_M + k_{-2} . M_{Ox} . XH_n \qquad (5.2.1.–6)$$

$$\frac{d}{dt} XH_n : 0 = +k_2 . X_M - k_{-2} . M_{Ox} . XH_n - k_3 . S_{Ox} . XH_n + k_{-3} . X_S \qquad (5.2.1.–7)$$

$$\frac{d}{dt} X_S : 0 = +k_3 . S_{Ox} . XH_n - k_{-3} . X_S - k_4 . X_S + k_{-4} . S_{Red} . X . \left[H^+ \right]^n \qquad (5.2.1.–8)$$

$$X_T = X + X_M + XH_n + X_S \qquad (5.2.1.–9)$$

Note this is a system of four equations, since one of the differential balances can always be written as linear combination of the remaining three. Resolution of this system of equations would yield the concentrations of each of the four biomass intermediates. However, a useful result should include measurable parameters instead of rate constants.

5.2.2. Definition of Half-saturation Constants

To illustrate how half-saturation constants – also known as affinity constants – might be used to substitute some of the rate constants, e.g. as input parameters, we should first review the original derivation of enzyme kinetics by Menten and Michaelis, with the modifications introduced by Briggs and Haldane (Menten and Michaelis, 1913; Briggs and Haldane, 1925). Consider an enzyme **E** that catalyses the conversion of substrate **S** into substrate **P**. Enzyme-substrate complexation is reversible, while conversion into product is irreversible. The following chemical equation applies,

$$E + S \underset{k_{-1}}{\overset{k_1}{\rightleftharpoons}} ES \xrightarrow{k_2} P$$

Writing the differential balance for the enzyme-substrate complex and applying the quasi-steady-state assumption,

$$\begin{aligned} &\frac{d}{dt}[ES] = +k_1.[E].[S] - k_{-1}.[ES] - k_2.[ES] = 0 \\ &\Rightarrow \frac{[E].[S]}{[ES]} = \frac{k_{-1} + k_2}{k_1} = K_S \end{aligned} \qquad (5.2.2.–1)$$

Thus, the half-saturation constant for substrate **S** is the sum of rate constants of reaction steps that directly contribute to reduce the concentration of complex **ES**, divided by the rate constant of the step that, using substrate **S**, contributes to increase the concentration of **ES**. Should there be multiple substrates instead of just **S**, this derivation would yield a half-saturation constant for their multiplicand, and stoichiometric coefficients would also appear as exponents. For instance,

$$E + a.A + b.B \underset{k_{-1}}{\overset{k_1}{\rightleftharpoons}} EA_aB_b \xrightarrow{k_2} P$$

$$\begin{aligned} &\frac{d}{dt}[EA_aB_b] = +k_1.[E].[A]^a.[B]^b - k_{-1}.[EA_aB_b] - k_2.[EA_aB_b] = 0 \\ &\Rightarrow \frac{[E].[A]^a.[B]^b}{[EA_aB_b]} = \frac{k_{-1} + k_2}{k_1} = K_{(A)^a.(B)^b} \end{aligned} \qquad (5.2.2.–2)$$

Such representations of half-saturation constants would be little more than a theoretical exercise without a method to convert them into their standard, measurable form. Two cases will be analysed: composite half-saturation constants, e.g. affinity for multiplicand (A).(B), and exponentiated half-saturation constants, e.g. affinity for $(S)^n$.

5.2.2.1. Composite Half-saturation Coefficients

Let's consider an enzymatic reaction with substrates A and B. Adapting the Michaelis-Menten approach (Menten and Michaelis, 1913; Briggs and Haldane, 1925),

$$E + A + B \underset{k_{-1}}{\overset{k_1}{\rightleftharpoons}} EAB \xrightarrow{k_2} P$$

$$\frac{d}{dt}[EAB] = +k_1.[E].[A].[B] - k_{-1}.[EAB] - k_2.[EAB] = 0$$
$$\Rightarrow \frac{[E].[A].[B]}{[EAB]} = \frac{k_{-1}+k_2}{k_1} = K_{(A).(B)} \quad (5.2.2.1.–1)$$

$$E_0 = [E] + [EAB] \Leftrightarrow [E] = E_0 - [EAB]$$
$$\Rightarrow \frac{(E_0 - [EAB]).[A].[B]}{[EAB]} = K_{(A).(B)} \Leftrightarrow [EAB] = E_0.\frac{[A].[B]}{K_{(A).(B)} + [A].[B]} \quad (5.2.2.1.–2)$$

$$r = \frac{d}{dt}[P] = +k_2.[EAB]$$
$$\Rightarrow r = +k_2.E_0.\frac{[A].[B]}{K_{(A).(B)} + [A].[B]} \quad (5.2.2.1.–3)$$

With this result, let us analyse scenarios where only one of the substrates is relevant. First, if there is an excess of **B** or a limitation in **A**, only the concentration of **A** is relevant for kinetic purposes. Mathematically,

$$[B] \gg K_B \vee [A] \ll K_A$$
$$\Rightarrow k_2.E_0.\frac{[A].[B]}{K_{(A).(B)} + [A].[B]} \approx k_2.E_0.\frac{[A]}{K_A + [A]}$$
$$\Leftrightarrow K_{(A).(B)} \approx [B].K_A \quad (5.2.2.1.–4)$$

Conversely, if there is an excess of **A** or a limitation in **B**, only the concentration of **B** is relevant,

$$[A] \gg K_A \vee [B] \ll K_B$$
$$\Rightarrow k_2.E_0.\frac{[A].[B]}{K_{(A).(B)} + [A].[B]} \approx k_2.E_0.\frac{[B]}{K_B + [B]}$$
$$\Leftrightarrow K_{(A).(B)} \approx [A].K_B \quad (5.2.2.1.–5)$$

This approach covers the opposite extremes where only one of the substrates is kinetically relevant. Thus, to estimate the composite half-saturation constant for any value in between the two extremes, a simple approximation is to sum the respective formula.

$$K_{(A).(B)} \approx [A].K_B + [B].K_A \quad (5.2.2.1.–6)$$

Noteworthy, the composite half-saturation constant is not, in fact constant – Figure 11 – and should thus be termed coefficient.

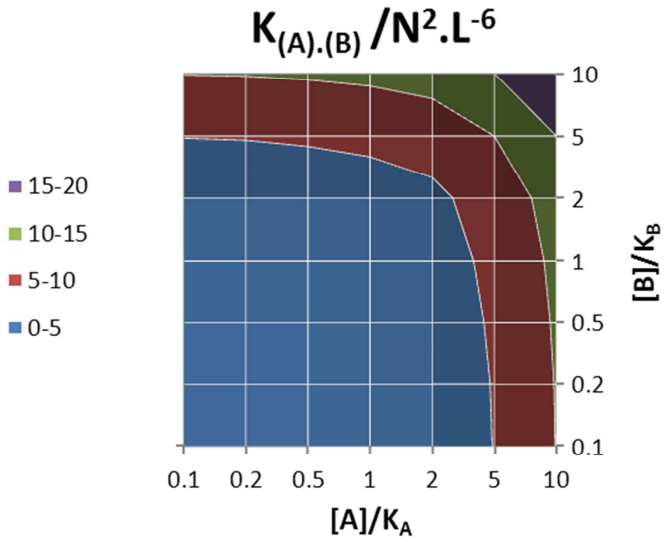

Figure 11 - Composite half-saturation coefficient as a function of the normalized concentrations of **A** and **B**. Since the substrate concentration for such an enzyme system is effectively **[A].[B]**, simultaneous variations of **A** and **B** towards high ($S>>K_S$) or low ($S<<K_S$) concentration ranges will, due to multiplication, be overrepresented in the overall rate equation. Hence why the composite half-saturation coefficient is also variable: to preserve the relative quantitative meaning of S and K_S. $\mathbf{K_{(A).(B)}}$ has units of squared concentration, e.g. $mmol^2.m^{-6}$.

5.2.2.2. Exponentiated Half-saturation Coefficients

Let us consider substrate **S** that contributes to an enzymatic reaction with more than one molecule, and write down two hypothetical stoichiometries,

$$E + a.S \underset{k_{-1}}{\overset{k_1}{\rightleftarrows}} ES_a \xrightarrow{k_2} P$$

$$E + b.S \underset{k_{-1}}{\overset{k_1}{\rightleftarrows}} ES_b \xrightarrow{k_2} P$$

Following the derivation procedure detailed in the previous sub-section,

$$r_a = +k_2.E_0.\frac{[S]^a}{K_{(S)^a} + [S]^a} \qquad (5.2.2.2.–1)$$

$$r_b = +k_2.E_0.\frac{[S]^b}{K_{(S)^b} + [S]^b} \qquad (5.2.2.2.–2)$$

The purpose of this derivation is to obtain rate-preserving conversion rules for exponentiated substrates. Mathematically, this is the same as saying the rates for stoichiometric coefficients ***a*** and ***b*** should be the same,

$$r_a = r_b \Leftrightarrow [S]^a.K_{(S)^b} = [S]^b.K_{(S)^a} \qquad (5.2.2.2.–3)$$

For b=1 and a=n,

$$K_{(S)^n} = [S]^{n-1}.K_S \qquad (5.2.2.2.–4)$$

Again, we realize the half-saturation constant is in fact not constant – see Figure 12 – and should thus be termed coefficient.

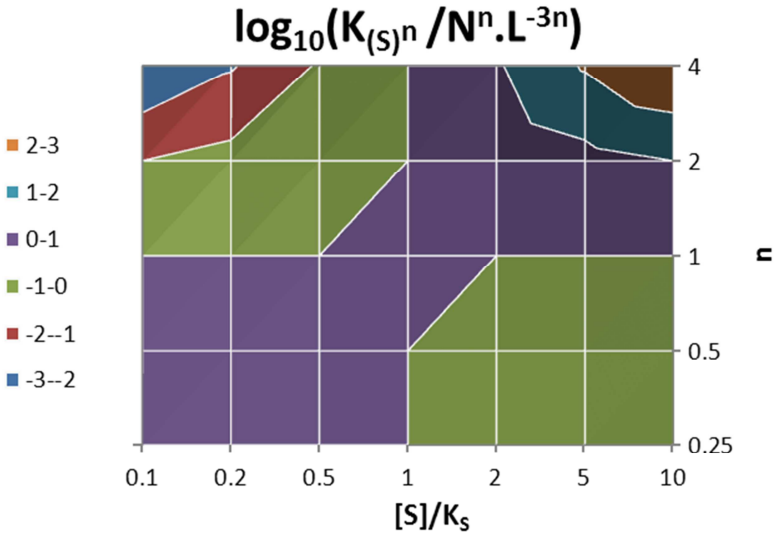

Figure 12 - Exponentiated half-saturation coefficient as a function of the normalized concentration of substrate **S**, and its stoichiometric coefficient **n**, for K_S = 1 $N.L^{-3}$. At high concentrations and n>>1, exponentiation of **[S]** causes an overrepresentation of **S** in the rate equation, thus the increase in magnitude of the exponentiated half-saturation coefficient may be interpreted as a correction to this overrepresentation. The opposite is also true for low concentration at n>>1.

Furthermore, it should be said this formulation of the half-saturation coefficient is similar to the one used in the Hill equation, with ***n*** being the Hill coefficient (Hill, 1910). Interestingly, today's knowledge of multi-ligand binding to macromolecules indicates the coefficient ***n*** is not strictly a measure of stoichiometry, but rather of cooperativity: if n>1, ligand affinity increases with every successive binding event; if n<1, the opposite is observed (Nelson and Cox, 2009). This may be something to keep in mind, since in this dissertation ***n*** is used to describe the number of electrons/protons simultaneously transferred to or from electron transport chains. The existence of cooperative behaviour in such a system would be highly relevant for BESs research, especially considering negative cooperativity is an obvious control mechanism to prevent respiratory overload, something that might happen if electrode potentials are poised too high or too low. Alas, this possibility won't be discussed any further.

5.2.2.3. Half-saturation Coefficients in MET

With the above derived conversion rules, we may safely write half-saturation coefficients for microbial kinetics, knowing the forthcoming rate equation is still applicable to real problems. Recalling the microbial portion of MET,

$$M_{Red} + X + n.H^+ \underset{k_{-1}}{\overset{k_1}{\rightleftarrows}} X_M \underset{k_{-2}}{\overset{k_2}{\rightleftarrows}} M_{Ox} + XH_n$$

$$S_{Ox} + XH_n \underset{k_{-3}}{\overset{k_3}{\rightleftarrows}} X_S \underset{k_{-4}}{\overset{k_4}{\rightleftarrows}} S_{Red} + X + n.H^+$$

straightforward application of the definition established in 5.2.2.Definition of Half-saturation Constants yields,

$$K_{M_{Red}\cdot\left(H^+\right)^n} = \frac{k_{-1}+k_2}{k_1} \Leftrightarrow k_1 = \frac{k_{-1}+k_2}{K_{M_{Red}\cdot\left(H^+\right)^n}} \qquad (5.2.2.3.\text{–}1)$$

$$K_{M_{Ox}} = \frac{k_{-1}+k_2}{k_{-2}} \Leftrightarrow k_{-2} = \frac{k_{-1}+k_2}{K_{M_{Ox}}} \qquad (5.2.2.3.\text{–}2)$$

$$K_{S_{Ox}} = \frac{k_{-3}+k_4}{k_3} \Leftrightarrow k_3 = \frac{k_{-3}+k_4}{K_{S_{Ox}}} \qquad (5.2.2.3.\text{–}3)$$

$$K_{S_{Red}\cdot\left(H^+\right)^n} = \frac{k_{-3}+k_4}{k_{-4}} \Leftrightarrow k_{-4} = \frac{k_{-3}+k_4}{K_{S_{Red}\cdot\left(H^+\right)^n}} \qquad (5.2.2.3.\text{–}4)$$

A total of eight rate constants must be substituted, meaning four additional definitions are necessary.

5.2.3. Definition of Maximum Rates

Maximum rates may also be defined by analogy with enzyme kinetics. Considering the basic Michaelis-Menten scheme,

$$\mathrm{E} + \mathrm{S} \underset{k_{-1}}{\overset{k_1}{\rightleftarrows}} \mathrm{ES} \xrightarrow{k_2} \mathrm{P}$$

$$r = +k_2.E_0.\frac{[S]}{K_S + [S]} \qquad (5.2.3.–1)$$

The maximum rate $\mathbf{V_{max}}$ is defined as

$$V_{max} = k_2.E_0 \qquad (5.2.3.–2)$$

This quantitative definition may be interpreted as follows: maximal reaction rates are observed when the total amount of biocatalyst is in the form of enzyme-substrate complex. Of course, this occurs when substrate is saturating, such that any free enzyme molecules are immediately complexed. Consulting the microbial section of MET,

$$\text{Reaction 1:}\quad \mathrm{M_{Red}} + \mathrm{X} + \mathrm{n}.\mathrm{H}^+ \underset{k_{-1}}{\overset{k_1}{\rightleftarrows}} \mathrm{X_M} \underset{k_{-2}}{\overset{k_2}{\rightleftarrows}} \mathrm{M_{Ox}} + \mathrm{XH_n}$$

$$\text{Reaction 2:}\quad \mathrm{S_{Ox}} + \mathrm{XH_n} \underset{k_{-3}}{\overset{k_3}{\rightleftarrows}} \mathrm{X_S} \underset{k_{-4}}{\overset{k_4}{\rightleftarrows}} \mathrm{S_{Red}} + \mathrm{X} + \mathrm{n}.\mathrm{H}^+$$

the following maximum forward and reverse rates may be defined,

$$\text{Reaction 1:}\ V_f = k_2.X_T\ ;\ V_r = k_{-1}.X_T \qquad (5.2.3.–3)$$

$$\text{Reaction 2:}\ V_f = k_4.X_T\ ;\ V_r = k_{-3}.X_T \qquad (5.2.3.–4)$$

Considering the maximum forward rate, evidently $\mathbf{V_f}$ cannot be the actual maximum of both reactions combined, since the total amount of biocatalyst can't be in two forms at once. Thus, $\mathbf{V_f}$ and $\mathbf{V_r}$ should be interpreted as the maximum rates if reactions 1 and 2 were isolated. For the combined system of chemical equations, and since the quasi-steady-state assumption imposes equal turnover for both reaction, we can expect the net maximum forward and reverse rates to be $\mathbf{V_f/2}$ and $\mathbf{V_r/2}$, respectively.

5.2.4. Biomass Distribution Equations

Substitution of the eight rate constants by the defined half-saturation coefficients and maximum rates, followed by resolution of the system of differential balances and mass balance to the biomass intermediate forms defined in 5.2.1.Quasi-steady-state, yields a set of biomass distribution equations,

$$\begin{aligned} Denominator\big|_{MET} = {} & V_f \cdot \left[\frac{M_{Red} \cdot \left[H^+\right]^n}{K_{M_{Red} \cdot \left(H^+\right)^n}} + 2. \frac{M_{Red} \cdot \left[H^+\right]^n}{K_{M_{Red} \cdot \left(H^+\right)^n}} \cdot \frac{S_{Ox}}{K_{S_{Ox}}} + \frac{S_{Ox}}{K_{S_{Ox}}} \right] \\ & + V_r \cdot \left[\frac{S_{Red} \cdot \left[H^+\right]^n}{K_{S_{Red} \cdot \left(H^+\right)^n}} + 2. \frac{S_{Red} \cdot \left[H^+\right]^n}{K_{S_{Red} \cdot \left(H^+\right)^n}} \cdot \frac{M_{Ox}}{K_{M_{Ox}}} + \frac{M_{Ox}}{K_{M_{Ox}}} \right] \\ & + \left(V_f + V_r\right) \cdot \left[\frac{M_{Red} \cdot \left[H^+\right]^n}{K_{M_{Red} \cdot \left(H^+\right)^n}} \cdot \frac{M_{Ox}}{K_{M_{Ox}}} + \frac{S_{Red} \cdot \left[H^+\right]^n}{K_{S_{Red} \cdot \left(H^+\right)^n}} \cdot \frac{S_{Ox}}{K_{S_{Ox}}} \right] \end{aligned} \tag{5.2.4.–1}$$

$$\frac{X}{X_T} = \frac{1}{Denominator\big|_{MET}} \cdot \left[V_f \cdot \frac{S_{Ox}}{K_{S_{Ox}}} + V_r \cdot \frac{M_{Ox}}{K_{M_{Ox}}} \right] \tag{5.2.4.–2}$$

$$\begin{aligned} \frac{X_M}{X_T} = {} & \frac{1}{Denominator\big|_{MET}} \cdot \left[V_f \cdot \frac{M_{Red} \cdot \left[H^+\right]^n}{K_{M_{Red} \cdot \left(H^+\right)^n}} \cdot \left(\frac{M_{Ox}}{K_{M_{Ox}}} + \frac{S_{Ox}}{K_{S_{Ox}}} \right) \right. \\ & \left. + V_r \cdot \frac{M_{Ox}}{K_{M_{Ox}}} \cdot \left(\frac{M_{Red} \cdot \left[H^+\right]^n}{K_{M_{Red} \cdot \left(H^+\right)^n}} + \frac{S_{Red} \cdot \left[H^+\right]^n}{K_{S_{Red} \cdot \left(H^+\right)^n}} \right) \right] \end{aligned} \tag{5.2.4.–3}$$

$$\frac{XH_n}{X_T} = \frac{1}{Denominator\big|_{MET}} \cdot \left[V_f \cdot \frac{M_{Red} \cdot \left[H^+\right]^n}{K_{M_{Red} \cdot \left(H^+\right)^n}} + V_r \cdot \frac{S_{Red} \cdot \left[H^+\right]^n}{K_{S_{Red} \cdot \left(H^+\right)^n}} \right] \tag{5.2.4.–4}$$

$$\frac{X_S}{X_T}=\frac{1}{Denominator\big|_{MET}}\cdot\left[V_f\cdot\frac{S_{Ox}}{K_{S_{Ox}}}\cdot\left(\frac{M_{Red}\cdot\left[H^+\right]^n}{K_{M_{Red}\cdot\left(H^+\right)^n}}+\frac{S_{Red}\cdot\left[H^+\right]^n}{K_{S_{Red}\cdot\left(H^+\right)^n}}\right)+V_r\cdot\frac{S_{Red}\cdot\left[H^+\right]^n}{K_{S_{Red}\cdot\left(H^+\right)^n}}\cdot\left(\frac{M_{Ox}}{K_{M_{Ox}}}+\frac{S_{Ox}}{K_{S_{Ox}}}\right)\right] \quad (5.2.4.–5)$$

These distribution equations are a relevant result in and of themselves. Namely, the possibility of experimentally measuring biomass redox states, or more specifically, cytochrome redox states, for instance through Confocal Raman Microscopy (Virdis et al., 2012) or UV/Vis Spectroscopy (Liu and Bond, 2012), would provide the necessary experimental verification of the analysis herein performed. Although other types of data can be used for fitting purposes, such as cyclic voltammetry results, i.e. current density *vs.* electrode potential curves, one may argue that any reasonably complex model with a large number of parameters can be successfully fitted to any macroscopic result. However, a model capable of accurately describing microscopic states is bound to provide mechanistic insights: it is thus a theory.

Although the aforementioned spectroscopic techniques are able to distinguish the reduced and oxidized forms of *c*-type cytochromes, so far, to the best of my knowledge, no data has been reported for biomass redox states at specific heights within living biofilms. Increased instrumentation resolution and more sophisticated data processing algorithms, especially ones capable of filtering out spectral noise, would alleviate technical difficulties.

5.2.5. Net Reversible Rate Equation and Equilibrium Constant

Knowing the quasi-steady-state assumption imposes equal turnovers on all chemical species involved in catabolism, the differential balance of any of those species is adequate as a starting point for a rate equation, e.g.

$$r_{cat}^{rev}=\frac{d}{dt}S_{Red}=+k_4.X_S-k_{-4}.S_{Red}.X.\left[H^+\right]^n \quad (5.2.5.–1)$$

Substitution of rate constants using the definitions in 5.2.2.3.Half-saturation Coefficients in MET and 5.2.3.Definition of Maximum Rates, and of X_S and X by the appropriate distribution equations yields the reversible catabolic rate equation for MET,

$$r_{cat}^{rev}=\frac{1}{Denominator\big|_{MET}}\cdot\left[V_f^2\cdot\frac{M_{Red}\cdot\left[H^+\right]^n}{K_{M_{Red}\cdot\left(H^+\right)^n}}\cdot\frac{S_{Ox}}{K_{S_{Ox}}}-V_r^2\cdot\frac{S_{Red}\cdot\left[H^+\right]^n}{K_{S_{Red}\cdot\left(H^+\right)^n}}\cdot\frac{M_{Ox}}{K_{M_{Ox}}}\right] \quad (5.2.5.–2)$$

Derivation of the corresponding equilibrium constant first requires specification of single-step equilibrium constants. Recalling the microbial portion of MET,

$$\mathrm{M_{Red}} + \mathrm{X} + \mathrm{n}.\mathrm{H}^{+} \underset{\mathrm{k_{-1}}}{\overset{\mathrm{k_1}}{\rightleftharpoons}} \mathrm{X_M} \underset{\mathrm{k_{-2}}}{\overset{\mathrm{k_2}}{\rightleftharpoons}} \mathrm{M_{Ox}} + \mathrm{XH_n}$$

$$\mathrm{S_{Ox}} + \mathrm{XH_n} \underset{\mathrm{k_{-3}}}{\overset{\mathrm{k_3}}{\rightleftharpoons}} \mathrm{X_S} \underset{\mathrm{k_{-4}}}{\overset{\mathrm{k_4}}{\rightleftharpoons}} \mathrm{S_{Red}} + \mathrm{X} + \mathrm{n}.\mathrm{H}^{+}$$

the following chemical equilibriums apply,

$$K_{eq,1} = \frac{k_1}{k_{-1}} = \left. \frac{X_M}{M_{Red}.X.\left[H^+\right]^n} \right|_{eq} \qquad (5.2.5.–3)$$

$$K_{eq,2} = \frac{k_2}{k_{-2}} = \left. \frac{M_{Ox}.XH_n}{X_M} \right|_{eq} \qquad (5.2.5.–4)$$

$$K_{eq,3} = \frac{k_3}{k_{-3}} = \left. \frac{X_S}{S_{Ox}.XH_n} \right|_{eq} \qquad (5.2.5.–5)$$

$$K_{eq,4} = \frac{k_4}{k_{-4}} = \left. \frac{S_{Red}.X.\left[H^+\right]^n}{X_S} \right|_{eq} \qquad (5.2.5.–6)$$

Also, by writing the net chemical equation and the respective homogeneous equilibrium,

$$\mathrm{M_{Red}} + \mathrm{S_{Ox}} \underset{\mathrm{k_r}}{\overset{\mathrm{k_f}}{\rightleftharpoons}} \mathrm{M_{Ox}} + \mathrm{S_{Red}}$$

$$K_{eq,cat}^{homogeneous} = \left. \frac{M_{Ox}.S_{Red}}{M_{Red}.S_{Ox}} \right|_{eq} \qquad (5.2.5.–7)$$

We observed the net equilibrium is the multiplicand of single-step equilibriums. Thus, and using the definitions in 5.2.2.3.Half-saturation Coefficients in MET and 5.2.3.Definition of Maximum Rates to substitute rate constants,

$$K_{eq,cat}^{homogeneous} = \frac{k_1.k_2.k_3.k_4}{k_{-1}.k_{-2}.k_{-3}.k_{-4}} = \frac{V_f^2}{V_r^2}.\frac{K_{M_{Ox}}.K_{S_{Red}\cdot\left(H^+\right)^n}}{K_{M_{Red}\cdot\left(H^+\right)^n}.K_{S_{Ox}}} \quad (5.2.5.–8)$$

This result is exactly the same as the one obtained by Cleland for Ping-Pong Bi-Bi enzyme kinetics, using the schematic method of King and Altman, thus validating the deductive approach herein developed (King and Altman, 1956; Cleland, 1963).

5.2.6. Maximum Rates as Thermodynamic Parameters

Besides the above derived formula for net chemical equilibrium, the same parameters may also be defined using its thermodynamic identity (Atkins and Paula, 2006),

$$\Delta_r G_{cat}^{\circ} = -R.T.\ln\left(K_{eq,cat}\right) \Leftrightarrow K_{eq,cat}^{homogeneous} = \exp\left(-\frac{\Delta_r G_{cat}^{\circ}}{R.T}\right) \quad (5.2.6.–1)$$

$$\Rightarrow \exp\left(-\frac{\Delta_r G_{cat}^{\circ}}{R.T}\right) = \frac{V_f^2}{V_r^2}.\frac{K_{M_{Ox}}.K_{S_{Red}\cdot\left(H^+\right)^n}}{K_{M_{Red}\cdot\left(H^+\right)^n}.K_{S_{Ox}}} \quad (5.2.6.–2)$$

where the standard Gibbs energy of catabolism refers to the net catabolic reaction,

$$\mathrm{M_{Red} + S_{Ox} \underset{k_r}{\overset{k_f}{\rightleftharpoons}} M_{Ox} + S_{Red}}$$

$$\Delta_r G_{cat}^{\circ} = -n.F.\left(E_{S_{Red}/S_{Ox}}^{\circ} - E_{M_{Red}/M_{Ox}}^{\circ}\right) \quad (5.2.6.–3)$$

Furthermore, recalling the discussion in 5.2.3.Definition of Maximum Rates, the maximum forward and reverse rates for the net catabolic reaction are $\mathbf{V_f/2}$ and $\mathbf{V_r/2}$, respectively. The difference between the two is the maximum net catabolic turnover, a measure of the capacity of electron transport chains, with a proposed value of 3.0 (mol-of-e^-).C-mol^{-1}.h^{-1} (Heijnen et al., 1992; Heijnen and Kleerebezem, 2010). The corresponding mathematical formulation would be,

$$\frac{q_{e,max}}{n}.X_T = \left|\frac{V_f}{2} - \frac{V_r}{2}\right| \quad (5.2.6.–4)$$

which, together with the two definitions for equilibrium constant yields,

$$V_f = 2.\frac{q_{e,max}}{n}.X_T.\frac{1}{\left|1-\exp\left(+\frac{1}{2}.\frac{\Delta_r G^o_{cat}}{R.T}\right).\left[\frac{K_{M_{Ox}}.K_{S_{Red}.\left(H^+\right)^n}}{K_{M_{Red}.\left(H^+\right)^n}.K_{S_{Ox}}}\right]^{1/2}\right|} \qquad (5.2.6.–5)$$

$$V_r = 2.\frac{q_{e,max}}{n}.X_T.\frac{1}{\left|\exp\left(-\frac{1}{2}.\frac{\Delta_r G^o_{cat}}{R.T}\right).\left[\frac{K_{M_{Red}.\left(H^+\right)^n}.K_{S_{Ox}}}{K_{M_{Ox}}.K_{S_{Red}.\left(H^+\right)^n}}\right]^{1/2}-1\right|} \qquad (5.2.6.–6)$$

thus highlighting the relation between maximum rates and thermodynamics, hypothesized in 4.2.Respiratory Reversibility. Besides the standard Gibbs energy of reaction, the defined maximum rates are also a function of half-saturation coefficients. These coefficients may also be interpreted as thermodynamic parameters. One of the purposes of homeostasis is to maintain cellular energetic fluxes, such that growth can proceed at a steady rate. Hypothetically, if the energy yield of a substrate decreases, e.g. the catabolic system approaches equilibrium due to preceding substrate consumption, bacteria have the ability to adjust the transcription levels of uptake system-encoding mRNA as a function of e.g. intracellular cAMP levels (Nelson and Cox, 2009). This would increase net metabolic molar turnovers in order to maintain constant energy yields, thus increasing the microbial affinity for said substrate.

A good example of such behaviour is the *lac* operon – a set of genes encoding the necessary enzymes for lactose metabolism, sharing the same regulatory elements – in *Escherichia coli*. Expression of the operon is regulated by two control mechanisms: the catabolite activator protein (CAP) (Busby and Ebright, 2001) and the lactose repressor (Gilbert and Müller-Hill, 1966). CAP is an activator that permits *lac* operon transcription once it binds to cAMP, while the lac repressor prevents *lac* operon transcription unless it is bound to lactose. Thus, only if lactose is present and high intracellular levels of cyclic AMP occur – a consequence of poor catabolic energy yields – will the expression of specialized lactose uptake systems be allowed. Therefore, diauxic growth, e.g. first glucose, then lactose, demonstrates the thermodynamic nature of microbial substrate affinities: at first the affinity for lactose is negligible, but becomes high upon glucose exhaustion.

5.2.7. Irreversible Rate Equations

Clarification of the properties of the derived reversible rate equation is best achieved by looking at the simplified irreversible case, observed when the reaction is far from equilibrium. For instance, if the availability of oxidized mediator and reduced

substrate is negligible, the rate equation will be macroscopically irreversible in the forward direction,

$$\begin{cases} M_{Ox} \to 0 \\ S_{Red} \cdot \left[H^+ \right]^n \to 0 \end{cases}$$

$$\Rightarrow r_{cat}^{irrev,f} = \frac{V_f^2 \cdot \frac{M_{Red} \cdot \left[H^+ \right]^n}{K_{M_{Red} \cdot \left(H^+ \right)^n}} \cdot \frac{S_{Ox}}{K_{S_{Ox}}}}{V_f \cdot \left[\frac{M_{Red} \cdot \left[H^+ \right]^n}{K_{M_{Red} \cdot \left(H^+ \right)^n}} + 2. \frac{M_{Red} \cdot \left[H^+ \right]^n}{K_{M_{Red} \cdot \left(H^+ \right)^n}} \cdot \frac{S_{Ox}}{K_{S_{Ox}}} + \frac{S_{Ox}}{K_{S_{Ox}}} \right]} \qquad (5.2.7.–1)$$

which, rewritten in a familiar form, is equivalent to a Monod law for dual substrate limitation with a correction factor,

$$r_{cat}^{irrev,f} = V_f \cdot \frac{M_{Red} \cdot \left[H^+ \right]^n}{K_{M_{Red} \cdot \left(H^+ \right)^n} + M_{Red} \cdot \left[H^+ \right]^n} \cdot \frac{S_{Ox}}{K_{S_{Ox}} + S_{Ox}} \times \frac{1}{\frac{M_{Red} \cdot \left[H^+ \right]^n}{K_{M_{Red} \cdot \left(H^+ \right)^n} + M_{Red} \cdot \left[H^+ \right]^n} + \frac{S_{Ox}}{K_{S_{Ox}} + S_{Ox}}} \qquad (5.2.7.–2)$$

This factor introduces corrections to both high and low concentration ranges, decreasing rates at the saturation limit and increasing them for very low substrate availabilities – see Figure 13 for an example and its interpretation. While the correction at high substrate concentrations is a direct consequence of the method used to define maximum forward and reverse rates in 5.2.3.Definition of Maximum Rates, the best way to interpret the acceleration at low substrate concentrations, specifically when both substrates are limiting, is the cumulative contribution of two substrates to drive the reaction, something that is not intrinsically accounted for in the dual substrate Monod model. Nevertheless, when approaching the low substrate range, inevitably we also approach equilibrium conditions, meaning the application of an irreversible rate equation may in and of itself be incorrect.

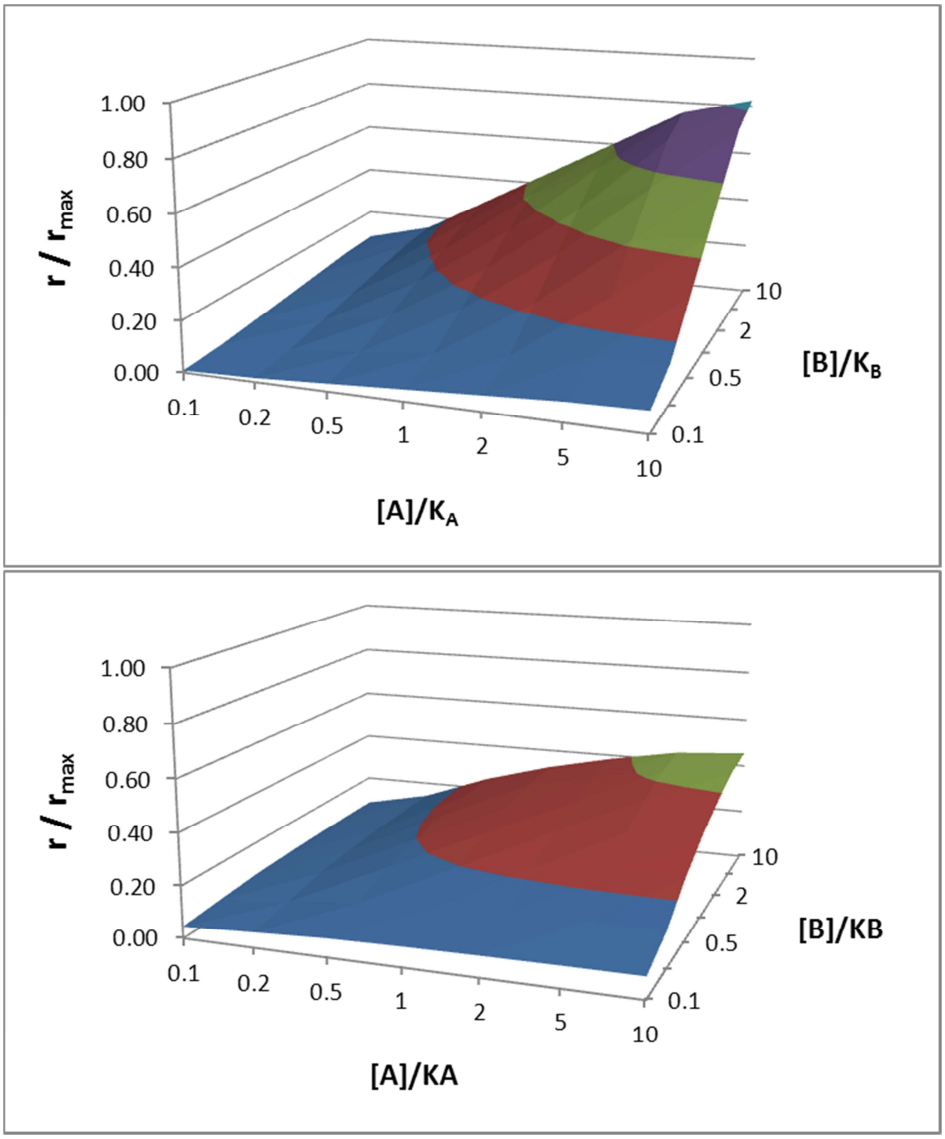

Figure 13 - Comparison between dual substrate Monod kinetics (**top**) and irreversible microbial MET kinetics (**bottom**) for substrates **A** and **B**. For microbial MET kinetics, the maximal achievable rate is half of the maximum rate, since this maximum was defined separately for each of the two microbial MET reactions: the combination of both means the biocatalyst will have to be – according to the quasi-steady-state assumption – evenly distributed among them. Also, at very low concentrations of both substrates, microbial MET kinetics is faster than dual substrate Monod, since dual limitation is alleviated, i.e. if **A** and **B** limit kinetics by a similar factor, the overall rate won't just be the multiplicand of factors, but will also take into account the fact that there are two substrates driving the reaction instead of just one.

Conversely, if the availability of reduced substrate and oxidized acceptor is negligible, the reaction approaches the irreversible reverse rate,

$$\begin{cases} M_{Red} \cdot \left[H^+ \right]^n \to 0 \\ S_{Ox} \to 0 \end{cases}$$

$$r_{cat}^{irrev,r} = \frac{-V_r^2 \cdot \frac{S_{Red} \cdot \left[H^+ \right]^n}{K_{S_{Red} \cdot \left(H^+ \right)^n}} \cdot \frac{M_{Ox}}{K_{M_{Ox}}}}{V_r \cdot \left[\frac{S_{Red} \cdot \left[H^+ \right]^n}{K_{S_{Red} \cdot \left(H^+ \right)^n}} + 2. \frac{S_{Red} \cdot \left[H^+ \right]^n}{K_{S_{Red} \cdot \left(H^+ \right)^n}} \cdot \frac{M_{Ox}}{K_{M_{Ox}}} + \frac{M_{Ox}}{K_{M_{Ox}}} \right]} \qquad (5.2.7.–3)$$

which is of course negative.

5.2.8. Example: Hydrogen Evolution using Methyl Viologen

To illustrate the application of the derived reversible rate equation and discuss some issues that may arise from a practical perspective, we will use the example of cathodic bioelectrocatalytic hydrogen evolution using methyl viologen as mediator, previously reported in multiple instances (e.g.: Lojou et al., 2002; Aulenta et al., 2008). First we should write down the half-oxidation and half-reduction reactions for methyl viologen and hydrogen, respectively,

$$\mathrm{MV^{\bullet +}(aq) \underset{\text{Reduction}}{\overset{\text{Oxidation}}{\rightleftharpoons}} MV^{2+}(aq) + e^-}$$

$$\mathrm{2.H^+(aq) + 2.e^- \underset{\text{Oxidation}}{\overset{\text{Reduction}}{\rightleftharpoons}} H_2(g)}$$

and proceed to define the appropriate conversion rules using the general notation defined in 4.3.A Generalized Notation, keeping in mind the half-oxidation of methyl viologen would have to be multiplied by two to match the number of electrons in the HER,

$$\begin{aligned} M_{Red} &= \left[MV^{\bullet +} \right]^2 \\ M_{Ox} &= \left[MV^{2+} \right]^2 \\ S_{Red} &= pH_2 \\ S_{Ox} &= \left[H^+ \right]^2 \end{aligned} \qquad (5.2.8.–1)$$

Furthermore, we will assume two electrons participate in biomass redox reactions. Thus, the chemical equations for microbial MET read as,

$$\begin{cases} M_{Red} + X + n.H^+ \underset{k_{-1}}{\overset{k_1}{\rightleftarrows}} X_M \underset{k_{-2}}{\overset{k_2}{\rightleftarrows}} M_{Ox} + XH_n \\ S_{Ox} + XH_n \underset{k_{-3}}{\overset{k_3}{\rightleftarrows}} X_S \underset{k_{-4}}{\overset{k_4}{\rightleftarrows}} S_{Red} + X + n.H^+ \end{cases}$$

$$\Rightarrow \begin{cases} 2.MV^{\bullet+}(aq) + X + 2.H^+(aq) \underset{k_{-1}}{\overset{k_1}{\rightleftarrows}} X_M^{4+} \underset{k_{-2}}{\overset{k_2}{\rightleftarrows}} 2.MV^{2+}(aq) + XH_2 \\ 2.H^+(aq) + XH_2 \underset{k_{-3}}{\overset{k_3}{\rightleftarrows}} X_S^{2+} \underset{k_{-4}}{\overset{k_4}{\rightleftarrows}} H_2(g) + X + 2.H^+(aq) \end{cases}$$

From the second chemical equation, it is evident that two types of protons participate in this reaction: protons that are captured/released by biomass intermediate X/XH_n to counterbalance the acceptance/donation of electrons, and protons that participate as substrate for hydrogen evolution. A third type of protons may be involved in the mediator reaction, e.g. for riboflavin or AQDS. Evidently, these protons are chemically equivalent: the difference is in how biomass interacts with them, and thus there is the possibility of different proton affinities for each type of interaction. Half-saturation constants/coefficients for biomass **c**ounter**b**alancing protons will be marked with the superscript ***cb*** to distinguish them from mediator- or substrate-associated protons. Furthermore, and to simplify the example, we will only look into the irreversible forward case. Recalling the conversion rules,

$$\begin{cases} Composition: K_{(A).(B)} \approx [A].K_B + [B].K_A \\ Exponentiation: K_{(S)^n} = [S]^{n-1}.K_S \end{cases} \qquad (5.2.8.–2)$$

and applying them to this example,

$$\begin{aligned} K_{M_{Red}.(H^+)^n} &= K_{(MV^{\bullet+})^2.(H^+)^2} \\ &= [MV^{\bullet+}]^2.K^{cb}_{(H^+)^2} + [H^+]^2.K_{(MV^{\bullet+})^2} \\ &= [MV^{\bullet+}]^2.[H^+].K^{cb}_{(H^+)} + [H^+]^2.[MV^{\bullet+}].K_{(MV^{\bullet+})} \end{aligned} \qquad (5.2.8.–3)$$

$$K_{S_{Ox}} = K_{(H^+)^2} = [H^+].K_{(H^+)} \qquad (5.2.8.–4)$$

There is no particular order when applying conversion rules. For instance, in the half-saturation coefficient for reduced mediator, the composition rule was applied first. However, if priority is given to the exponentiation rule, the final result is the same,

$$
\begin{aligned}
K_{M_{Red}\cdot\left(H^+\right)^n} &= K_{\left(MV^{\bullet+}\right)^2\cdot\left(H^+\right)^2} \\
&= \left[MV^{\bullet+}\right].\left[H^+\right].K_{\left(MV^{\bullet+}\right)\cdot\left(H^+\right)} \\
&= \left[MV^{\bullet+}\right].\left[H^+\right].\left(\left[MV^{\bullet+}\right].K^{cb}_{\left(H^+\right)} + \left[H^+\right].K_{\left(MV^{\bullet+}\right)}\right) \\
&= \left[MV^{\bullet+}\right]^2.\left[H^+\right].K^{cb}_{\left(H^+\right)} + \left[H^+\right]^2.\left[MV^{\bullet+}\right].K_{\left(MV^{\bullet+}\right)}
\end{aligned}
\qquad (5.2.8.–5)
$$

Recalling the irreversible forward rate equation,

$$
r^{irrev,f}_{cat} = \frac{V_f^2.\dfrac{M_{Red}.\left[H^+\right]^n}{K_{M_{Red}\cdot\left(H^+\right)^n}}.\dfrac{S_{Ox}}{K_{S_{Ox}}}}{V_f.\left[\dfrac{M_{Red}.\left[H^+\right]^n}{K_{M_{Red}\cdot\left(H^+\right)^n}} + 2.\dfrac{M_{Red}.\left[H^+\right]^n}{K_{M_{Red}\cdot\left(H^+\right)^n}}.\dfrac{S_{Ox}}{K_{S_{Ox}}} + \dfrac{S_{Ox}}{K_{S_{Ox}}}\right]}
\qquad (5.2.8.–6)
$$

application of all conversion rules and subsequent simplification yields the following result,

$$
\Leftrightarrow r^{irrev,f}_{cat} = \frac{V_f.\dfrac{\left[MV^{\bullet+}\right].\left[H^+\right]}{\left[MV^{\bullet+}\right].K^{cb}_{\left(H^+\right)} + \left[H^+\right].K_{\left(MV^{\bullet+}\right)}}.\dfrac{\left[H^+\right]}{K_{\left(H^+\right)}}}{\left[\dfrac{\left[MV^{\bullet+}\right].\left[H^+\right]}{\left[MV^{\bullet+}\right].K^{cb}_{\left(H^+\right)} + \left[H^+\right].K_{\left(MV^{\bullet+}\right)}} + \dfrac{\left[H^+\right]}{K_{\left(H^+\right)}} + 2.\dfrac{\left[MV^{\bullet+}\right].\left[H^+\right]}{\left[MV^{\bullet+}\right].K^{cb}_{\left(H^+\right)} + \left[H^+\right].K_{\left(MV^{\bullet+}\right)}}.\dfrac{\left[H^+\right]}{K_{\left(H^+\right)}}\right]}
\qquad (5.2.8.–8)
$$

Further simplification is possible, namely by simultaneous elimination of protons from numerator and denominator, which, although mathematically sound, would contradict the *a priori* assigned meaning of those protons.

5.2.8.1. Influence of pH in Catabolism

The distinction between mediator protons, substrate protons and biomass counterbalancing protons may yet provide clues on how to include the effects of pH in previously derived reversible rate equations. Microbial life – and indeed all life as we know

it – is inhibited by sufficiently acidic environments. The threshold for inhibition varies greatly. While most known bacteria grow well at pH~7, acidophiles have optimal growth at pH values somewhere between 1 and 6, and alkaliphiles between 9 and 11 (Singleton and Sainsbury, 2006).

On the other hand, and as we just saw, a universal method capable of accounting for proton inhibition should not rely on mediator or substrate protons: if e.g. the mediator is methyl viologen and the external substrate is Fe^{2+}/Fe^{3+}, neither of those types of protons will be present. However, counterbalancing protons are always present, and could thus be an adequate pivot to express pH inhibition. Rigorous derivation of the necessary formulae would require the complete analysis of possible side reactions between biomass and protons. However, a reasonable approximation might be achieved through analogy with the classical substrate inhibition case (Bommarius and Riebel-Bommarius, 2007). Consider the formula for Michaelis-Menten kinetics with counterbalancing protons as substrate, with and without substrate inhibition. Respectively,

$$r = k_2.E_0.\frac{\left[H^+\right]}{K^{cb}_{S,\left(H^+\right)} + \left[H^+\right].\left(1 + \frac{\left[H^+\right]}{K^{cb}_{I,\left(H^+\right)}}\right)} \qquad (5.2.8.1.–1)$$

$$r = k_2.E_0.\frac{\left[H^+\right]}{K^{cb}_{App,\left(H^+\right)} + \left[H^+\right]} \qquad (5.2.8.1.–2)$$

The intended result of this derivation is an apparent, rate preserving, half-saturation constant that implicitly represents both productive and inhibitory interactions, such that this apparent constant could be used to express pH inhibition without having to re-derive the rate equations for MET. A method to obtain this constant is to equal the rates of the above two equations,

$$k_2.E_0.\frac{\left[H^+\right]}{K^{cb}_{S,\left(H^+\right)} + \left[H^+\right].\left(1 + \frac{\left[H^+\right]}{K^{cb}_{I,\left(H^+\right)}}\right)} = k_2.E_0.\frac{\left[H^+\right]}{K^{cb}_{App,\left(H^+\right)} + \left[H^+\right]} \qquad (5.2.8.1.–3)$$

$$\Rightarrow K^{cb}_{App,\left(H^+\right)} = K^{cb}_{S,\left(H^+\right)} + \frac{\left[H^+\right]^2}{K^{cb}_{I,\left(H^+\right)}} \qquad (5.2.8.1.–4)$$

which results in a variable, apparent half-saturation coefficient, including substrate half-saturation and inhibition half-saturation constants, allowing for fine tuning of pH-dependent kinetics – see Figure 14. This is especially relevant in the field of Bioelectrochemical Systems, since it has been shown that excessive acidification of bioanodes (Picioreanu et al., 2010a) and alkalinisation of cathodes (Popat et al., 2012) are two of the main hindrances to continuous BESs operation. This effect is caused by migration of ions other than hydronium or hydroxide through the compartment-separating membrane. Recalling the discussion in 2.1.Bioelectrochemical Systems, the relative abundance of ions such as sodium results in closure of the ionic circuit by those ions instead of hydronium, thus causing a counterproductive pH gradient between the two compartments (Harnisch and Schröder, 2009).

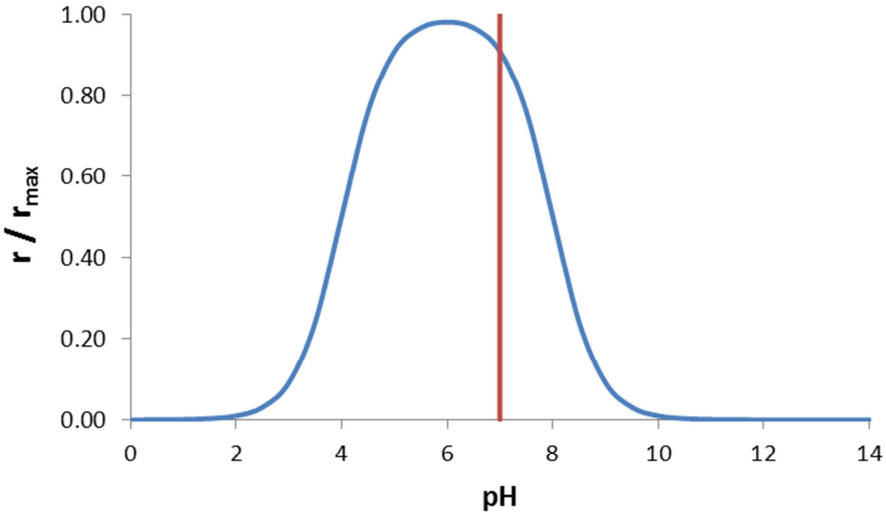

Figure 14 - Michaelis-Menten kinetics with apparent proton half-saturation coefficient: affinity constant at pH=8 and inhibition constant at pH=4. Maximal rates are observed at the pH average of the two constants. Also, if the difference between the two constants is larger, the bell shaped growth curve will also be broader. Thus, usage of the apparent coefficient to express simultaneous productive and inhibitory interactions makes it possible to effectively manipulate rate equations into having maximum values at any pH, with any desired sensitivity to hydronium concentration. For details, see 5.2.8.1.Influence of pH in Catabolism.

6. Catabolic Rate of Direct Electron Transfer

For DET, as the name implies, there is no intermediate redox shuttle, meaning the biomass redox intermediate directly interacts with the electrode or, in long-range DET, the biofilm matrix. Thus, e.g. for cathodic processes, the heterogeneous component of kinetics is the conversion of oxidized biomass **X** into reduced biomass $\mathbf{XH_n}$. Therefore, rates are best expressed using heterogeneous current densities – a measure of how many electrons are exchanged between electrode or matrix and the underlying liquid solution. The following chemical equations apply,

$$\begin{cases} \text{Half-oxidation}: XH_n \underset{\text{Reduction}}{\overset{\text{Oxidation}}{\rightleftharpoons}} X + n.H^+ + n.e^- \\ \text{Half-reduction}: S_{Ox} + n.e^- \underset{\text{Oxidation}}{\overset{\text{Reduction}}{\rightleftharpoons}} S_{Red} \end{cases}$$

$$\Rightarrow \begin{cases} \text{Heterogeneous}: X + n.H^+ + n.e^- \underset{k_a}{\overset{k_c}{\rightleftharpoons}} XH_n \\ \text{Homogeneous}: S_{Ox} + XH_n \underset{k_{-1}}{\overset{k_1}{\rightleftharpoons}} X_S \underset{k_{-2}}{\overset{k_2}{\rightleftharpoons}} S_{Red} + X + n.H^+ \end{cases}$$

As in 5.Catabolic Rate of Mediated Electron Transfer, chemical equations are written such that the forward direction is cathodic and the reverse direction is anodic. This formulation differs from the one proposed by Hamelers and co-workers (Hamelers et al., 2011), specifically in the implicit properties of biomass intermediates. Namely, in their representation, oxidized biomass is depicted as X_{Ox}, and reduced biomass as X_{Red}. These are not idealized species such as S_{Ox} and S_{Red}, but instead have the same meaning as X and XH_n, respectively. Since protons are not accounted for in the Butler-Volmer-Monod model, at least one of their stable biomass intermediates has a net electrical charge, which, as discussed in 5.2.Microbial Kinetics in MET, should not happen, given that electron transport chains always carry electrons accompanied by protons.

Many of the elements necessary to the derivation of a reversible rate equation for DET are similar to their counterparts in MET, and won't be discussed in great detail.

6.1.Heterogeneous Kinetics

The first necessary element is a method to describe the kinetics of the heterogeneous cell-conductive matrix electron transfer reaction. Here, the Butler-Volmer model is applied in much the same formulation as in 5.1.Electrode Kinetics in MET,

$$X + n.H^+ + n.e^- \underset{k_a}{\overset{k_c}{\rightleftharpoons}} XH_n$$

$$j = n.F.\left(k_a.XH_n - k_c.\left[H^+\right]^n.X\right) \qquad (6.1.–1)$$

$$k_a = k^\circ.\exp\left(+\alpha_a.\frac{n.F}{R.T}.\left\{\left[\varphi_{matrix} - \varphi_{solution}\right] - E^o_{XH_n/X}\right\}\right) \qquad (6.1.–2)$$

$$k_c = \frac{k^\circ}{\left(\left[H^+\right]^\circ\right)^n}.\exp\left(-\alpha_c.\frac{n.F}{R.T}.\left\{\left[\varphi_{matrix} - \varphi_{solution}\right] - E^o_{XH_n/X}\right\}\right) \qquad (6.1.–3)$$

the only difference being substitution of electrode potential $\varphi_{electrode}$ by matrix potential φ_{matrix}, since long-range DET can occur at any height within the biofilm: the apparently conductive matrix behaves as an extension of the electrode. The standard biomass reduction potential may be estimated from the standard reduction potentials of abundant metabolic redox intermediates, such as NADH/NAD^+ or OmcA in *Shewanella oneidensis* (Carmona-Martínez et al., 2012), although rigor mandates its determination by fitting of experimental data.

6.2.Differential and Mass Biomass Balances

Substitution of XH_n and X in the Butler-Volmer equation by their respective biomass distribution formula is the next obvious step. Recalling the chemical equations for DET,

$$\mathrm{X + n.H^+ + n.e^- \underset{k_a}{\overset{k_c}{\rightleftharpoons}} XH_n}$$

$$\mathrm{S_{Ox} + XH_n \underset{k_{-1}}{\overset{k_1}{\rightleftharpoons}} X_S \underset{k_{-2}}{\overset{k_2}{\rightleftharpoons}} S_{Red} + X + n.H^+}$$

And applying the quasi-steady-state assumption, extensively discussed in 5.2.1.Quasi-steady-state, and a mass balance to the biocatalyst,

$$\frac{d}{dt}X : 0 = +k_2.X_S - k_{-2}.S_{Red}.\left[H^+\right]^n.X - k_c.\left[H^+\right]^n.X.\frac{A_r}{V_r} + k_a.XH_n.\frac{A_r}{V_r} \qquad (6.2.–1)$$

$$\frac{d}{dt}X_S : 0 = +k_1.S_{Ox}.XH_n - k_{-1}.X_S - k_2.X_S + k_{-2}.S_{Red}.\left[H^+\right]^n.X \qquad (6.2.–2)$$

$$\frac{d}{dt}XH_n : 0 = -k_1.S_{Ox}.XH_n + k_{-1}.X_S + k_c.\left[H^+\right]^n.X.\frac{A_r}{V_r} - k_a.XH_n.\frac{A_r}{V_r} \qquad (6.2.–3)$$

$$X_T = X + X_S + XH_n \qquad (6.2.–4)$$

As previously, it is always possible to write one of the differential balances as a linear combination of the remaining two, meaning the above four expressions form a system of three equations and three variables. Noteworthy, the homogeneous or heterogeneous nature of each kinetic step is accounted for in the above expressions. Namely, when dealing with heterogeneous steps, the rates of consumption/generation are converted into equivalent homogeneous rates using the volumetric surface area $\mathbf{A_r/V_r}$, something that was lacking in the Butler-Volmer-Monod model (Hamelers et al., 2011). For example,

$$\left[\mathrm{k_a} . \mathrm{XH_n} . \frac{\mathrm{A_r}}{\mathrm{V_r}} \right] = \frac{\mathrm{m}}{\mathrm{s}} . \frac{\mathrm{mol}}{\mathrm{m^3}} . \frac{\mathrm{m^2}}{\mathrm{m^3}} = \frac{\mathrm{mol}}{\mathrm{m^3 . s}}$$

instead of

$$\left[\mathrm{k_a} . \mathrm{XH_n} \right] = \frac{\mathrm{m}}{\mathrm{s}} . \frac{\mathrm{mol}}{\mathrm{m^3}} = \frac{\mathrm{mol}}{\mathrm{m^2 . s}}$$

Qualitatively, the substance that reacts or is produced at surface A_r will, respectively, depopulate or populate the adjacent solution volume V_r, hence the need to convert turnovers per unit area into turnovers per unit volume. The conversion could also be performed the other way around, that is, homogeneous rates into heterogeneous rates, resulting in differentials for surface concentrations. For instance, for oxidized biomass,

$$\frac{d}{dt}\Gamma_X : 0 = +k_2 . X_S . \frac{V_r}{A_r} - k_{-2} . S_{Red} . \left[H^+ \right]^n . X . \frac{V_r}{A_r} - k_c . \left[H^+ \right]^n . X + k_a . XH_n \qquad (6.2.–5)$$

6.3. Half-saturation Coefficients and Peak Current Densities

Concerning rate constants and coefficients, $\mathbf{k_a}$ and $\mathbf{k_c}$ are defined by the Butler-Volmer model, meaning only the homogeneous rate constant pose a problem. Recalling the homogeneous component of DET and following the procedure discussed in 5.2.2.Definition of Half-saturation Constants,

$$\mathrm{S_{Ox}} + \mathrm{XH_n} \underset{\mathrm{k_{-1}}}{\overset{\mathrm{k_1}}{\rightleftarrows}} \mathrm{X_S} \underset{\mathrm{k_{-2}}}{\overset{\mathrm{k_2}}{\rightleftarrows}} \mathrm{S_{Red}} + \mathrm{X} + \mathrm{n} . \mathrm{H^+}$$

$$K_{S_{Ox}} = \frac{k_{-1} + k_2}{k_1} \Leftrightarrow k_1 = \frac{k_{-1} + k_2}{K_{S_{Ox}}} \qquad (6.3.–1)$$

$$K_{S_{Red}\cdot\left(H^+\right)^n} = \frac{k_{-1}+k_2}{k_{-2}} \Leftrightarrow k_{-2} = \frac{k_{-1}+k_2}{K_{S_{Red}\cdot\left(H^+\right)^n}} \quad (6.3.–2)$$

The concepts developed in 5.2.3.Definition of Maximum Rates also apply to DET, albeit in a slightly different manner. Unlike in MET, the intended result of this derivation is not a rate equation *per se*, but an expression for heterogeneous current density. Thus, and considering chemical equations were written in the cathodic direction, the equivalent to maximum forward rate is the peak cathodic current density, and the equivalent to maximum reverse rate is the peak anodic current density. Furthermore, and following the approach proposed by Hamelers and co-workers (Hamelers et al., 2011) microbial kinetics is assumed to be limiting, since – ignoring hypothetical electrode side reactions – electrode potentials can be manipulated at will, such that the (lack of) electrochemical driving force is never an unavoidable restriction. If microbial kinetics is limiting, the cathodic reaction will be fastest when all biomass is being converted into the cathodic substrate **X**,

$$\left(-j_{pc}\right) = n.F.k_2.X_T.\frac{V_r}{A_r} \Leftrightarrow k_2 = \frac{\left(-j_{pc}\right)}{n.F.X_T}.\frac{A_r}{V_r} \quad (6.3.–3)$$

where the peak cathodic current density is accompanied by a minus sign since cathodic currents are negative by definition. Similarly, the anodic reaction will be fastest when all biomass is being converted into the anodic substrate XH_n,

$$\left(+j_{pa}\right) = n.F.k_{-1}.X_T.\frac{V_r}{A_r} \Leftrightarrow k_{-1} = \frac{\left(+j_{pa}\right)}{n.F.X_T}.\frac{A_r}{V_r} \quad (6.3.–4)$$

Experimentally, peak cathodic and anodic currents can be measured using different voltammetric techniques, the most popular being cyclic voltammetry (CV) (Logan, 2012; Harnisch and Rabaey, 2012) – see (Harnisch and Freguia, 2012) for a tutorial on CV.

6.4.Biomass Distribution Equations

Using the rate constant definitions established in the previous chapter, the system of equation derived in 6.2.Differential and Mass Biomass Balances yields the following biomass distribution equations,

$$Denominator\Big|_{DET} = \frac{K_{(S_{Red}).(H^+)^n} + S_{Red}.\left[H^+\right]^n}{K_{(S_{Red}).(H^+)^n}}.\left[\frac{\left(-j_{pc}\right)}{n.F.X_T}.\frac{S_{Ox}}{K_{S_{Ox}}} + k_a\right] + \frac{K_{S_{Ox}} + S_{Ox}}{K_{S_{Ox}}}.\left[\frac{\left(+j_{pa}\right)}{n.F.X_T}.\frac{S_{Red}.\left[H^+\right]^n}{K_{(S_{Red}).(H^+)^n}} + k_c.\left[H^+\right]^n\right] \quad (6.4.–1)$$

$$\frac{X}{X_T} = \frac{1}{Denominator\Big|_{DET}}.\left[\frac{\left(-j_{pc}\right)}{n.F.X_T}.\frac{S_{Ox}}{K_{S_{Ox}}} + k_a\right] \quad (6.4.–2)$$

$$\frac{X_S}{X_T} = \frac{1}{Denominator\Big|_{DET}}.\left[\frac{S_{Red}.\left[H^+\right]^n}{K_{S_{Red}.(H^+)^n}}.\left(\frac{\left(-j_{pc}\right)}{n.F.X_T}.\frac{S_{Ox}}{K_{S_{Ox}}} + k_a\right) + \frac{S_{Ox}}{K_{S_{Ox}}}.\left(\frac{\left(+j_{pa}\right)}{n.F.X_T}.\frac{S_{Red}.\left[H^+\right]^n}{K_{S_{Red}.(H^+)^n}} + k_c.\left[H^+\right]^n\right)\right] \quad (6.4.–3)$$

$$\frac{XH_n}{X_T} = \frac{1}{Denominator\Big|_{DET}}.\left[\frac{\left(+j_{pa}\right)}{n.F.X_T}.\frac{S_{Red}.\left[H^+\right]^n}{K_{S_{Red}.(H^+)^n}} + k_c.\left[H^+\right]^n\right] \quad (6.4.–4)$$

The discussion in 5.2.4.Biomass Distribution Equations also applies to this set of biomass distribution equations: they allow verification of localized redox states within EABs, thus potentially endowing the mathematical construct herein developed with the status of theory.

6.5.Heterogeneous Current Density and Equilibrium Constant

Direct substitution of the biomass distribution equations for **X** and $\mathbf{XH_n}$ into the main Butler-Volmer equation,

$$j = n.F.\left(k_a.XH_n - k_c.\left[H^+\right]^n.X\right) \quad (6.5.–1)$$

yields the reversible heterogeneous current density equation,

$$j = \frac{1}{Denominator\big|_{DET}} . \left[\left(+j_{pa}\right) . \frac{S_{Red} . \left[H^+\right]^n}{K_{\left(S_{Red}\right) . \left(H^+\right)^n}} . k_a - \left(-j_{pc}\right) . \frac{S_{Ox}}{K_{S_{Ox}}} . k_c . \left[H^+\right]^n \right] \quad (6.5.–2)$$

Furthermore, following a procedure similar to the one employed in 5.2.5.Net Reversible Rate Equation and Equilibrium Constant, derivation of the heterogeneous equilibrium constant for DET yields,

$$K_{eq,cat}^{heterogeneous} = \frac{k_c . k_1 . k_2}{k_a . k_{-1} . k_{-2}} = \frac{\left(-j_{pc}\right)}{\left(+j_{pa}\right)} . \frac{K_{S_{Red} . \left(H^+\right)^n}}{K_{S_{Ox}}} . \frac{k_c}{k_a} \quad (6.5.–3)$$

6.6.Peak Current Densities as Thermodynamic Parameters

The procedure described in 5.2.6.Maximum Rates as Thermodynamic Parameters may also be applied to DET. The thermodynamic definition of equilibrium constant is valid as always,

$$K_{eq,cat}^{heterogeneous} = \exp\left(-\frac{\Delta_r G_{cat}^{\circ}}{R.T} \right) \quad (6.6.–1)$$

$$\Rightarrow \exp\left(-\frac{\Delta_r G_{cat}^{\circ}}{R.T} \right) = \frac{\left(-j_{pc}\right)}{\left(+j_{pa}\right)} . \frac{K_{S_{Red} . \left(H^+\right)^n}}{K_{S_{Ox}}} . \frac{k_c}{k_a} \quad (6.6.–2)$$

The standard Gibbs energy of reaction refers to net catabolism, that is, reduction/oxidation of an external substrate by an electrode or conductive matrix at a certain potential **φ**. Thus, representing the net heterogeneous reaction, and applying the approach used to derive the fundamental one-step, one-electron Butler-Volmer law (Bard and Faulkner, 2001).

$$S_{Ox} + n . e^- \underset{Anodic}{\overset{Cathodic}{\rightleftharpoons}} S_{Red}$$

$$\Delta_r G_{cat}^{\circ} = -n.F. \left(E_{S_{Red}/S_{Ox}}^{\circ} - \left[\varphi_{matrix} - \varphi_{solution} \right] \right) \quad (6.6.–3)$$

By definition, $[\boldsymbol{\varphi_{matrix} - \varphi_{solution}}]$ is the reduction potential of the interacting solid: the lower (more cathodic) this potential, the higher is the solid's tendency to reduce the external substrate **S**. Writing down the actual Gibbs energy of reaction,

$$\Delta_r G_{cat} = \Delta_r G^{\circ}_{cat} + R.T.\ln\left(\frac{S_{Red}}{S_{Ox}}\right)$$

$$\Leftrightarrow \frac{\Delta_r G_{cat}}{-n.F} = \left(E^{\circ}_{S_{Red}/S_{Ox}} - \left[\varphi_{matrix} - \varphi_{solution}\right]\right) - \frac{R.T}{n.F}.\ln\left(\frac{S_{Red}}{S_{Ox}}\right) \qquad (6.6.–4)$$

$$\Leftrightarrow E_{cat} = E_{S_{Red}/S_{Ox}} - \left[\varphi_{matrix} - \varphi_{solution}\right]$$

On the other hand, as was the case for maximum forward and reverse rates in MET, the maximum DET rate is the difference between anodic and cathodic peak current densities. Since reactions were written in the cathodic direction, cathodic peaks correspond to forward maxima and anodic peaks to reverse maxima. Thus, with the appropriate heterogeneous-homogeneous conversions,

$$\frac{q_{e,max}}{n}.X_T = \frac{1}{n.F}.\frac{A_r}{V_r}.\left|\left(-j_{pc}\right) - \left(+j_{pa}\right)\right| \qquad (6.6.–5)$$

which, combining with the two definitions of equilibrium constant, yields,

$$\left(-j_{pc}\right) = \frac{q_{e,max}}{n}.n.F.X_T.\frac{V_r}{A_r}.\frac{1}{\left|1 - \exp\left(+\frac{\Delta_r G^{\circ}_{cat}}{R.T}\right).\frac{K_{S_{Red}.\left(H^+\right)^n}}{K_{S_{Ox}}}.\frac{k_c}{k_a}\right|} \qquad (6.6.–6)$$

$$\left(+j_{pa}\right) = \frac{q_{e,max}}{n}.n.F.X_T.\frac{V_r}{A_r}.\frac{1}{\left|\exp\left(-\frac{\Delta_r G^{\circ}_{cat}}{R.T}\right).\frac{K_{S_{Ox}}}{K_{S_{Red}.\left(H^+\right)^n}}.\frac{k_a}{k_c} - 1\right|} \qquad (6.6.–7)$$

These results may be further simplified using the definitions for $\mathbf{k_c}$ and $\mathbf{k_a}$. Recalling the Butler-Volmer formula described in 6.1.Heterogeneous Kinetics, and taking into account that, by definition,

$$\alpha_a + \alpha_c = 1 \qquad (6.6.–8)$$

$$\Rightarrow \frac{k_c}{k_a} = \frac{1}{\left(\left[H^+\right]^\circ\right)^n}.\exp\left(-\frac{n.F}{R.T}.\left\{\left[\varphi_{matrix} - \varphi_{solution}\right] - E^o_{XH_n/X}\right\}\right)$$
$$\Leftrightarrow \frac{k_a}{k_c} = \left(\left[H^+\right]^\circ\right)^n.\exp\left(+\frac{n.F}{R.T}.\left\{\left[\varphi_{matrix} - \varphi_{solution}\right] - E^o_{XH_n/X}\right\}\right) \quad (6.6.–9)$$

Substituting also the formula for standard Gibbs energy of reaction,

$$\left(-j_{pc}\right) = \frac{q_{e,max}}{n}.n.F.X_T.\frac{V_r}{A_r}.\frac{1}{\left|1 - \frac{1}{\left(\left[H^+\right]^\circ\right)^n}.\exp\left(-\frac{n.F}{R.T}.\left\{E^\circ_{S_{Red}/S_{Ox}} - E^o_{XH_n/X}\right\}\right).\frac{K_{S_{Red}.\left(H^+\right)^n}}{K_{S_{Ox}}}\right|} \quad (6.6.–10)$$

$$\left(+j_{pa}\right) = \frac{q_{e,max}}{n}.n.F.X_T.\frac{V_r}{A_r}.\frac{1}{\left|\left(\left[H^+\right]^\circ\right)^n.\exp\left(+\frac{n.F}{R.T}.\left\{E^\circ_{S_{Red}/S_{Ox}} - E^o_{XH_n/X}\right\}\right).\frac{K_{S_{Ox}}}{K_{S_{Red}.\left(H^+\right)^n}} - 1\right|} \quad (6.6.–11)$$

Besides the fundamental relevance of discussing the thermodynamic nature of maximum rates in 5.2.6.Maximum Rates as Thermodynamic Parameters, this result provides a simple method to determine the substrate affinities of EABs from voltammetric data. The only problematic parameter is the standard reduction potential of biomass. As discussed in 5.2.Microbial Kinetics in MET, one of the metabolic intermediates that best represents the abstract concept of biomass redox state is the pair NADH/NAD^+: thus, its standard reduction potential, -0.113V (Rabaey et al., 2010), could be used as a reasonable approximation. Furthermore, and according to the assumption that microbial kinetics is limiting in 6.3.Half-saturation Coefficients and Peak Current Densities, peak current densities are ultimately not a function of electrode potentials.

6.7.Irreversible Kinetics

Irreversible DET kinetics is observed if either S_{Red} or S_{Ox} is absent or present in negligible amounts. If there is no reduced substrate, EET will be purely cathodic (Figure 15),

$$S_{Red} \to 0$$

$$\Rightarrow j_c = \frac{-\left(-j_{pc}\right).\frac{S_{Ox}}{K_{S_{Ox}}}.k_c.\left[H^+\right]^n}{\frac{S_{Ox}}{K_{S_{Ox}}}.\left[\frac{\left(-j_{pc}\right)}{n.F.X_T}+k_c.\left[H^+\right]^n\right]+k_a+k_c.\left[H^+\right]^n} \qquad (6.7.–1)$$

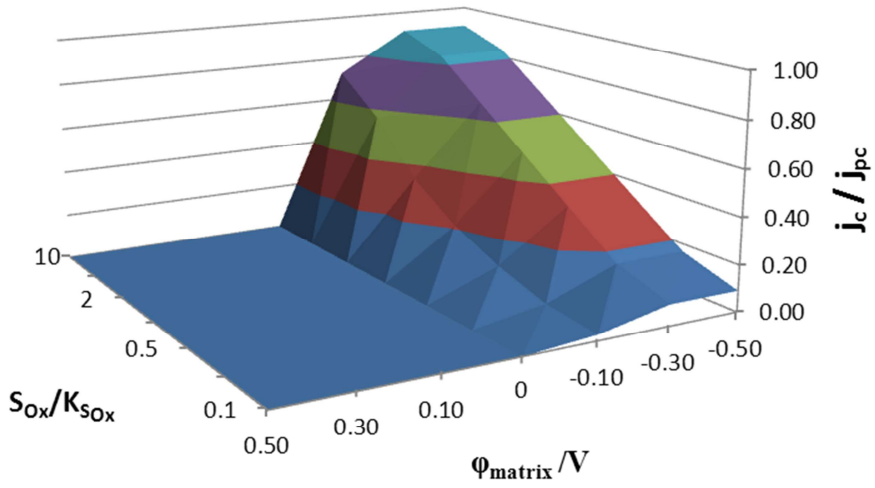

Figure 15 - Irreversible cathodic EET observed in the absence of reduced substrate S_{Red}. If the electrode or matrix potential is too high (too anodic), the reaction is halted: the nearly infinite chemical (concentration) potential caused by the absence of S_{Red} is counterbalanced by the nearly infinite electrochemical potential favoring anodic processes, thus highlighting the interaction of the two types of driving forces in bioelectrochemical systems, as discussed in 3.1.2.Kinetics in MET. Parameters: $pH=pH_{reference}=7$; n=2; F=96485 $C.mol^{-1}$; R=8.3145 $J.K^{-1}.mol^{-1}$; T=298.15 K; $\varphi_{solution}=0$ V; $X_T=4000$ $C\text{-}mol.m^{-3}$, equivalent to roughly $100g.L^{-1}$; $k°=10^{-6}m.s^{-1}$, calculated from (Tatsumi et al., 1999); $\alpha_a=\alpha_c=0.5$; $E^o_{XH_n/X}$ = –0.113 V, based on the standard reduction potential of $NADH/NAD^+$ (Rabaey et al., 2010).

Noteworthy, even though the microbial reaction is irreversible due to lack of reduced substrate, the equilibrium of anodic and cathodic processes at the matrix-biomass intermediate interface is still relevant, given that $\mathbf{k_a}$ is still present in the denominator. Thus, when EET is predominantly cathodic and too much biomass is reduced, some of the electrons may flow back into the electrode without reaching the external substrate, as expected from Butler-Volmer kinetics: microbial kinetics doesn't seem to affect electrochemical reversibility. This rational may also be adapted to the predominantly anodic case,

$$S_{Ox} \to 0$$

$$\Rightarrow j_a = \frac{\left(+j_{pa}\right).\dfrac{S_{Red}.\left[H^+\right]^n}{K_{(S_{Red}).\left(H^+\right)^n}}.k_a}{\dfrac{S_{Red}.\left[H^+\right]^n}{K_{(S_{Red}).\left(H^+\right)^n}}.\left[\dfrac{\left(+j_{pa}\right)}{n.F.X_T}+k_a\right]+k_a+k_c.\left[H^+\right]^n} \qquad (6.7.–2)$$

7. Anabolic Rates

Derivation of an expression for growth rate first requires an anabolic stoichiometry that is compatible with both mediated and direct electron transfer, and also remains unchanged upon catabolic inversion, e.g. from an anode to a cathode. Let us consider the case of organo-hetero-trophic metabolism with acetate as substrate (Nelson and Cox, 2009). Acetate is both the source of energy, reducing equivalents and carbon, albeit through separate pathways. As an energy source, acetate is oxidized intracellularly to bicarbonate, with concomitant reduction of NAD^+ to NADH. NADH then donates electrons to an electron transport chain, which then generates a proton motive force convertible into ADP phosphorylation, thus completing the catabolic pathway of oxidative phosphorylation. However, NADH may also be used as source of reducing equivalents for biosynthetic purposes, meaning acetate is ultimately the source of reducing equivalents. Furthermore, in organo-hetero-trophic growth, the source of energy and carbon is usually the same, with a small fraction of metabolized acetate receiving electrons from NADH to promote its reduction to ultimately biomass (Nelson and Cox, 2009). From an electrochemical perspective, this is but a dismutation of the pool of acetate: spontaneous oxidation into bicarbonate is coupled to unspontaneous reduction into biomass. The redox broker coupling both reactions is $NADH/NAD^+$, which as discussed multiple times in previous chapters, is one of the prime contributors to the overall biomass redox state.

Catabolic inversion in organo-hetero-trophic growth is unlikely, especially if also aerobic. However, lithotrophy helps solidify the concept of mandatory redox intermediates. For instance, in litho-hetero-trophic growth, organic compounds are used solely as sources of carbon. As for energy, electron donors are external inorganics. The source of reducing equivalents is also the same donor. If the reduction potential of said donor is too high, reversed electron transport is necessary: electron transport chains (ETCs) consume proton motive force (PMF) in order to momentarily operate with reversed electron flux (Singleton and Sainsbury, 2006). This decreases the reduction potential of electrons provided by the donor, such that reduction of NAD+ becomes possible. And as usual, the resulting NADH is then the intermediate electron donor for anabolism.

Thus, in all cases, electrons provided by a donor go through a redox intermediate before reaching anabolism. Even if the external donor changes, e.g. in the event of catabolic inversion, the redox intermediate remains the same. Thus, the *de facto* reductant for anabolism is XH_n/X.

7.1. Stoichiometry of Growth

Let's consider the model organic substrate acetate and write a tentative chemical scheme, including also ammonium as nitrogen source, biomass as synthesis product, protons for charge balancing purposes and water to balance oxygen and hydrogen,

$$a.CH_3COO^- + b.NH_4^+ + c.H^+ + d.\left(XH_n - X\right) + 1.CH_{1.8}O_{0.5}N_{0.2} + e.H_2O = 0 \quad (7.1.–1)$$

Hydroxide could have been used instead of hydronium, since the intracellular medium is kept roughly at neutral pH (Nelson and Cox, 2009). The five stoichiometric coefficients may be calculated using elemental balances to carbon, nitrogen, oxygen and hydrogen, and a charge balance. Briefly,

$$\begin{cases} \mathrm{C}: 2.a + 1 = 0 \\ \mathrm{N}: b + 0.2 = 0 \\ \mathrm{O}: 2.a + 0.5 + e = 0 \\ \mathrm{H}: 3.a + 4.b + c + n.d + 1.8 + 2.e = 0 \\ Charge: -a + b + c = 0 \end{cases} \Leftrightarrow \begin{cases} a = -0.5 \\ b = -0.2 \\ c = -0.3 \\ d = -0.2\dfrac{1}{n} \\ e = +0.5 \end{cases} \quad (7.1.–2)$$

Thus, the following chemical equation applies to anabolic consumption of acetate,

$$0.5\,\mathrm{CH_3COO^-(aq)} + 0.2\,\mathrm{NH_4^+(aq)} + \left(0.3 + 0.2\frac{1}{\mathrm{n}}\mathrm{n}\right)\mathrm{H^+(aq)} + 0.2\frac{1}{\mathrm{n}}\mathrm{XH_n}$$
$$\underset{\text{decay}}{\overset{\text{biosynthesis}}{\rightleftharpoons}} \mathrm{CH_{1.8}O_{0.5}N_{0.2}(s)} + 0.5\,\mathrm{H_2O(l)} + 0.2\frac{1}{\mathrm{n}}\mathrm{X} + 0.2\frac{1}{\mathrm{n}}\mathrm{n\,H^+(aq)}$$

Some protons are also represented into right-hand side of the equation, to distinguish the protons released by the half-oxidation of XH_n, from those consumed in the half-reduction of acetate. Evidently, this reaction is reversible, the opposite of growth being endogenous respiration, which generates reduced biomass intermediates capable of acting as donors for respiration, thus providing maintenance energy in the absence of an external electron donor (Heijnen et al., 1992; Heijnen and Kleerebezem, 2010).

7.2. Thermodynamics of Growth

According to Heijnen and co-workers (Heijnen et al., 1992; Heijnen and Kleerebezem, 2010), there are four main thermodynamic sub-units in microbial growth systems: catabolism, anabolism, dissipation and maintenance. Of the four processes, only catabolism is spontaneous, meaning growth is only possible if catabolism generates enough energy to compensate for dissipation and sustain maintenance. If catabolism produces insufficient energy, anabolism will be reversed to sustain maintenance: the cell oxidises non-essential biomolecules in order to generate the energy necessary to compensate for membrane leakage and spontaneous denaturation events, in a process known as endogenous respiration (Heijnen et al., 1992; Heijnen and Kleerebezem, 2010). Evidently, since

biomass is oxidizing itself in order to stay alive, endogenous respiration eventually leads to cellular death: otherwise the cycle of carbon-source-into-biomass followed by biomass-into-carbon-source would correspond to a perpetual motion machine, violating the first and second laws of thermodynamics.

7.2.1. Catabolism

The thermodynamics of catabolism is represented by its Gibbs energy of reaction. For MET, and considering the net catabolic reaction in the cathodic direction,

$$\mathrm{M_{Red}} + \mathrm{S_{Ox}} \underset{\text{Anodic}}{\overset{\text{Cathodic}}{\rightleftharpoons}} \mathrm{M_{Ox}} + \mathrm{S_{Red}}$$

$$\Delta_r G^{\circ}_{cat}\Big|_{MET} = -n.F.\left(E^{\circ}_{S_{Red}/S_{Ox}} - E^{\circ}_{M_{Red}/M_{Ox}} \right) \qquad (7.2.1.–1)$$

$$\Delta_r G_{cat}\Big|_{MET} = \Delta_r G^{\circ}_{cat}\Big|_{MET} + R.T.\ln\left(\frac{M_{Ox}.S_{Red}}{M_{Red}.S_{Ox}} \right) \qquad (7.2.1.–2)$$

For DET, as discussed in 6.6.Peak Current Densities as Thermodynamic Parameters, the net catabolic reaction – in the cathodic direction – and the respective Gibbs energy of reaction read as,

$$\mathrm{S_{Ox}} + \mathrm{n\,.\,e^-} \underset{\text{Anodic}}{\overset{\text{Cathodic}}{\rightleftharpoons}} \mathrm{S_{Red}}$$

$$\Delta_r G^{\circ}_{cat}\Big|_{DET} = -n.F.\left(E^{\circ}_{S_{Red}/S_{Ox}} - [\varphi_{matrix} - \varphi_{solution}] \right) \qquad (7.2.1.–3)$$

$$\begin{aligned} &\Delta_r G_{cat}\Big|_{DET} = \Delta_r G^{\circ}_{cat}\Big|_{DET} + R.T.\ln\left(\frac{S_{Red}}{S_{Ox}} \right) \\ &\Leftrightarrow E_{cat}\Big|_{DET} = E_{S_{Red}/S_{Ox}} - [\varphi_{matrix} - \varphi_{solution}] \end{aligned} \qquad (7.2.1.–4)$$

7.2.2. Anabolism

As for anabolism, again with acetate as an example, and recalling the previously derived stoichiometry,

$$0.5\,CH_3COO^-(aq) + 0.2\,NH_4^+(aq) + \left(0.3 + 0.2\frac{1}{n}\right)H^+(aq) + 0.2\frac{1}{n}XH_n$$
$$\underset{\text{decay}}{\overset{\text{biosynthesis}}{\rightleftarrows}} CH_{1.8}O_{0.5}N_{0.2}(s) + 0.5\,H_2O(l) + 0.2\frac{1}{n}X + 0.2\frac{1}{n}n\,H^+(aq)$$

$$\begin{aligned}\Delta_r G^\circ_{an} = &\left[\Delta_f G^\circ_{CH_{1.8}O_{0.5}N_{0.2}} + 0.5\Delta_f G^\circ_{H_2O}\right] \\ &-\left[0.5\Delta_f G^\circ_{CH_3COO^-} + 0.2\Delta_f G^\circ_{NH_4^+} + \left(0.3 + 0.2\frac{1}{n}\right)\Delta_f G^\circ_{H^+}\right] \\ &-0.2\frac{1}{n}\left(-n.F.E^\circ_{XH_n/X}\right)\end{aligned} \qquad (7.2.2.–1)$$

$$\Delta_r G_{an} = \Delta_r G^\circ_{an} + R.T.\ln\left(\left[CH_3COO^-\right]^{-0.5}.\left[NH_4^+\right]^{-0.2}.\left[H^+\right]^{-0.3}.\left(\frac{\left[XH_n\right]}{\left[X\right]}\right)^{-0.2\frac{1}{n}}\right) \qquad (7.2.2.–2)$$

The Gibbs energy of formation for biomass is estimated at –67 kJ.C-mol^{-1} (Heijnen et al., 1992; Heijnen and Kleerebezem, 2010). Regarding the standard Gibbs energy of anabolism, inevitably the biomass redox intermediate must be accounted for via its standard reduction potential, since it's not explicitly defined and thus it is not possible to assign a value to the Gibbs energy of formation of either oxidized or reduced form. Furthermore, this reduction potential implicitly accounts for those protons released upon biomass redox intermediate half-oxidation, thus requiring their explicit representation in the net stoichiometry to avoid potential miscalculations.

Concerning the actual Gibbs energy of reaction, biomass and water, being solid and liquid respectively, are not represented in the reaction quotient. The physical state of the biomass redox intermediates XH_n and X is not clearly defined. If we consider them to be NADH/NAD$^+$, then they are solutes and should be included in the reaction quotient. If they were to be a certain cytochrome, they could either be solutes or membrane anchored, which doesn't mean they should be regard as inert solids. From an electrochemical perspective, membrane anchored cytochromes are part of circuits ultimately connecting both aqueous interfaces of the membrane – these circuits are also known as electron transport chains. As discussed in 6.6.Peak Current Densities as Thermodynamic Parameters, the Gibbs energy of electrons present in such circuits, e.g. the external circuit of a BES and respective

electrodes, can be accounted for via their electrical potential, whose meaning is equivalent to reduction potential. If this is the case, and according to the Nernst equation, such a potential is a function of the reduced/oxidized ratio of the carrier. For a metal, this would correspond to the density of electrons *vs.* electron-holes (Atkins et al., 2009), whilst for a membrane anchored cytochrome, C_{Red}/C_{Ox} would suffice. Therefore, the inclusion of XH_n and X in the reaction quotient would justified even if they were explicitly membrane anchored cytochromes.

7.2.3. Dissipation

Coupling of catabolism and anabolism is not direct. In fact, the main purpose of electron transport chains is to generate proton motive force, which is then converted into ADP phosphorylation. Even considering the simplest possible coupling, energy would be lost as heat upon: donor oxidation; electron transfer along the ETC; PMF generation; acceptor reduction; PMF conversion into ADP phosphorylation; NAD^+ reduction by a donor; and finally NADH oxidation by the carbon source coupled with ATP hydrolysis. If metabolism is organo-hetero-trophic, then the minimal number of individual reactions is larger, since organic donors such as acetate are first oxidized by NAD^+, and then separately, the co-enzyme reduces an intermediate acceptor in the ETC. The number of individual reactions and potential energy dissipation events will chiefly depend on the reduction potential of the carbon source. Specifically, how far this potential is from the reduction potential of biomass will determine how much energy must be invested to bring the potential of the carbon source to the right level. Based on experimental data, Heijnen and co-workers (Heijnen et al., 1992) proposed a correlation to calculate the dissipation energy for a given carbon source,

$$\begin{cases} \text{without} \quad \text{RET}: \Delta G_{diss} = -\left[200 + 18.\left(6 - \#C\right)^{1.8} + \exp\left\{ \left(\left(3.8 - \gamma_C\right)^2 \right)^{0.16} .\left(3.6 + 0.4\#C\right) \right\} \right] \\ \text{with} \quad \text{RET}: \Delta G_{diss} = -3500 \end{cases} \tag{7.2.3.–1}$$

with dissipation energy in kJ.C-mol^{-1} of newly synthesized biomass, where **#C** is the number of carbon atoms per source molecule and $\boldsymbol{\gamma_C}$ is the degree of reduction in number of electrons per carbon atom. ΔG_{diss} is negative since it represents energy lost as heat, mainly. A thorough explanation of this correlation and concepts such as degree of reduction is provided in (Heijnen and Kleerebezem, 2010), suffice to say the degree of reduction of acetate is +4 mol of e- / C-mol. Whether or not reversed electron transport (RET) is needed, as discussed in 7.Anabolic Rate, depends on whether the reduction potential of the electron donor is sufficiently low to reduce the carbon source spontaneously. As a rule of thumb, Heijnen and co-workers (Heijnen et al., 1992) state RET

is only relevant for autotrophic growth, since the pair acetate/bicarbonate has a standard biochemical reduction potential of –0.278 V, lower than most microbiological electron donors (Rabaey et al., 2010).

However, with the structure developed in this model, it is possible to refine the criteria for RET. Firstly, by virtue of reversibility, the reduction potential of the biomass redox intermediate XH_n/X is always between that of the electron donor and the electron acceptor. Mathematically,

$$\begin{aligned}
&\text{MET}:\\
&\rightarrow \text{Cathodic}: E_{S_{Red}/S_{Ox}} > E_{M_{Red}/M_{Ox}} \Rightarrow E_{S_{Red}/S_{Ox}} > E_{XH_n/X} > E_{M_{Red}/M_{Ox}}\\
&\rightarrow \text{Anodic}: E_{S_{Red}/S_{Ox}} < E_{M_{Red}/M_{Ox}} \Rightarrow E_{S_{Red}/S_{Ox}} < E_{XH_n/X} < E_{M_{Red}/M_{Ox}}\\
&\rightarrow \text{Equilibrium}: E_{S_{Red}/S_{Ox}} = E_{M_{Red}/M_{Ox}} \Rightarrow E_{S_{Red}/S_{Ox}} = E_{XH_n/X} = E_{M_{Red}/M_{Ox}}
\end{aligned} \qquad (7.2.3.–2)$$

$$\begin{aligned}
&\text{DET}:\\
&\rightarrow \text{Cathodic}: E_{S_{Red}/S_{Ox}} > [\varphi_{matrix} - \varphi_{solution}] \Rightarrow E_{S_{Red}/S_{Ox}} > E_{XH_n/X} > [\varphi_{matrix} - \varphi_{solution}]\\
&\rightarrow \text{Anodic}: E_{S_{Red}/S_{Ox}} < [\varphi_{matrix} - \varphi_{solution}] \Rightarrow E_{S_{Red}/S_{Ox}} < E_{XH_n/X} < [\varphi_{matrix} - \varphi_{solution}]\\
&\rightarrow \text{Equilibrium}: E_{S_{Red}/S_{Ox}} = [\varphi_{matrix} - \varphi_{solution}] \Rightarrow E_{S_{Red}/S_{Ox}} = E_{XH_n/X} = [\varphi_{matrix} - \varphi_{solution}]
\end{aligned} \qquad (7.2.3.–3)$$

Thus, if the actual reduction potential of the biomass intermediate is equal or higher than that of the electron donor, and if the reduction potential of said donor is higher than that of the carbon source, naturally the reduction potential of the biomass intermediate is also higher than that of the carbon source. Mathematically,

$$E_{D_{Red}/D_{Ox}} > E_{Biomass/Carbon\ Source} \wedge E_{XH_n/X} > E_{D_{Red}/D_{Ox}} \Rightarrow E_{XH_n/X} > E_{Biomass/Carbon\ Source} \qquad (7.2.3.–4)$$

Thus, for any donor and any carbon source, reversed electron transport is needed when the biomass intermediate can't spontaneously reduce the carbon source into biomass, that is, when the Gibbs energy of reaction for anabolism, as defined in this dissertation, is positive,

$$\begin{cases} \Delta_r G_{an} < 0 \Rightarrow \text{without} \quad \text{RET} \\ \Delta_r G_{an} > 0 \Rightarrow \text{with} \quad \text{RET} \end{cases} \qquad (7.2.3.–5)$$

with dissipation energy in kJ.C-mol^{-1} of newly synthesized biomass. Noteworthy, this conclusion highlights a sort of self-regulation of anabolism: if RET is required, dissipation increases and anabolism slows down, resulting in accumulation of reduced biomass redox intermediate, which in turn lowers the reduction potential of the pair XH_n/X, returning $\Delta_r G_{an}$ to zero. If RET is not required, the opposite will happen, ultimately restoring $\Delta_r G_{an}$ to zero as well. Thus, the anabolic reaction *per se* should always have a near neutral energy balance, and most catabolic energy is consumed by dissipation and maintenance. Thus, from a thermodynamics perspective, perhaps the difference between autotrophy and heterotrophy is simply how many intermediate steps are required to couple catabolism and anabolism.

However, the argument herein develop transcends the scope of the Heijnen correlation. If we want to be sure that dissipation energy estimations are reasonably accurate, we should abide by the conditional formulation described by the authors (Heijnen et al., 1992). Thus,

$$\begin{cases} \mathrm{C_{source}} \;\; \text{is} \;\; \text{organic} : \Delta G_{diss} = -\left[200 + 18.\left(6 - \#C\right)^{1.8} + \exp\left\{ \left(\left(3.8 - \gamma_C\right)^2 \right)^{0.16} .\left(3.6 + 0.4\#C\right) \right\} \right] \\ \mathrm{C_{source}} \;\; \text{is} \;\; \text{inorganic} : \Delta G_{diss} = -3500 \end{cases} \qquad (7.2.3.–6)$$

7.2.4. Maintenance

Maintenance energy is chiefly required for two purposes: recycling denatured biomolecules and correcting membrane leakage. Denaturation of biomolecules, namely proteins, is a probabilistic event: even in intracellular conditions it will occasionally happen (Buxbaum, 2007). Likewise, membrane leakage is also a continuous process of gradient dissipation by diffusion across the cytoplasmic membrane, and must be correct by the cell to maintain homeostasis (Nelson and Cox, 2009). Suffice to say that at 25°C, maintenance energy is estimated at m_G = 4.5 kJ.C-mol^{-1}.h^{-1} (Heijnen et al., 1992), relative to total existing biomass.

7.3.Localized Specific Growth Rate

The specific growth rate **μ** may be obtained by equating the rate of energy generation by catabolism to the sum of energy consumption rates, that is, by a power balance. The energy generated by catabolism is simply the multiplicand of reaction rate and Gibbs energy of reaction,

$$\begin{cases} \text{MET}: q_G^{Generated}\big|_{MET}.X_T = -r_{cat}^{rev}.\Delta_r G_{cat}\big|_{MET} \\ \text{DET}: q_G^{Generated}\big|_{DET}.X_T = \dfrac{j}{n.F}.\dfrac{A_r}{V_r}.\Delta_r G_{cat}\big|_{DET} \end{cases} \tag{7.3.–1}$$

No minus sign is necessary in the DET generation rate since, in this work, the forward direction in catabolic kinetics is cathodic, meaning $\boldsymbol{j}$ and $\Delta_r G_{cat}$ have the same sign. If inversion occurs, the signs in rates and Gibbs energies change, which simply means the dominant reaction direction is the opposite of what was expected. As for energy consumption, dissipation is expressed in energy per C-mol of newly synthesized biomass. Thus,

$$q_G^{Consumed}.X_T = \mu.X_T.\left(\Delta_r G_{an} - \Delta G_{diss}\right) + m_G.X_T \tag{7.3.–2}$$

with m_G positive and ΔG_{diss} negative. Since consumption and generation must be equal,

$$q_G^{Generated}.X_T = q_G^{Consumed}.X_T \tag{7.3.–3}$$

$$\Rightarrow \begin{cases} \text{MET}: \mu = \dfrac{-\dfrac{r_{cat}^{rev}}{X_T}.\Delta_r G_{cat} - m_G}{\Delta_r G_{an} - \Delta G_{diss}} \\ \text{DET}: \mu = \dfrac{\dfrac{j}{F.X_T}.\dfrac{A_r}{V_r}.\Delta_r G_{cat} - m_G}{\Delta_r G_{an} - \Delta G_{diss}} \end{cases} \tag{7.3.–4}$$

Together with the concept of reversibility, this result highlights why life, if possible, evolves to exploit redox systems far from equilibrium. Although energy can theoretically be obtained from forward or reverse reactions, near equilibrium there is a band where $q_G^{Generated}$ is not sufficient to offset maintenance: the endogenous respiration band (Figure 16).

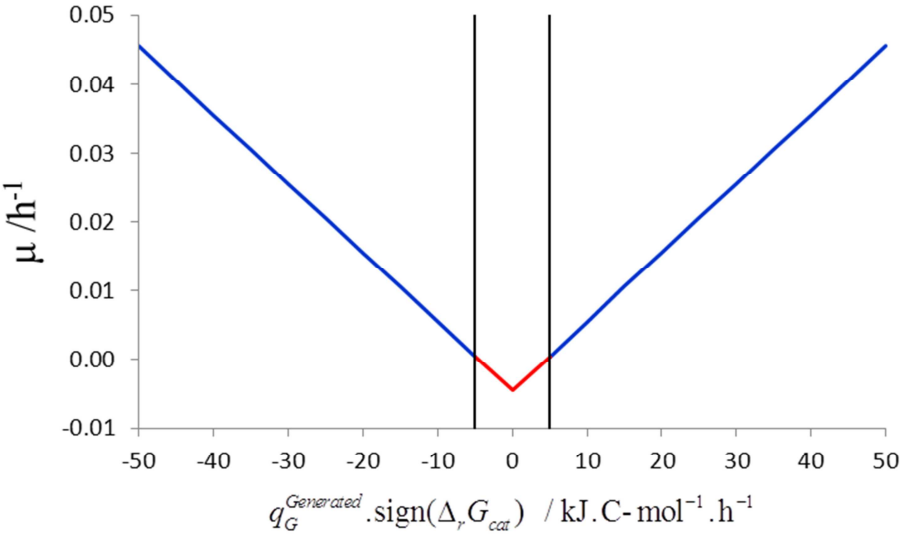

Figure 16 - Endogenous respiration band. If the catabolic reaction is too close to equilibrium, the energy generated is not enough to offset maintenance, thus forcing the cell to oxidize some of its components to remain alive. Hence the negative specific growth rate, representative of decay or endogenous respiration. Parameters: m_G = 4.5 kJ.C-mol^{-1}.h^{-1}, $\Delta_r G_{an}$ = 0 kJ.C-mol^{-1}, ΔG_{diss} = –1000 kJ.C-mol^{-1}.

7.4.Net Biofilm Growth Rate

Derivation of a net biofilm growth rate requires reapplication of the principle used to justify the quasi-steady-state assumption: biofilms grow in volume without major rapid changes in localized density. Thus, the net biofilm growth rate is the velocity at which the biofilm boundary moves, as a result of growth and endogenous respiration. Firstly, we should convert the rate at which biomass concentration would vary into a formula that represents volume variation. The growth rate applicable to suspended cultures,

$$r_X = \mu.X_T \quad \left[\mathrm{C\text{-}mol.m^{-3}.s^{-1}}\right] \qquad (7.4.–1)$$

may be converted into a molar turnover using the geometry in Figure 17,

$$\mu.X_T.A.dx \quad \left[\mathrm{C\text{-}mol.s^{-1}}\right] \qquad (7.4.–2)$$

which may in turn be converted into volume turnover using mass per C-mol and biomass density,

$$\mu.X_T.A.dx.\frac{M_X}{\rho_X} \quad \left[\mathrm{m^3.s^{-1}}\right] \qquad (7.4.–3)$$

However, by definition,

$$X_T = \frac{\rho_X}{M_X} \tag{7.4.–4}$$

$$\Rightarrow \mu.X_T.A_{biofilm}.dx.\frac{M_X}{\rho_X} = \mu.A_{biofilm}.dx \ \left[\mathrm{m}^3.\mathrm{s}^{-1}\right] \tag{7.4.–5}$$

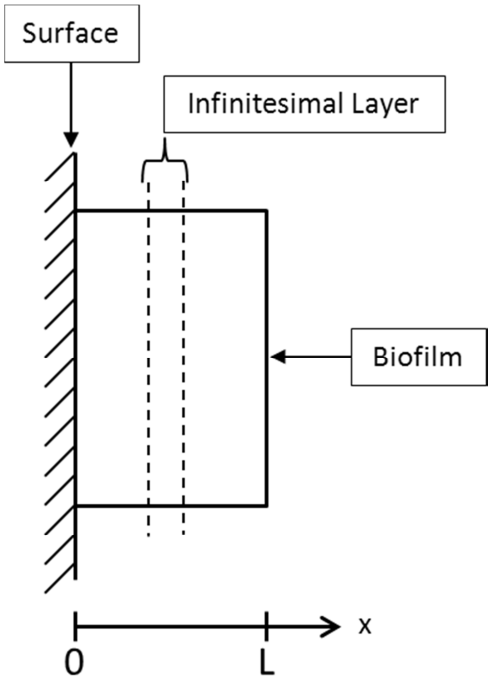

Figure 17 - Framework for derivation of the net biofilm growth rate: idealized smooth biofilm growing perpendicular to its substratum.

Since the biofilm is assumed to be growing uni-directionally, the change in thickness of the infinitesimal layer is simply the previous formula divided by the section area,

$$\mu.dx \ \left[\mathrm{m}.\mathrm{s}^{-1}\right] \tag{7.4.–6}$$

and naturally the change in thickness of the whole biofilm is the sum of changes in infinitesimal layers,

$$v_{biofilm} = \int_0^L \mu.dx \ \left[\mathrm{m}.\mathrm{s}^{-1}\right] \tag{7.4.–7}$$

This result is literally the velocity at which the biofilm expands or contracts, and is applicable to all types of biofilms, so long as there is a method to calculate localized specific growth rates. Interestingly, the reversible rate equation described in 5.2.5.Net Reversible Rate Equation and Equilibrium Constant is applicable to any biofilm: the mediator is equivalent to a donor and the external substrate to an acceptor: determination of localized concentrations becomes a simple simultaneous diffusion and reaction problem.

This formula also highlights how the thickness of a steady-state biofilm is self-regulated. In a non-electrochemically active biofilm feed with an endless supply of substrate, e.g. continuous culture, the thin layer on top of the biofilm will grow relatively quickly, while the deeper layers will be nutrient starved and thus undergo endogenous respiration. According to the integral for biofilm growth velocity, a top thin layer with a large specific growth rate can be balanced out by a deeper thicker layer undergoing slow decay. Thus, the biofilm will either growth or decay, depending on conditions, until a steady-state is reached. Of course, external factors such as shear stress will also affect biofilm dynamics and contribute to a steady-state thickness. However, such factors do not appear to be strictly necessary.

Furthermore, the formula for biofilm growth velocity predicts average behaviour over long periods of time. First, we should keep in mind the products of endogenous respiration are soluble, such that dying cells will leave behind empty space, including their own former volume and also that of oxidized EPS. The biofilm may then re-arrange, causing a steady collapse in volume, or not, triggering an increase in porosity near the substratum, which eventually leads to sloughing followed by regrowth. In both cases, and provided the supply of substrate is constant, over long periods of time and on average, the biofilm thickness fluctuates around a steady-state value.

8. Electron Transport

Electron transport is rather different in MET and DET. In MET, since electrons are carried by soluble mediators, electron transport is simply a problem of diffusion, migration and convection of the mediator. As discussed in 3.1.1.Transport in MET, the Nernst-Planck equation applies,

$$J_M = -D_M.\nabla C_M - z_M.\frac{D_M}{R.T}F.C_M.\nabla\varphi + u.C_M \qquad (8.–1)$$

where **M** refers to mediator, either the oxidized or reduced form. In DET, and given the approach in this dissertation is conduction-based, electron transport across the biofilm matrix is modelled through Ohm's law,

$$i_{matrix} = -\sigma_{matrix}.\nabla\left[\varphi_{matrix} - \varphi_{solution}\right] \qquad (8.–2)$$

According to Ohm's law, the driving force for electron transport is electrical potential, here specifically the difference between matrix potential and solution potential at each point in the biofilm. Since matrix-solution electron transfer is spread along the height of conductive biofilms, one can expect the homogeneous current density $\boldsymbol{i_{matrix}}$ to decrease as the distance to the electrode surface increases, until $\boldsymbol{i_{matrix}}$=0 at the biofilm edge. If $\boldsymbol{i_{matrix}}$ is not constant, and according to Ohm's law, one can expect the matrix potential gradient to be non-linear. The conceptual basis of the approach presented below is not too different from the one proposed by Marcus and co-workers (Marcus et al., 2007).

8.1.Poisson's Equation for Matrix Potential

Figure 18 and Figure 19 provide the geometrical basis necessary to derive the matrix potential profile, based on the cathodic case. From Figure 19, and assuming both biofilm porosity and matrix conductivity are constant, we may write an infinitesimal current balance,

$$\begin{aligned}&\text{Input} - \text{Output} = \text{Transfer} + \text{Growth}\\ &\Leftrightarrow i_{matrix}(x).L_y.L_z.\left(1-\varepsilon_{biofilm}\right) - i_{matrix}(x+dx).L_y.L_z.\left(1-\varepsilon_{biofilm}\right)\\ &= +j_{transfer}.L_y.dx + j_{growth}.H\left(-j_{transfer}.\mu\right).L_y.dx\end{aligned} \qquad (8.1.–1)$$

meaning electrons removed from the conductive matrix are either transferred to the liquid phase as a part of catabolism or retained for growth at the matrix-solution interface.

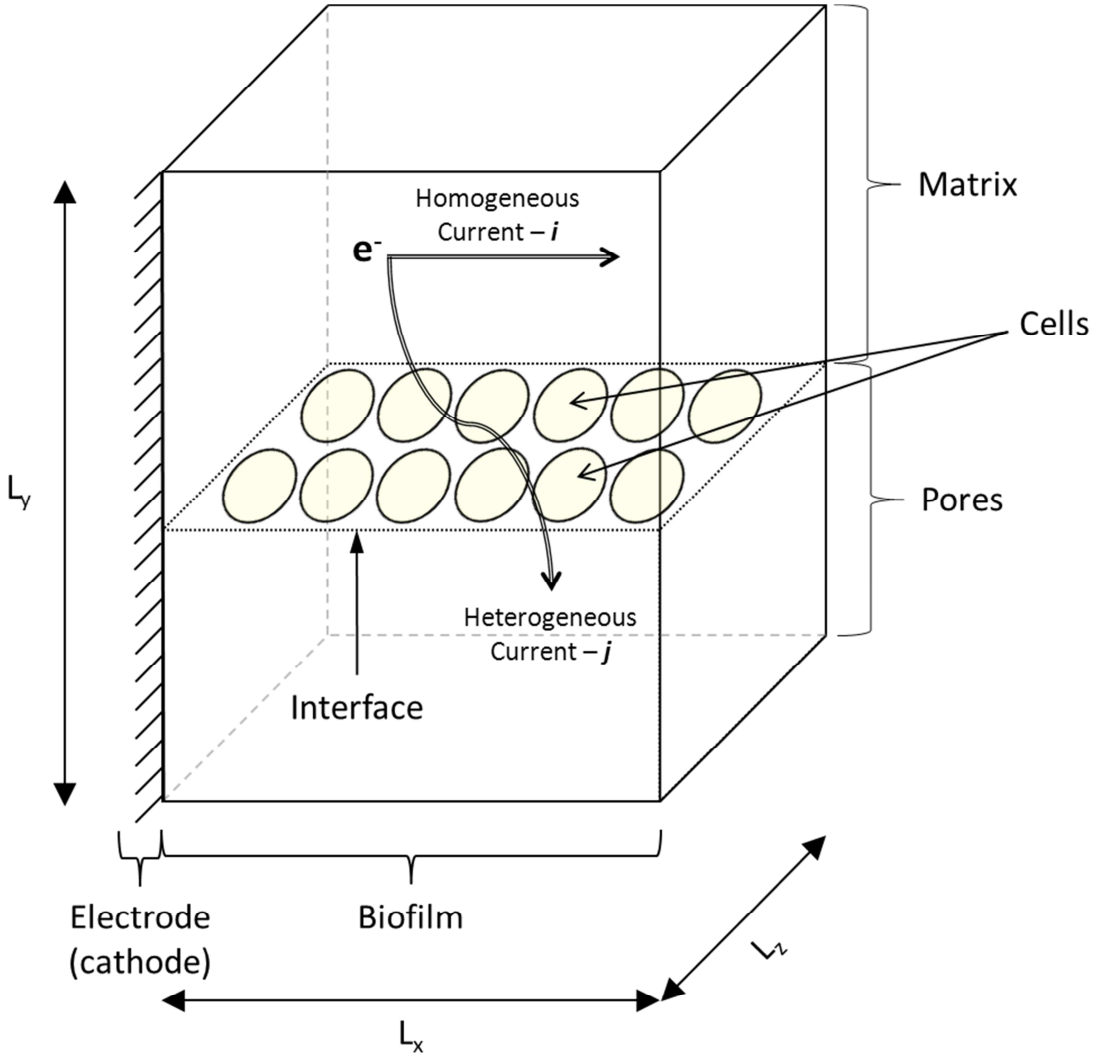

Figure 18 - Schematics for electron transport in conduction-based long-range direct electron transfer. Here, the cathodic process is depicted: the anodic process is similar, only reversed. Electrons exiting the cathode are conducted by the EPS matrix – homogeneous current ***i*** – which for long-range DET is proposed to have conductive properties, see 3.2.DET Models. Cells growing at the interface between conductive EPS and solution contained in biofilm pores will utilize those electrons for catabolic purposes, thus transferring them to an acceptor located in the liquid phase – heterogeneous current ***j***. Noteworthy, cells performing DET must, without exception, be located at the matrix-solution interface, such that e.g. in cathodic DET, electrons can be retrieved from the matrix into an electron transport chain, and eventually transferred to a soluble acceptor. Furthermore, a fraction of electrons is retained at the interface for anabolic purposes (not shown).

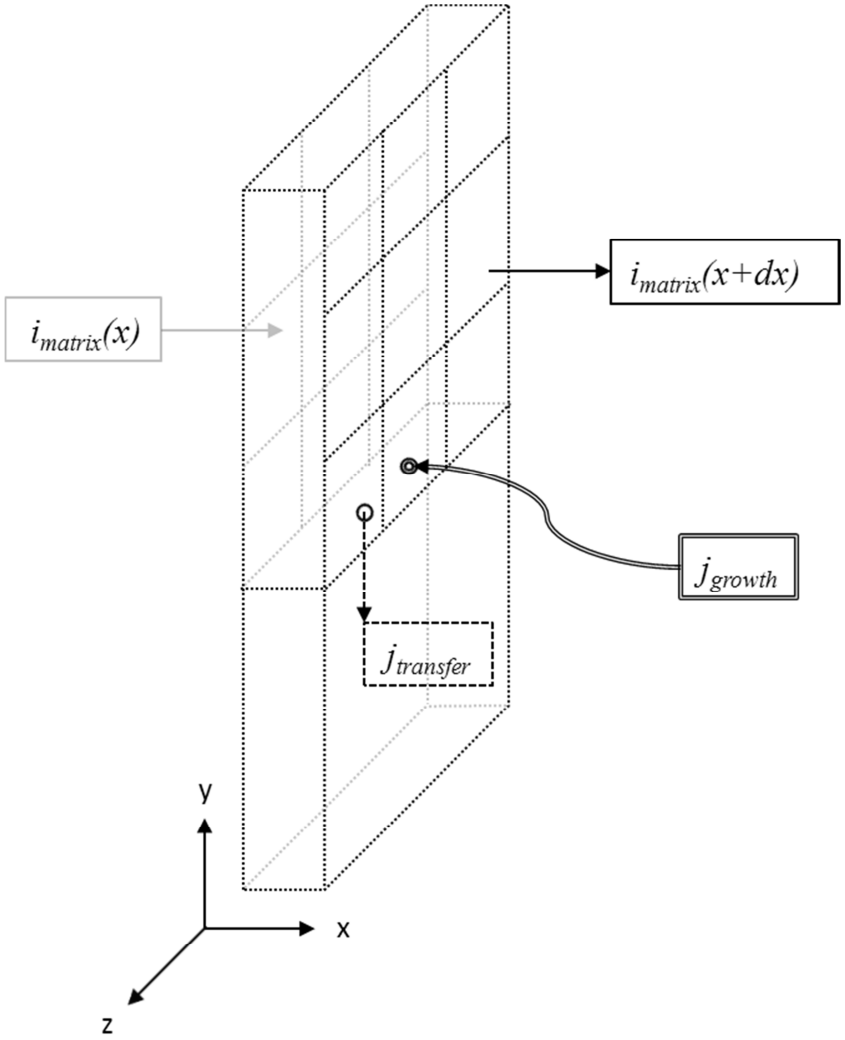

Figure 19 - Infinitesimal cut in a long-range DET biofilm (complementary information in Figure 18). In infinitesimal thickness ***dx***, the variation in homogeneous current density ***i*** will be equal to the sum of localized heterogeneous current densities, both transferred to the liquid and retained at the interface for biosynthetic purposes.

Re-arranging the infinitesimal balance,

$$-\frac{d}{dx} i_{matrix} = \frac{j_{transfer}}{L_z.\left(1-\varepsilon_{biofilm}\right)} + \frac{j_{growth}}{L_z.\left(1-\varepsilon_{biofilm}\right)}.H\left(-j_{transfer}.\mu\right) \qquad (8.1.–2)$$

Each of the three terms – homogeneous current, transferred current and growth current – will be discussed separately.

8.1.1. Homogeneous Current Density

The homogeneous component in the differential current balance may be substituted using Ohm's law. For the uni-dimensional case, and assuming constant matrix conductivity, Ohm's law reads as,

$$\begin{aligned} & i_{matrix} = -\sigma_{matrix} . \frac{d}{dx} [\varphi_{matrix} - \varphi_{solution}] \\ & \Leftrightarrow -\frac{d}{dx} i_{matrix} = \sigma_{matrix} . \frac{d^2}{dx^2} [\varphi_{matrix} - \varphi_{solution}] \end{aligned} \tag{8.1.1.–1}$$

Substituting,

$$\sigma_{matrix} . \frac{d^2}{dx^2} [\varphi_{matrix} - \varphi_{solution}] = \frac{j_{transfer}}{L_z . \left(1 - \varepsilon_{biofilm}\right)} + \frac{j_{growth}}{L_z . \left(1 - \varepsilon_{biofilm}\right)} . H\left(-j_{transfer} . \mu\right) \tag{8.1.1.–2}$$

This type of partial differential equation is known as Poisson's equation (Polyanin, 2002), whose general formulation in Euclidean space, with dependent variable φ and source term f, reads as,

$$\nabla^2 \varphi = f \tag{8.1.1.–3}$$

8.1.2. Heterogeneous Current Density

The heterogeneous current density $j_{transfer}$ is calculated as derived in 6.5. Heterogeneous Current Density and Equilibrium Constant, and is simply the result of DET catabolism. Recalling the general result,

$$j = j_{transfer} = \frac{1}{Denominator\big|_{DET}} . \left[\left(+j_{pa}\right) . \frac{S_{Red} . \left[H^+\right]^n}{K_{(S_{Red}) . \left(H^+\right)^n}} . k_a - \left(-j_{pc}\right) . \frac{S_{Ox}}{K_{S_{Ox}}} . k_c . \left[H^+\right]^n \right] \tag{8.1.2.–1}$$

$$\begin{aligned} Denominator\big|_{DET} = & \frac{K_{(S_{Red}) . \left(H^+\right)^n} + S_{Red} . \left[H^+\right]^n}{K_{(S_{Red}) . \left(H^+\right)^n}} . \left[\frac{\left(-j_{pc}\right)}{n.F.X_T} . \frac{S_{Ox}}{K_{S_{Ox}}} + k_a \right] \\ & + \frac{K_{S_{Ox}} + S_{Ox}}{K_{S_{Ox}}} . \left[\frac{\left(+j_{pa}\right)}{n.F.X_T} . \frac{S_{Red} . \left[H^+\right]^n}{K_{(S_{Red}) . \left(H^+\right)^n}} + k_c . \left[H^+\right]^n \right] \end{aligned} \tag{8.1.2.–2}$$

Noteworthy, the spatial organization in Figure 18 is merely for derivation purposes. Specifically, the heterogeneous reaction surface for electron transfer is the entire internal biofilm area. From Figure 18,

$$a_{biofilm} = \frac{L_y.dx}{L_y.dx.L_z} = \frac{1}{L_z} \qquad (8.1.2.–3)$$

where $\boldsymbol{a_{biofilm}}$ is the internal biofilm surface area per unit volume. Substituting in the differential current balance,

$$\sigma_{matrix}.\frac{d^2}{dx^2}[\varphi_{matrix} - \varphi_{solution}] = a_{biofilm}.\frac{j_{transfer}}{1-\varepsilon_{biofilm}} + a_{biofilm}.\frac{j_{growth}}{1-\varepsilon_{biofilm}}.H\left(-j_{transfer}.\mu\right) \qquad (8.1.2.–4)$$

8.1.3. Growth

The growth-related term on the right-hand side of the differential current balance encompasses both growth and endogenous respiration, and is valid for anodic and cathodic processes. The fate of growth-related electrons varies with each specific set of conditions. Firstly, let us write down the mathematical conditions that distinguish anodes from cathodes and growth from decay,

$$\begin{cases} Anode \Leftrightarrow j_{transfer} > 0 \\ Cathode \Leftrightarrow j_{transfer} < 0 \end{cases} \qquad (8.1.3.–1)$$

$$\begin{cases} Growth \Leftrightarrow \mu > 0 \\ Decay \Leftrightarrow \mu < 0 \end{cases} \qquad (8.1.3.–2)$$

Recalling chapter 7.3.Localized Specific Growth Rate, the specific growth rate $\boldsymbol{\mu}$ may be slightly negative if catabolism operates too close to equilibrium, corresponding to endogenous respiration. Furthermore, let us analyse each specific combination of conditions, regarding the fate of growth-related electrons,

1.Anode+Growth: Electrons are provided by a chemical donor and don't reach the conductive matrix. ➔ No need to account for them in the matrix current balance

2.Anode+Decay: Electrons are released onto the conductive matrix upon endogenous respiration. ➔ They must be added in the matrix current balance.

3.Cathode+Growth: Electrons for growth are provided by the conductive matrix. ➔ They must be subtracted in the matrix current balance.

4.Cathode+Decay: Electrons produced by endogenous respiration are donated to soluble, chemical acceptor. ➔ No influence in the matrix current balance.

Thus, anabolism-related electrons should only be included in the matrix current balance in cases 2 and 3. Furthermore, cases 1-4 may also be classified using the sign of the product $\boldsymbol{j_{transfer}.\mu}$,

$$\begin{cases} 1.Anode + Growth \Rightarrow j_{transfer}.\mu > 0 \\ 2.Anode + Decay \Rightarrow j_{transfer}.\mu < 0 \\ 3.Cathode + Growth \Rightarrow j_{transfer}.\mu < 0 \\ 4.Cathode + Decay \Rightarrow j_{transfer}.\mu > 0 \end{cases} \qquad (8.1.3.–3)$$

Thus, if the product $\boldsymbol{j_{transfer}.\mu}$ is negative, the matrix current balance must account for growth-related electrons. If $\boldsymbol{j_{transfer}.\mu}$ is positive, this is not necessary. And of course, if the product is null, there is no growth or decay. This property may be used together with the Heaviside step function, providing a growth-related term applicable to all cases,

$$\frac{j_{growth}}{L_z.\left(1-\varepsilon_{biofilm}\right)}.H\left(-j_{transfer}.\mu\right) \qquad (8.1.3.–4)$$

Regarding $\boldsymbol{j_{growth}}$ specifically, is simply the growth rate multiplied by the number of electrons exchange per newly formed C-mol. Recalling the anabolic stoichiometry with acetate as carbon source,

$$0.5\,CH_3COO^-(aq) + 0.2\,NH_4^+(aq) + \left(0.3 + 0.2\frac{1}{n}\right)H^+(aq) + 0.2\frac{1}{n}XH_n$$
$$\xrightleftharpoons[\text{decay}]{\text{biosynthesis}} CH_{1.8}O_{0.5}N_{0.2}(s) + 0.5\,H_2O(l) + 0.2\frac{1}{n}X + 0.2\frac{1}{n}n\,H^+(aq)$$

And applying the necessary conversion,

$$j_{growth} = v_X^{Anabolism}.n.z_e.F.\mu.X_T.\frac{L_y.L_z.dx}{L_y.dx} = -0.2F.\mu.X_T.L_z \qquad (8.1.3.–5)$$

where $v_X^{Anabolism}$ is the stoichiometric coefficient of **X** and z_e is the electronic charge number, z_e=–1, included in the equation to compensate for the positive convention used to express current directions. Substitution in the differential current balance yields,

$$\sigma_{matrix}.\frac{d^2}{dx^2}[\varphi_{matrix}-\varphi_{solution}]=a_{biofilm}.\frac{j_{transfer}}{1-\varepsilon_{biofilm}}+\frac{v_X^{Anabolism}.n.z_e.F.\mu.X_T}{1-\varepsilon_{biofilm}}.H\left(-j_{transfer}.\mu\right) \quad (8.1.3.–6)$$

where both $\boldsymbol{j_{transfer}}$ and $\boldsymbol{\mu}$ are a function of local matrix potential and chemical species concentrations, meaning they are also indirectly a function of position $\boldsymbol{x}$.

8.2.Boundary Conditions

Two boundary conditions are required to solve Poisson's equation. Firstly, at the electrode surface, the matrix potential must be equal to the electrode potential, such that the Dirichlet boundary condition (Polyanin, 2002) applies,

$$\text{Dirichlet Boundary Condition}:[\varphi_{matrix}-\varphi_{solution}]\big|_{x=0}=[\varphi_{electrode}-\varphi_{solution}] \quad (8.2.–1)$$

Secondly, at the biofilm boundary, the homogeneous current density must be zero, simply because the conductive matrix doesn't extend any further. From Ohm's law, we may define a Neumann boundary (Polyanin, 2002) condition,

$$i_{matrix}\big|_{x=L_x}=0\Rightarrow\frac{d}{dx}[\varphi_{matrix}-\varphi_{solution}]=0 \quad (8.2.–2)$$

However, applying the principal of electric potential continuity, a Dirichlet boundary condition may also be defined at the same point,

$$[\varphi_{matrix}-\varphi_{solution}]\big|_{x=L_x}=\varphi_{solution} \quad (8.2.–3)$$

Thus, the second boundary condition is of the Cauchy type (Polyanin, 2002),

$$\text{Cauchy Boundary Condition}:\begin{cases}\dfrac{d}{dx}[\varphi_{matrix}-\varphi_{solution}]=0\\ [\varphi_{matrix}-\varphi_{solution}]\big|_{x=L_x}=\varphi_{solution}\end{cases} \quad (8.2.–4)$$

With these conditions, Poisson's equation may be computationally solved and the resulting matrix potential profile may be used to calculate the homogeneous current density through Ohm's law. Interestingly, the matrix potential is the *de facto* substrate for DET catabolism, meaning the two equations must be solved simultaneously.

9. Final Remarks

The initial objective proposed in 1.Motivation – deriving reversible rate equations capable of explaining the results report by Rozendal and co-workers (Rozendal et al., 2008) – has been achieved and greatly surpassed. Rates for all measurable macroscopic process in EABs are provided: current generation, microbial kinetics and biofilm growth. These results are based on clearly identified assumptions, namely, quasi-steady-state: biofilms have approximately constant localized densities. Furthermore, predictions of biomass redox states – a concept that in and of itself is discussed and applied with unprecedented detail – are also made, thus providing a zooming tool into today's black box EAB, potentially granting the model herein developed with the status of theory.

Other results are also extremely useful from a practical perspective. For instance, the relation between peak current densities and substrate affinities for biofilms performing DET, if proven correct, would render the quantification of EAB substrate affinities almost trivial, and certainly much simpler and accurate than in regular biofilms. Not to mention the results derived for the microbial portion of MET are applicable to all biofilms growing on soluble electron donors and acceptors, ultimately resulting in a mechanistic equation for biofilm growth velocity.

These results weren't just derived from a theoretical perspective. The development of a universal notation, easily converted into any concrete example, was a primary concern. The same concern also propelled the derivation of conversion rules for composite and exponentiated half-saturation coefficients into their standard counterparts, a result which in and of itself allows the extension of classical models such as Michaelis-Menten/Monod in previously unforeseen ways.

Last but not least, and because equations are just another way to express ideas, this report is not just about Mathematics or Physical Chemistry: whenever necessary, concepts where discussed at length to ensure the equations that arise from them are accessible to the largest possible variety of specialists. The prolonged introduction provided by chapters 2, 3 and 4 serves this purpose. Also, the biological and biochemical component of arguments was never forgotten.

The experimental work that should follow is lengthy and complex, since this is the type of modelling that requires dedicated experiments for validation purposes. Such details, I admit, are not fully within my grasp, for I have dedicated most of my time to theory building. However, there is one derivation I haven't quite managed to finish: full unification of MET and DET. The reason for this is mediator affinity: so far I haven't been able to identify a parameter in DET that is conceptually equivalent. This I believe is the next key theoretical goal, and would enable direct comparison of MET and DET.

References

Alpkvist E, Picioreanu C, Loosdrecht M, Heyden A. Three-dimensional biofilm model with individual cells and continuum EPS matrix. Biotechnol Bioeng 94:961-79, 2006.

Andrieux C, Savéant J. Electron transfer through redox polymer films. J Electroanal Chem 111:377-81, 1980.

Atkins P, Overton T, Rourke J, Weller M, Armstrong F. Shriver and Atkins' Inorganic Chemistry, 5th ed.. Oxford University Press, 2009.

Atkins P, Paula J. *Atkins' Physical Chemistry, 8th ed.*. W.H. Freeman, 2006.

Aulenta F, Catervi A, Majone M, Panero S, Reale P, Rossetti S. Electron transfer from a solid-state electrode assisted by methyl viologen sustains efficient microbial reductive dechlorination of TCE. Environ Sci Technol 41:2554-9, 2007.

Aulenta F, Canosa A, Majone M, Panero S, Reale P, Rossetti S. Trichloroethene dechlorination and H_2 evolution are alternative biological pathways of electric charge utilization by a dechlorinating culture in a bioelectrochemical system. Environ Sci Technol 42:6185-90, 2008.

Aulenta F, Canosa A, Reale P, Rossetti S, Panero S, Majone M. Microbial reductive dechlorination of trichloroethene to ethane with electrodes serving as electron donors without the external addition of redox mediators. Biotechnol Bioeng 103:85-91, 2009.

Aulenta F, Reale P, Canosa A, Rossetti S, Panero S, Majone M. Characterization of an electro-active biocathode capable of dechlorinating trichloroethene and *cis*-dichloroethene to ethene. Biosens Bioelectron 25:1796-1802, 2010a.

Aulenta F, Maio V, Ferri T, Majone M. The humic acid analogue anthraquinone-2,6-disulfonate (AQDS) serves as an electron shuttle in the electricity-driven microbial dechlorination of trichloroethene to *cis*-dichloroethene. Bioresouce Technol 101:9728-33, 2010b.

Bard A, Faulkner L. Electrochemical methods: Fundamentals and applications, 2nd ed.. Wiley, 2001.

Batchelor-McAuley C, Li Q, Dapin S, Compton R. Voltammetric characterization of DNA intercalators across the full pH range: Anthraquinone-2,6-disulfonate and anthraquinone-2-sulfonate. J Phys Chem B 114:4094-100, 2010.

Beech I, Campbell S. Accelerated low water corrosion of carbon steel in the presence of a biofilm harbouring sulphate-reducing and sulphur-oxidising bacteria recovered from a marine sediment. Electrochim Acta 54:14-21, 2008.

Blauch D, Savéant J. Dynamics of electron hopping in assemblies of redox centers: Percolation and diffusion. J Am Chem Soc 114:3323-32, 1992.

Bommarius A, Riebel-Bommarius B. Biocatalysis: Fundamentals and applications. Wiley, 2007.

Bond D, Strycharz-Glaven S, Tender L, Torres C. On electron transport through *Geobacter* biofilms. ChemSusChem 5:1099-105, 2012.

Briggs G, Haldane J. A note on the kinematics of enzyme action. Biochem J 19:338-9, 1925.

Busby S, Ebright R. Transcription activation by catabolite activator protein (CAP). J Mol Biol 293:199-213, 2001.

Buxbaum E. Fundamentals of protein structure and function, 1st ed.. Springer, 2007.

Canstein H, Ogawa J, Shimizu S, Lloyd J. Secretion of flavins by *Shewanella* species and their role in extracellular electron transfer. Appl Environ Microb 74:615-23, 2008.

Carmona-Martínez A, Harnisch F, Kuhlicke U, Neu T, Schröder U. Electron transfer and biofilm formation of *Shewanella putrefaciens* as function of anode potential. Bioelectrochemistry, Corrected Proof, 2012.

Cecchini G, Schröder I, Gunsalus R, Maklashina E. Succinate dehydrogenase and fumarate reductase from *Escherichia coli*. Biochim Biophys Acta 1553:140-157, 2002.

Cleland W. The kinetics of enzyme-catalyzed reactions with two or more substrates or products. I. Nomenclature and rate equations. Biochim Biophys Acta 67:104-37, 1963.

Condon C, Cammack R, Patil D, Owen P. The succinate dehydrogenase of *Escherichia coli*. Immunochemical resolution and biophysical characterization of a 4-subunit enzyme complex. J Biol Chem 260:9427-34, 1985.

Cracknell J, Vincent K, Armstrong F. Enzymes as working or inspirational electrocatalysts for fuel cells and electrolysis. Chem Rev 108:2439-61, 2008.

Dalton E, Surridge N, Jerningan J, Wilbourn K, Facci J, Murray R. Charge transport in electroactive polymers consisting of fixed molecular redox sites. Chem Phys 141:143-57, 1990.

Delaney G, Bennetto H, Mason J, Roller S, Stirling J, Thurston C. Electron-transfer coupling in microbial fuel cells. 2. Performance of fuel cells containing selected microorganism-mediator-substrate combinatons. J Chem Tech Biot B 34:13-27, 1984.

Gilbert W, Müller-Hill B. Isolation of the lac repressor. Proc Natl Acad Sci USA 56:1891-8, 1966.

Hamelers H, Heijne A, Stein N, Rozendal R, Buisman C. Butler-Volmer-Monod model for describing bio-anode polarization curves. Bioresource Technol 102:381-7, 2011.

Harnisch F, Freguia S. A basic tutorial on cyclic voltammetry for the investigation of electroactive microbial biofilms. Chem Asian J 7:466:75, 2012.

Harnisch F, Rabaey K. The diversity of techniques to study electrochemically active biofilms highlights the need for standardization. ChemSusChem 5:1027-38, 2012.

Harnisch F, Schröder U. Selectivity versus mobility: Separation of anode and cathode in microbial bioelectrochemical systems. ChemSusChem 2:921-6, 2009.

Harnisch F, Schröder U. From MFC to MXC: Chemical and biological cathodes and their potential for microbial bioelectrochemical systems. Chem Soc Rev 39:4433-48, 2010.

Harnisch F, Schröder U. Biofilms, electroactive. In: Encyclopedia of Applied Electrochemistry, Springer, 2012.

Heidelberg J, Paulsen I, Nelson K, Gaidos E, Nelson W, Read T, Eisen J, Seshadri R, Ward N, Methé B, Clayton R, Meyer T, Tsapin A, Scott J, Beanan M, Brinkac L, Daugherty S, DeBoy R, Dodson R, Durkin A, Haft D, Kolonay J, Madupu R, Peterson J, Umayam L, White O, Wolf A, Vamathevan J, Weidman J, Impraim M, Lee K, Berry K, Lee C, Mueller J, Khouri H, Gill J, Utterback T, MacDonald L, Feldblyum T, Smith H, Venter J, Nealson K, Fraser C. Genome sequence of the dissimilatory metal ion-reduction bacterium *Shewanella oneidensis*. Nature 20:1118-23, 2002.

Hernandez M, Newman D. Extracellular electron transfer. Cell Mol Life Sci 58:1562-71, 2001.

Heijnen J, Kleerebezem R. Bioenergetics of microbial growth. **In:** Encyclopedia of Industrial Biotechnology: Bioprocess, Bioseparation, and Cell Technology. Wiley, 2010.

Heijnen J, Loosdrecht M, Tijhuis L. A black box model to calculate auto- and heterotrophic biomass yields based on Gibbs energy dissipation. Biotechnol Bioeng 40:1139-54, 1992.

Hill A. The possible effects of the aggregation of the molecules of hæmoglobin on its dissociation curves. J Physiol 40(Suppl):iv-vii, 1910.

Inoue K, Leang C, Franks A, Woodard T, Nevin K, Lovley D. Specific localization of the *c*-type cytochrome OmcZ at the anode surface in current-producing biofilms of *Geobacter sulfurreducens*. Environ Microbiol Rep 3:211-7, 2011.

Iverson T, Chavez C, Cecchini G, Rees D. Structure of the *Escherichia coli* fumarate reductase respiratory complex. Science 284:1961-6, 1999.

Jacq J. Schema Carre – Etablissement et discussion de l'equation generale de la courbe intensite-potentiel en regime stationnaire et diffusion convective. J Electroanal Chem 29:149-80, 1971.

Johnson K, Goody R. The original Michaelis constant: Translation of the 1913 Michaelis-Menten paper. Biochemistry 50:8264-9, 2011.

Kaufman F, Engler E. Solid-state spectroelectrochemistry of cross-linked donor bound polymer films. J Am Chem Soc 101, 547-9, 1979.

King E, Altman C. A schematic method of deriving the rate laws for enzyme-catalyzed reactions. J Phys Chem 60:1375-8, 1956.

Lapinsonnière L, Picot M, Barrière F. Enzymatic versus microbial bio-catalyzed electrodes in bio-electrochemical systems. ChemSusChem 5:995-1005, 2012.

Laviron E. A multilayer model for the study of space distributed redox modified electrodes: Part I. Description and discussion of the model. J Electroanal Chem 112:1-9, 1980.

Laviron E, Roulier L, Degrand C. A multilayer model for the study of space distributed redox modified electrodes: Part II. Theory and application of linear potential sweep voltammetry for a simple reaction. J Electroanal Chem 112:11-23, 1980.

Leang C, Qian X, Mester T, Lovley D. Alignment of the c-type cytochrome OmcS along pili of *Geobacter sulfurreducens*. Appl Environ Microb 76:4080-4, 2010.

Lee H, Torres C, Rittmann B. Effects of substrate diffusion and anode potential on kinetic parameters for anode-respiring bacteria. Environ Sci Technol 43:7571-7, 2009.

Liu Y, Bond D. Long-distance electron transfer by *G. sulfurreducens* biofilms results in accumulation of reduced *c*-type cytochromes. ChemSusChem 5:1047-53, 2012.

Logan B. Exoelectrogenic bacteria that power microbial fuel cells. Nat Rev Microbiol 7:375-81, 2009.

Logan B. Essential data and techniques for conducting microbial fuel cell and other types of bioelectrochemical system experiments. ChemSusChem 5:988-94, 2012.

Lohner S, Becker D, Mangold K, Tiehm A. Sequential reductive and oxidative biodegradation of chloroethenes stimulated in a coupled bioelectro-process. Environ Sci Technol 45:6491-7, 2011.

Lojou E, Durand M, Dolla A, Bianco P. Hydrogenase activity control at *Desulfovibrio vulgaris* cell-coated carbon electrodes: Biochemical and chemical factors influencing the mediated bioelectrocatalysis. Electroanalysis 14:913-22, 2002.

Lovley D. The microbe electric: conversion of organic matter to electricity. Curr Opin Biotech 19:564-71, 2008.

Malvankar N, Vargas M, Nevin K, Franks A, Leang C, Kim B, Inoue K, Mester T, Covalla S, Johnson J, Rotello V, Tuominen M, Lovley D. Tunable metallic-like conductivity in microbial nanowire networks. Nat Nanotechnol 6:573-9, 2011.

Malvankar N, Lovley D. Microbial nanowires: A new paradigm for biological electron transfer and bioelectronics. ChemSusChem 5:1039-46, 2012.

March J. Advanced organic chemistry: Reactions, mechanisms, and structure, 3rd ed.. Wiley, 1985.

Marcus A, Torres C, Rittman B. Conduction-based modeling of the biofilm anode of a microbial fuel cell. Biotechnol Bioeng 98:1171-82, 2007.

Marsili E, Baron D, Shikhare I, Coursolle D, Gralnick J, Bond D. *Shewanella* secretes flavins that mediate extracellular electron transfer. P Natl Acad Sci USA 105:3968-73, 2008.

McNaught A, Wilkinson A. *Editors of* IUPAC Compendium of chemical terminology, 2nd ed.. Blackwell, 1997.

Menten L, Michaelis M. Die Kinetik der Invertinwirkung. Biochem Z 49:333-69, 1913.

Methé B, Nelson K, Eisen J, Paulsen I, Nelson W, Heidelberg J, Wu D, Wu M, Ward N, Beanan M, Dodson R, Madupu R, Brinkac L, Daugherty S, DeBoy R, Durkin A, Gwinn M, Kolonay J, Sullivan S, Haft D, Selengut J, Davidsen T, Zafar N, White O, Tran B, Romero C, Forberger H, Weidman J, Khouri H, Feldblyum T, Utterback T, Aken S, Lovley D, Fraser C. Genome of *Geobacter sulfurreducens*: Metal reduction in subsurface environments. Science 302:1967-9, 2003.

Monod J. The growth of bacterial cultures. Annu Rev Microbiol 3:371-94, 1949.

Morgado L, Paixão V, Schiffer M, Pokkuluri P, Bruix M, Salgueiro C. Revealing the structural origin of the redox-Bohr effect: The first solution structure of a cytochrome from *Geobacter sulfurreducens*. Biochem J 441:179-187, 2012.

Nelson D, Cox M. Lehninger Principles of Biochemistry, 5th ed.. W.H. Freeman, 2009.

Nielsen L, Petersen N, Fossing H, Christensen P, Sayama M. Electric currents couple spatially separated biogeochemical processes in marine sediment. Nature 463:1071-4, 2010.

Okamoto A, Hashimoto K, Nakamura R. Long-range electron conduction of *Shewanella* biofilms mediated by outer membrane *c*-type cytochromes. Bioelectrochemistry 85:61-65, 2012.

Picioreanu C, Loosdrecht M. A mathematical model for initiation of microbiologically influenced corrosion by differential aeration. J Electrochem Soc 149:B211-23, 2002.

Picioreanu C, Head I, Katuri K, Loosdrecht M, Scott K. A computational model for biofilm-based microbial fuel cells. Water Res 41:2921-40, 2007.

Picioreanu C, Katuri K, Head I, Loosdrecht M, Scott K. Mathematical model for microbial fuel cells with anodic biofilms and anaerobic digestion. Water Sci Technol 57:965-71, 2008.

Picioreanu C, Loosdrecht M, Curtis T, Scott K. Model based evaluation of the effect of pH and electrode geometry on microbial fuel cell performance. Bioelectrochemistry 78:8-24, 2010a.

Picioreanu C, Katuri K, Loosdrecht M, Head I, Scott K. Modelling microbial fuel cells with suspended cells and added electron transfer mediator. J Appl Electrochem 40:151-62, 2010b.

Polyanin A. Handbook of linear partial differential equations for engineers and scientists. CRC Press, 2002.

Popat S, Ki D, Rittmann B, Torres C. Importance of OH^- transport from cathodes in microbial fuel cells. ChemSusChem 5:1071-9, 2012.

Rabaey K, Angenent L, Schröder U, Keller J. **Editors of:** Bioelectrochemical systems: From extracellular electron transfer to biotechnological application, 1st ed.. IWA Publishing, 2010.

Rabaey K, Rozendal R. Microbial electrosynthesis – revisiting the electrical route for microbial production. Nat Rev Microbiol 8:706-16, 2010.

Reguera G, McCarthy K, Mehta T, Nicoll J, Tuominen M, Lovley D. Extracellular electron transfer via microbial nanowires. Nature 435:1098-101, 2005.

Richter H, Nevin K, Jia H, Lowy D, Lovley D, Tender L. Cyclic voltammetry of biofilms of wild type and mutant *Geobacter sulfurreducens* on fuel cell anodes indicates possible roles of OmcB, OmcZ, type IV pili, and protons in extracellular electron transfer. Energy Environ Sci 2:506-16, 2009.

Richter K, Schicklberger M, Gescher J. Dissimilatory reduction of extracellular electron acceptors in anaerobic respiration. Appl Environ Microbiol 78:913-21, 2012.

Roller S, Bennetto H, Delaney G, Mason J, Stirling J, Thurston C. Electron-transfer coupling in microbial fuel cells: 1. Comparison of redox-mediator reduction rates and respiratory rates of bacteria. J Chem Tech Biot B 34:3-12, 1984.

Rosenbaum M, Aulenta F, Villano M, Angenent L. Cathodes as electron donors for microbial metabolism: Which extracellular electron transfer mechanisms are involved? Bioresource Technol 102:324-33, 2011.

Rozendal R, Jeremiasse A, Hamelers H, Buisman C. Hydrogen production with a microbial biocathodes. Environ Sci Technol 42:629-34, 2008.

Savéant J. Electron hopping between fixed sites: Equivalent diffusion and migration laws. J Electroanal Chem 201:211-3, 1986.

Schröder U. Anodic electron transfer mechanisms in microbial fuel cells and their energy efficiency. Phys Chem Chem Phys 9:2619-29, 2007.

Singleton P, Sainsbury D. Dictionary of Microbiology and Molecular Biology, 3rd ed.. Wiley, 2006.

Stein N, Keesman K, Hamelers H, Straten G. Kinetic models for detection of toxicity in a microbial fuel cell based biosensor. Biosens Bioelectron 26:3115-20, 2011.

Strycharz-Glaven S, Gannon S, Boles A, Franks A, Nevin K, Lovley D. Reductive dechlorination of 2-chlorophenol by *Anaeromyxobacter dehalogenans* with an electrode serving as the electron donor. Environ Microbiol Rep 2:289-94, 2010.

Strycharz S, Malanoski A, Snider R, Yi H, Lovley D, Tender L. Application of cyclic voltammetry to investigate enhanced catalytic current generation by biofilm-modified anodes of *Geobacter sulfurreducens* strain DL1 *vs.* variant strain KN400. Energy Environ Sci 4:896-913, 2011.

Strycharz-Glaven S, Snider R, Guiseppi-Elie A, Tender L. On the electrical conductivity of microbial nanowires and biofilms. Energy Environ Sci 4:4366-79, 2011.

Strycharz-Glaven S, Tender L. Study of the mechanism of catalytic activity of *G. sulfurreducens* biofilm anodes during biofilm growth. ChemSusChem 5:1106-18, 2012.

Tatsumi H, Takagi K, Fujita M, Kano K, Ikeda T. Electrochemical study of reversible hydrogenase reaction of *Desulfovibrio vulgaris* cells with methyl viologen as an electron carrier. Anal Chem 71:1753-9, 1999.

Torres C, Marcus A, Parameswaran P, Rittmann B. Kinetic experiments for evaluating the Nernst-Monod model for anode-respiring bacteria (ARB) in a biofilm anode. Environ Sci Technol 42:6593-7, 2008.

Torres C, Marcus A, Lee H, Parameswaran P, Brown R, Rittmann B. A kinetic perspective on extracellular electron transfer by anode-respiring bacteria. FEMS Microbiol Rev 34:3-17, 2010.

Virdis B, Harnisch F, Batstone D, Rabaey K, Donose B. Non-invasive characterization of electrochemically active microbial biofilms using confocal Raman microscopy. Energy Environ Sci 5:7017-24, 2012.